Induction Kinetics of the PhoQ-PhoP Two-Component System in *Escherichia coli*

Michael E. Salazar, Jr.

A.B. Physics
Princeton University, Princeton, NJ, 08544

SUBMITTED TO THE DEPARTMENT OF BIOLOGY IN PARTIAL FULFILLMENT OF THE REQUIREMENTS FOR THE DEGREE OF

DOCTOR OF PHILOSOPHY IN BIOLOGY
AT THE
MASSACHUSETTS INSTITUTE OF TECHNOLOGY

APRIL 2016
[June 2016]

The author hereby grants MIT permission to reproduce and distribute publicly paper and electronic copies of this thesis document in whole or in part

Signature of Author:___ Signature redacted
Michael E. Salazar, Jr.
Department of Biology
April 20th, 2016

Certified by:_____ Signature redacted
Michael T. Laub
Professor of Biology
Thesis Supervisor

Accepted by:_____ Signature redacted
Amy E. Keating
Professor of Biology
Co-Chair, Biology Graduate Committee

Induction Kinetics of the PhoQ-PhoP Two-Component System in *Escherichia coli*

by

Michael E. Salazar, Jr.

Advisor: Professor Michael Laub

Submitted to the Department of Biology on April 29th, 2016

In partial fulfillment of the requirements for the degree of Doctor of Philosophy in Biology at the Massachusetts Institute of Technology

Abstract

Cells rely on signal transduction systems to sense and respond to changes in their enviroments. When a stimulus is present, the corresponding signal transduction system will activate and enact the appropriate biological response, often by modulating target gene expression. In many cases, the temporal dynamics of the activation of target gene expression in the presence of constant stimulus is complex, and often exhibits one or several pulses. How these complex temporal dynamics are regulated at the molecular level is unknown for many signal transduction systems. In this thesis, I discuss the molecular regulation of the temporal dynamics of PhoQ-PhoP induction in *Escherichia coli*. The PhoQ-PhoP pathway is a canonical two-component system that responds to low extracellular Mg^{++}, certain antimicrobial peptides, and potentially other unknown factors. Upon activation, the bifunctional histidine kinase PhoQ autophosphorylates and subsequently phosphotransfers to the response regulator PhoP, thereby activating it to increase transcription of PhoP target genes. Because PhoQ is bifunctional, PhoQ acts as a phosphatase on phosphorylated PhoP in the absence of stimulus, thereby keeping the system inactivated. When the PhoQ-PhoP system is strongly induced, PhoP target genes exhibit impulse kinetics, meaning gene expression increases to a maximal level and subsequently decreases to an eventual steady state. We discovered that this impulse response is caused by a negative feedback loop in which active PhoP transcribes *mgrB*, a gene encoding a small membrane protein that interacts directly with PhoQ to repress the output of the system. MgrB selectively inhibits the ability of PhoQ to phosphorylate PhoP, and permits PhoQ to act as a phosphatase on phosphorylated PhoP. This change in PhoQ activity causes a decrease in the level of active PhoP and the level of PhoP target genes. This thesis reveals how negative feedback loops and histidine kinase bifunctionality can drive the kinetics of two-component system induction in bacteria, and more generally explores how cells regulate changes in gene expression over time.

Acknowledgements

First and foremost, I would like to thank my advisor, Michael Laub, for his support and mentorship during my PhD. Your lab is a terrific place to learn and to grow as a scientist, and I am grateful to have been a part of it.

I would like to thank my committee, Alan Grossman, Amy Keating, and Jeff Gore, for providing me with advice and insightful questions about my research. I also thank the Ned Wingreen, Zemer Gitai, and the Princeton ISC faculty for helping me become excited about research and encouraging me to attend graduate school.

Thank you to all the members of the Laub Lab, past and present who have helped make this a great working environment. Anna, thank you for taking me under your wing as a rotatoe and as a new member of the lab, my thesis would look very different if it weren't for your guidance. I also want to thank the other Laub Lab members who were already in the lab when I joined; Josh, Chris, Emily, Emma, Christos, Tung, Barrett, Leonor, and Diane, who were especially helpful in welcoming me to the lab and teaching me how to do science. Diane, I want to additionally thank you for being a great baymate after I graduated from working on the short bench. Thanks to Peter and Anjana for making Room 2 a fun and supportive place to work, and also thanks to Katie and Conor for many good PhoQ-PhoP related discussions. Thanks to Team UCSF for their biochemistry/*E. coli* expertise and for reminding us all to chill out. To the newer members of the lab and to everyone else, thanks for being great co-workers and I am excited to see how your research turns out.

I also would like to thank other labs in building 68, particularly the Sauer, Baker, and Grossman labs for their help and advice throughout the years. Thank you to the Bio Education and Financial Offices for keeping everything running.

And finally, I would like to thank my family and friends their support through graduate school.

Table of Contents

Chapter I:

An introduction to two-component systems and the temporal dynamics of gene expression

A subset of this chapter was published as Salazar, M.E., Laub M.T. *Curr Opin Microbiol* 24, 7-14, April 2015. Permission was received to reprint in thesis.

Cells rely on signal transduction systems to detect external stimuli and to initiate the necessary physiological responses. These responses often include the modulation of gene expression, either through gene activation or repression, and can occur over timescales ranging from minutes to days (López-Maury et al., 2008; Yosef and Regev, 2011). It is often assumed that the relationship between signal input and pathway output is relatively simple, and that a constant level of stimulus results in a constant level of output. However, the temporal dynamics of gene expression during signal transduction can be quite complex, even when the level of stimulus remains constant. The recent development of technologies, such as time-lapse fluorescence microscopy (Locke and Elowitz, 2009) and genome wide expression analysis (RNA-seq, microarrays, etc.), allows researchers to observe changes in gene expression during signal transduction with high temporal precision and across the entire genome. Now that many examples of signal transduction pathways containing complex induction kinetics have been identified, researchers are beginning to discover how molecular level interactions lead to the regulation of these temporal dynamics and what physiological benefit these dynamics confer to the organism. In this chapter, I review the current literature of the signal transduction systems, with a focus on the temporal dynamics of signal transduction systems and two-component signaling systems in bacteria.

Temporal Dynamics of Gene Expression

I. The Impulse Response

One of the most common kinetic profiles for the expression level of targets in signal transduction pathways is the impulse response (Chechik et al., 2008; Yosef and Regev, 2011) (Fig. 1.1A). During the impulse response, gene expression level rapidly increases

(or decreases) from its original level in response to a constant stimulus, but then partially adapts to a new steady state expression level between the original and maximal (or minimal) levels. Impulse responses have been observed in a wide range of species, and are often caused by a rapid change in heat, salinity, or osmotic pressure (Chechik et al., 2008; Gasch et al., 2000; Litvak et al., 2009; Salazar and Laub, 2015; Shin et al., 2006; Yosef and Regev, 2011). Generally, these kinetics can be beneficial in biological systems because an impulse response of gene expression can translate into a more rapid production of proteins necessary to respond to the activating stimulus, while maintaining a low steady state level of expression at longer timescales (Chechik et al., 2008; Yosef and Regev, 2011).

The environmental stress response (ESR) in yeast is classic example of how environmental stimuli can trigger a genome-wide impulse response (Gasch et al., 2000; Taymaz-Nikerel et al., 2016; Yosef and Regev, 2011). Many different environmental signals trigger the ESR response, including sudden changes in temperature, changes in osmolarity, exposure to oxidative or reductive environments, amino acid starvation, nitrogen depletion, and entrance into stationary phase (Gasch et al., 2000). Once the ESR is initiated, a conserved set of approximately 900 genes is either activated or repressed. Activated genes, such as genes involved in redox reactions, protein folding, and DNA damage repair, are necessary to respond to stressful environmental conditions. Repressed genes, on the other hand, are genes that are normally expressed in rapidly growing cells, such genes involved in protein synthesis. The repression of these genes typically results in slow the rate of cell growth (Gasch et al., 2000). The activation and repression kinetics of ESR target genes mimics an impulse response,

resulting in the gene expression of ESR regulated genes to reach a maximal or minimal level and to subsequently adapt to a final steady state (Gasch et al., 2000; Yosef and Regev, 2011). Once the stressors are removed from the environment, the cells reactivate the downregulated ESR genes and downregulate the previously activated ESR genes. The kinetics of this second change in gene expression levels also mimic an impulse response (Gasch et al., 2000).

Another classic example of the impulse response in signal transduction is the heat shock response (HSR) in *Escherichia coli* (Guisbert et al., 2008; T Yura et al., 1993). The HSR activates a set of heat shock proteins (HSPs) through the σ^{32} transcription factor in response to an increase in temperature. Following temperature upshift from 37°F to 42°F, the level and activity of σ^{32} increase until they reach their peak at ~5 minutes post-shift, and subsequently decrease to reach a new steady state after ~10 minutes (Guisbert et al., 2008).

The molecular mechanisms behind the *E. coli* HSR impulse response have been well characterized and involve two negative feedback loops (Guisbert et al., 2008; T Yura et al., 1993). First, σ^{32} is activated by the upshift in temperature which directly increases its rate of production. The increase in σ^{32} levels results in the increased production of HSPs, including chaperones DnaKJ and GroEL/S and the protease FtsH. These newly produced chaperones and protease will bind to and degrade proteins that have become misfolded due to the increase in temperature. Eventually, σ^{32} produces DnaKJ, GroEL/S, and FtsH in excess relative to the amount of misfolded proteins. The excess chaperones then bind to and inactivate σ^{32} while FtsH targets σ^{32} for degradation. These

processes reduce the intracellular level of σ^{32} until a new steady state level of active σ^{32} is reached (Guisbert et al., 2008).

II. Pulsing

Some signal transduction systems produce multiple pulses of target gene expression in succession when exposed to a constant level of stimulus (Levine et al., 2013) (Fig. 1.1B). Although pulsing is similar to transcriptional bursting in that target gene expression levels increase and decrease repetitively, pulsing is regulated by genetic circuits that repetitively activate and deactivate pathway output regulators instead of relying on stochastic gene expression (Levine et al., 2013; Raj and van Oudenaarden, 2008). Pulsing can be beneficial during signal transduction by allowing cells to respond in ways that would be difficult to achieve with a simpler response (Levine et al., 2013).

The response of p53 to double strand breaks in mammalian cells is a well-studied example of pulsing in genetic circuits (Batchelor et al., 2008, 2009, 2011; Levine et al., 2013). In response to γ-irradiation mediated DNA damage, ATM kinase activates the tumor suppressor protein, p53, via phosphorylation. Once activated, p53 initiates two negative feedback loops by activating the E3 ubiquitin ligase Mdm2 and the phosphatase Wip1. Mdm2 targets p53 for degradation through ubiquitination, and Wip1 dephosphorylates, and therefore destabilizes, p53 (Batchelor et al., 2011; Levine et al., 2013). Wip1 also targets ATM kinase, which requires phosphorylation in order to be in the active state. Therefore, the increased activity of Wip1 silences ATM kinase, which prevents the activation of p53. If DNA damage persists in the cell, ATM kinase activates p53 once more after Wip1 expression levels have subsided. Pulsing of p53 activity results in cell-cycle arrest and DNA repair, and continues until DNA damage has been

completely repaired (Batchelor et al., 2011; Levine et al., 2013). Interestingly, ultraviolet irradiation also activates p53, but activates p53 at a constant level instead of pulsing. When ultraviolet irradiation produces ssDNA, ATR kinase activates p53 instead of ATM kinase. However, Wip1 does not act on ATR kinase. Because ATR kinase does not become dephosphorylated, p53 activity level remains relatively constant. Instead of leading to cell-cycle arrest, continual activity of p53 activates the apoptosis pathway and initiates cell death (Batchelor et al., 2011; Levine et al., 2013). Therefore, p53 can activate more than one cellular process depending on the temporal dynamics of its activation, and the kinetics of p53 activation are crucial for determining cell fate (Batchelor et al., 2008, 2009, 2011; Levine et al., 2013).

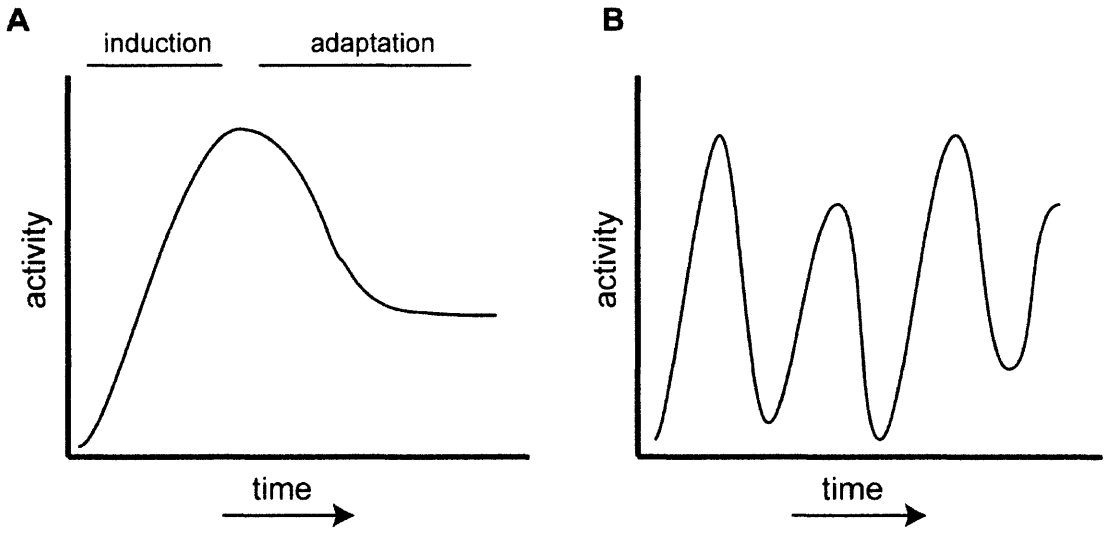

Figure 1.1: Examples of complex signal induction. A. Impulse response. Activity starts in the OFF state, increases during induction until a maximum activity level is reached, and then enters adaptation and approaches a lower steady state level. **B.** Pulsing. Activity increases and decreases periodically while stimulus is present.

Two-Component Systems - Structure and Function

Bacteria frequently sense and respond to changes in their environments through the use of two-component signal transduction systems. The canonical two-component

system involves a sensor histidine kinase that autophosphorylates in the presence of a stimulus, and then transfers the phosphoryl group to a cognate response regulator (Fig. 1.2). Once phosphorylated, response regulators are typically active, initiating cellular responses appropriate for the stimulus or environmental change that activated the system, often by changing gene expression (Stock et al., 2000). Given the wide diversity of environmental signals that most bacteria must detect, individual species typically encode dozens to hundreds of unique two-component systems, each responding to a different stimulus and activating a different cellular response (Capra and Laub, 2012; Galperin, 2005; Krell et al., 2010; Podgornaia and Laub, 2013). Although two-component pathways are often depicted as static entities that simply switch ON and OFF, recent work has demonstrated that these signaling pathways are sophisticated information-processing devices that exhibit complex dynamics upon induction.

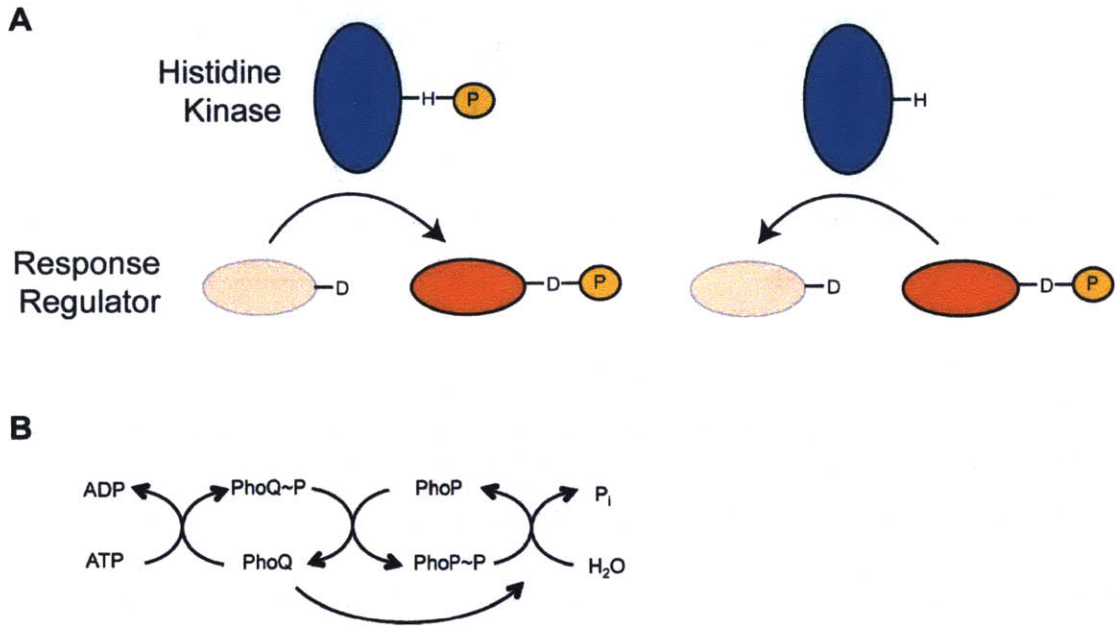

Figure 1.2: Diagram of a canonical two-component system. A. A typical histidine kinase is able to both phosphorylate (after an initial autophosphorylation step) and

dephosphorylate its cognate response regulator. Once phosphorylated, the response regulator is able to activate the output of the pathway. **B.** Diagram of the phosphotransfer steps in two-component signaling.

I. Histidine Kinases

As with many signal transduction proteins, histidine kinases are highly modular (Gao and Stock, 2009). The canonical histidine kinase contains a C-terminal catalytic and ATP binding domain and a dimerization and histidine phosphotransfer domain (Gao and Stock, 2009). Histidine kinases typically operate as homodimers, and the residues dictating dimerization specificity are located in the dimerization domain (Ashenberg et al., 2011). When stimulated, the ATP binding domain hydrolyzes ATP to ADP and transfers the resulting phosphoryl group to a conserved histidine residue in the dimerization and histidine phosphotransfer domain to form a phosphoramidate (Gao and Stock, 2009). Histidine kinase homodimers can autophosphorylate in *cis* (in which each monomeric unit phosphorylates itself) or in *trans* (in which subunits phosphorylate their binding partner), and the helix bundle loop at the base of the dimerization domain plays a role in determining which method of autophosphorylation the kinase will perform (Ashenberg et al., 2013). The N-P bond between histidine residue and the phosphoryl group is both high-energy and unstable, resulting in the phosphorylated histidines being efficient phosphotransfer intermediates (Gao and Stock, 2009).

In 75% of histidine kinases, the phosphoryl group can then be transferred directly to a conserved aspartate on the kinase's cognate response regulator (Gao and Stock, 2009). The interaction between cognate kinases and regulators are highly specific, allowing the kinase to interact only with its cognate regulator and avoid unwanted cross-talk between separate two-component systems (Capra et al., 2010, 2012a; Podgornaia

and Laub, 2013, 2015; Skerker et al., 2005, 2008). However, in the 25% of histidine kinases classified as hybrid kinases, the phosphoryl group is first transferred to an aspartate on a receiver domain fused to the C-terminus of the histidine kinase. The phosphoryl group is subsequently transferred to a histidine on a histidine phosphotransferase, and then finally transferred to the kinase's cognate response regulator (Capra and Laub, 2012; Gao and Stock, 2009). In hybrid kinases, the specificity between the kinase's dimerization and REC domain is less than in canonical two-component systems, likely resulting from spatial proximity of the two domains relaxing the selective pressure on the system to not interact with non-cognate proteins (Capra et al., 2012b).

Histidine kinases often rely on one or several input domains at their N-terminus to sense a diverse set of stimuli, such as small molecules, light, and cell envelope stress (Gao and Stock, 2009; Mascher et al., 2006; Szurmant et al., 2007). Because of the diversity in histidine kinase sensory domains, the stimuli and mechanisms of action for most histidine kinase sensory domains have not been characterized (Gao and Stock, 2009). However, several common topologies of histidine kinase sensory domains have been identified (Gao and Stock, 2009; Mascher et al., 2006). In most cases, histidine kinases have a sensory domain outside the cytoplasm between two transmembrane helices (Gao and Stock, 2009). Once the sensory domain detects its stimuli, the signal will be internalized through the membrane to stimulate the protein's enzymatic activities. Other histidine kinases have many transmembrane helices, but unlike the former case, do not contain any sensory domains between them. These histidine kinases are thought to primarily detect changes to cell membrane integrity. It is also common for histidine

kinases to exist entirely in the cytoplasm and detect intracellular signals (Gao and Stock, 2009).

Histidine kinases are also unique in that most are also functional phosphatases on their cognate response regulators (Gao and Stock, 2009; Russo and Silhavy, 1993; Stock et al., 2000) (Fig. 1.2). The dimerization and histidine phosphotransfer domain is required for functional phosphatase activity, and response regulator dephosphorylation can be performed through multiple mechanisms. In the reverse phosphotransfer method of response regulator dephosphorylation, observed in the EnvZ-OmpR two-component system, the phosphoryl group is transferred from the phosphorylated response regulator back to the conserved histidine on the dimerization and histidine phosphotransfer domain of the histidine kinase (Dutta and Inouye, 1996; Gao and Stock, 2009; Hsing and Silhavy, 1997; Zhu et al., 2000). In other two-component systems, the histidine kinase is able to dephosphorylate its response regulator in a manner independent of the conserved histidine residue, indicating that other mechanisms of histidine kinase phosphatase activity exist (Carmany et al., 2003; Chamnongpol et al., 2003; Gao and Stock, 2009). A conserved threonine located in close proximity to the phosphorylated histidine has been shown to play a role in the phosphatase activity of certain histidine kinases (Miyashiro and Goulian, 2008). To regulate the net level of phosphorylated response regulators, some histidine kinases, such as CpxA and LuxN, respond to stimuli by activating kinase activity, while others, like KdpD, respond by modulating phosphatase activity (Brandon et al., 2000; Fleischer et al., 2007; Gao and Stock, 2009; Timmen et al., 2006). Some histidine kinases, such as NtrB and PhoQ, respond to

stimuli by modulating both kinase and phosphatase reactions (Chamnongpol et al., 2003; Gao and Stock, 2009; Jiang et al., 2000).

II. Response Regulators

Like histidine kinases, proteins in the response regulator family are highly modular, and typically contain an N-terminal receiver domain and a C-terminal effector domain (Gao and Stock, 2009; Stock et al., 2000). In the canonical response regulator, the conserved N-terminal receiver domain recognizes and interacts with the cognate histidine kinase to facilitate the transfer of the phosphoryl group to the receiver domain's conserved aspartate (Gao and Stock, 2009). Recently, the first structure of a response regulator and histidine kinase interaction has been solved (Casino et al., 2009), and the interaction seems largely similar even when the interacting regions have been mutated to match the interacting regions of other two-component system cognate pairs (Podgornaia et al., 2013). Structural experiments using NMR show that receiver domains can exist in two states, one active and one inactive. Phosphorylation of the receiver domain drives the active state of the response regulator, and unphosphorylated receiver domains are typically found in the inactive state. Response regulators rapidly sample both active and inactive forms, but the most likely conformation is determined by the phosphorylation state of the protein (Gao and Stock, 2009; Gardino and Kern, 2007). When the receiver domain is the in active state, the C-terminal effector domain initiates the appropriate response of the two-component system by binding DNA and modulating gene expression, by catalyzing enzymatic reactions, or by binding another protein (Gao and Stock, 2009). In rare cases, receiver domains exist without effector domains, and are normally related to the regulation of chemotaxis (e.x., CheY, which

influences flagellar rotation by interacting with FliN in the C-ring of the flagellar motor (Sarkar et al., 2010)) or serve as phosphotransferases in complex phosphorelays (e.x., Spo0F, which phosphorylates the phosphotransferase, Spo0B (Burbulys et al., 1991)) (Gao and Stock, 2009; Hilbert and Piggot, 2004).

Response regulators play an active enzymatic role in controlling their own phosphorylation state (Gao and Stock, 2009). In addition to being phosphorylated by their cognate histidine kinases, most response regulators are phosphorylated by small, high-energy molecules found in bacterial cells, such as acetyl phosphate, although phosphorylation by these molecules has high K_m values and is slower than phosphorylation by cognate histidine kinases (Da Re et al., 1999; Gao and Stock, 2009; Lukat et al., 1992). This suggests that response regulator autophosphorylation is relatively insignificant compared to traditional histidine kinase dependent phosphotransfer, but it has been shown that acetyl phosphate can slightly perturb response regulator phosphorylation state under certain physiological conditions (Gao and Stock, 2009; Wolfe, 2005). Response regulators can also be phosphorylated by non-cognate histidine kinases. However, non-cognate kinases phosphorylate response regulators at slow rates relative to cognate kinases, and the phosphatase activity of cognate kinases typically prevents accumulation of unwanted cross-talk between systems (Siryaporn and Goulian, 2008).

Response regulators also have a rate of intrinsic autodephosphorylation (Gao and Stock, 2009). Because phosphorylated aspartates are highly unstable, typically having half-lives of six hours in typical conditions *in vitro*, the phosphorylated aspartate on response regulators passively lose their phosphoryl group (Gao and Stock, 2009).

Additionally, response regulators can actively catalyze autodephosphorylation to increase the phosphoryl group's detachment rate (Gao and Stock, 2009). Lastly, some response regulators are dephosphorylated by proteins other than their cognate histidine kinases (Gao and Stock, 2009; Perego, 2001; Zhao et al., 2002).

Dynamics of Two-Component Systems

I. Temporal Dynamics

Although bacterial signaling pathways typically involve fewer components than their eukaryotic counterparts, they still possess features that enable them to regulate downstream targets with a high degree of sophistication and control. One such feature, as discussed above, is the dual kinase and phosphatase activity, or bifunctionality, of histidine kinases. Early studies demonstrated that, in addition to phosphorylating their cognate response regulators when a stimulus is present, most histidine kinases also act as phosphatases for the same response regulators in the absence of stimulus (Hsing et al., 1998; Huynh et al., 2010; Igo et al., 1989; Russo and Silhavy, 1993). Thus, the phosphorylation level of a response regulator is ultimately controlled by the balance of these two activities. If the rate of either the kinase or phosphatase reaction is altered, the steady-state level of active response regulator will change accordingly (Gao and Stock, 2013a; Hsing et al., 1998). The phosphatase activity of histidine kinases also helps to prevent cross-talk between different pathways, suppressing the activation of a response regulator by a non-cognate histidine kinase or by promiscuous phosphodonors such as acetyl-phosphate (Boll and Hendrixson, 2011; Groban et al., 2009; Siryaporn and Goulian, 2008). Recent work has further proposed that the bifunctionality of histidine kinases may serve to suppress latent bistability in two-

component pathways (Ram and Goulian, 2013). In *Escherichia coli*, a variant PhoQ kinase engineered to selectively lack phosphatase activity led to bistability in the levels of its phosphorylated partner, PhoP, in individual cells, with some cells switching to and staying in the ON state, even once the stimulus was removed, an effect that severely undermined fitness.

Other features of two-component pathways that yield complex temporal dynamics are positive and negative feedback loops. Using reporter genes activated by a given response regulator or direct measurements of mRNAs from target genes, several groups have observed impulse responses, or partial adaptation (Gao and Stock, 2013a; Hutchings et al., 2006; Shin et al., 2006; Yamamoto and Ishihama, 2005). Instead of increasing monotonically to a new steady-state level after exposure to inducing conditions, the gene expression driven by a response regulator will first increase to a high, maximal level, and subsequently decrease to reach a new steady-state level intermediate to the initial and maximal levels.

The molecular basis of partial adaptation in two-component systems is unclear, but likely involves feedback loops. The *Salmonella* PhoQ-PhoP system, which responds to low extracellular magnesium and antimicrobial peptides, involves a positive feedback loop wherein phosphorylated PhoP positively autoregulates *phoPQ* transcription. One early study suggested that eliminating this positive feedback loop, by constitutively expressing *phoP*, diminished adaptation, or impulse-like behavior (Shin et al., 2006). However, mathematical modeling has indicated that negative feedback is ultimately required for an impulse response of two-component systems (Ray and Igoshin, 2010) with subsequent work suggesting two potential sources of such feedback. One model

posits that the PhoQ kinase retains ADP in its catalytic domain after autophosphorylation, promoting the phosphatase state of PhoQ and driving a decrease in phosphorylated PhoP (Yeo et al., 2012). Whether the ADP to ATP exchange rate for PhoQ is low enough *in vivo* that ADP would be retained for long periods of time is unclear; however, at least *in vitro*, histidine kinases likely undergo multiple rounds of autophosphorylation and phosphotransfer, implying high rates of nucleotide exchange. Another potential source of negative feedback for the PhoQ-PhoP system was revealed with the discovery of the small membrane protein MgrB (Lippa and Goulian, 2009). Transcription of *mgrB* is directly stimulated by phosphorylated PhoP, and MgrB interacts with PhoQ in the membrane to reduce output from the PhoQ-PhoP system. PhoQ also interacts with another small protein, SafA, although it activates PhoQ autophosphorylation only under certain conditions in response to a different two-component pathway and thus does not form a feedback loop (Eguchi et al., 2012a).

How positive feedback loops influence the steady-state output of two-component pathways is still unresolved, and may differ between individual systems. For the PhoQ-PhoP system, strains with and without positive autoregulation have similar steady-state outputs over a large range of input stimuli, even though a strain lacking positive autoregulation has lower total levels of PhoP than the wild type (Miyashiro and Goulian, 2008; Shin et al., 2006). By contrast, for the *E. coli* PhoR-PhoB pathway, autoregulation plays a critical role in tuning both total PhoB levels and pathway output (Gao and Stock, 2013b). In phosphate-replete conditions, PhoB levels are low. As cells are depleted of inorganic phosphate, PhoR activates PhoB, which drives increased expression of PhoR and PhoB, leading to higher PhoB levels and activation of the full Pho regulon.

Strikingly, the level of PhoB achieved through positive autoregulation is close to optimal. Forcing higher overall levels of PhoB does not significantly increase the amount of phosphorylated PhoB, and leads to the selection of mutations that restore a lower, optimal level of PhoB (Gao and Stock, 2013b).

Even more complex temporal dynamics have been described for so-called phosphorelays. Although the majority of two-component pathways involve a single histidine kinase and its cognate response regulator, phosphorelays involve additional components: the phosphoryl group from a kinase is first transferred to one response regulator, then to a histidine phosphotransferase, and finally to a terminal response regulator. One such phosphorelay regulates the initiation of sporulation in *Bacillus subtilus* and involves five different kinases, each of which can phosphorylate the response regulator Spo0F. The phosphotransferase Spo0B then shuttles phosphoryl groups from Spo0F to Spo0A, the master regulator of sporulation initiation (Hilbert and Piggot, 2004). Strikingly, upon shift to nutrient-limited conditions, Spo0A phosphorylation levels exhibit a series of pulses over the course of several cell cycles until sporulation is ultimately initiated (Levine and Elowitz, 2014; Levine et al., 2012; Veening et al., 2009). Each pulse becomes successively larger in amplitude, likely until a threshold of phosphorylated Spo0A is reached, which then allows commitment to sporulation. Which regulatory features of the sporulation pathway drive these pulses is unclear. There are several different feedback loops involving Spo0A and various phosphorelay components, but eliminating individual feedback loops did not disrupt pulsatile behavior.

The biological function of Spo0A pulsing is also not yet clear, although the gradual increase in magnitude of the pulses may represent a time-delay mechanism. Because sporulation is a costly, irreversible decision, cells may use the time it takes to ramp up Spo0A pulses to ensure that prevailing conditions warrant a commitment to sporulation. Additionally, the gradual accumulation of phosphorylated Spo0A may help coordinate the expression of genes needed for sporulation initiation (Fujita and Losick, 2005). Genes with high affinity Spo0A binding sites are expressed early when active Spo0A first begins to accumulate, with lower affinity promoters expressed later as active Spo0A accumulates to higher levels (Fujita et al., 2005).

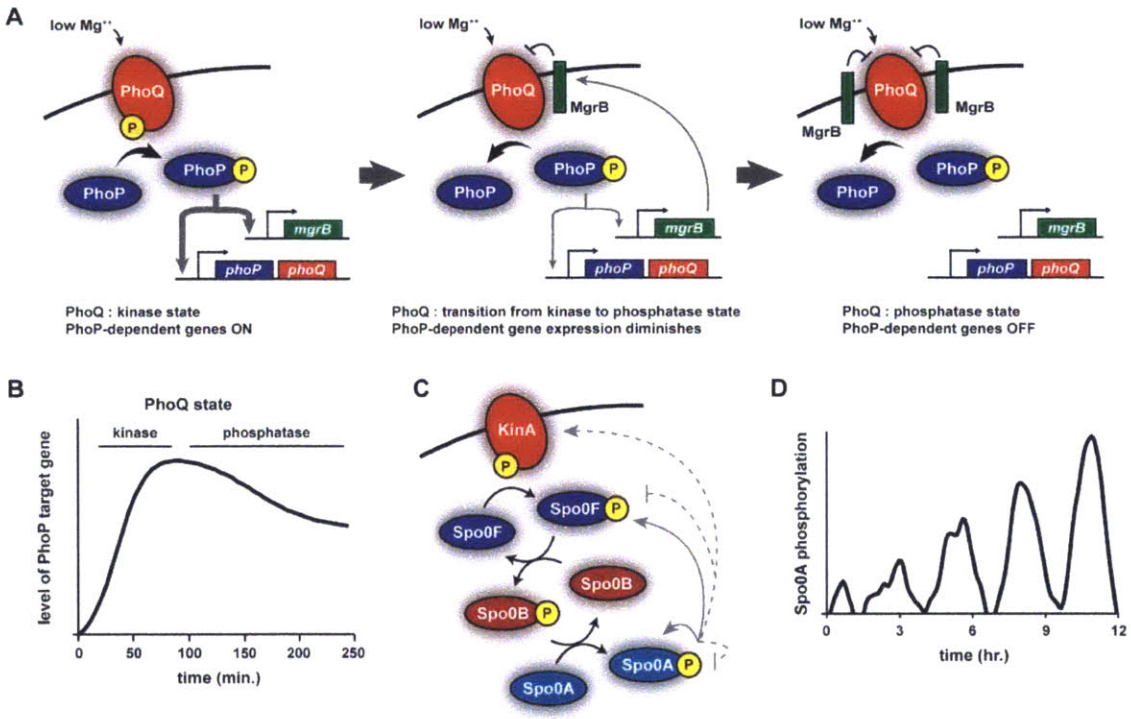

Figure 1.3: Temporal dynamics of two-component systems. (A) PhoQ-PhoP is a canonical two-component system that is activated by low extracellular Mg^{++}, changes in pH, and certain antimicrobial peptides. Upon sensing a stimulus, PhoQ is initially in the kinase state, driving PhoP phosphorylation and the increased expression of PhoP target genes, including *phoPQ* and *mgrB* (left). As MgrB accumulates, it helps drive a switch of PhoQ from the kinase to the phosphatase state (middle). Eventually PhoQ is predominantly a phosphatase, limiting expression of PhoP-

dependent genes (right). (B) This negative feedback loop mediated by MgrB likely accounts for the partial adaptation in pathway output. (C) Sporulation in *B. subtilis* is initiated by a four step phosphorelay. KinA (shown) or KinB/C/D/E first autophosphorylate; a phosphoryl group is then transferred to the response regulator Spo0F, then to the histidine phosphotransferase Spo0B, and finally to Spo0A (black arrows). Phosphorylated Spo0A directly promotes expression of itself and Spo0F (solid grey arrows), and indirectly promotes the production of KinA (dashed grey arrow). Phosphorylated Spo0A also indirectly drives dephosphorylation of itself and Spo0F (dashed grey lines). (D) Somehow these feedback loops produce pulses of phosphorylated Spo0A in sporulation-inducing conditions. Each pulse exhibits higher levels until a threshold level is reached to initiate sporulation.

It is tempting to speculate that the pulsatile dynamics of Spo0A stem in part from the four-step architecture of the phosphorelay, as such pulsing behavior has not been seen yet with canonical two-component systems. Alternatively, the multi-step phosphorelay could simply enable the integration of multiple signals by providing more points of control. The phosphorelay may also represent a noise generator (Chastanet et al., 2010; Jong et al., 2010), such that only some cells in a population ultimately achieve the levels of phosphorylated Spo0A needed for sporulation to initiate. Whatever the case, further studies of the *B. subtilis* sporulation phosphorelay promise to provide important insights into the temporal dynamics of two-component pathways.

Finally, we note that the temporal dynamics of two-component signaling pathways are often inferred from the behavior of downstream reporter genes, but this approach is inherently indirect and potentially misleading. For example, in *E. coli*, two different PhoB-dependent reporters yield different temporal profiles of activation, likely reflecting differential regulation by other transcription factors (Kinoshita et al., 2009). A more direct method for measuring response regulator phosphorylation levels *in vivo* involves Phos-Tag technology, in which the phosphorylated and unphosphorylated forms of a regulator can be distinguished in protein gels (Kinoshita et al., 2009). This approach has enabled the direct measurement of both total and phosphorylated PhoB levels during phosphate

starvation in *E. coli*. Importantly, this study demonstrated that only ~30% of PhoB molecules are phosphorylated during the phosphate starvation response. This set point is, in part, a consequence of the higher total levels of PhoB compared to its kinase PhoR during phosphate limitation, and high regulator:kinase ratios are a common feature of two-component pathways (Cai and Inouye, 2002; Li et al., 2014; Yeo et al., 2012).

II. Evolutionary Dynamics

In addition to complex temporal dynamics, two-component signaling pathways also exhibit a striking degree of evolutionary change and plasticity. Over the course of evolution, two-component systems have grown dramatically in number within many bacterial genomes, enabling organisms to sense and respond to diverse environmental stimuli. This expansion has been driven primarily through gene duplication and the subsequent divergence of paralogous systems (Alm et al., 2006). However, the individual mutations responsible for establishing new pathways post-duplication and the order in which these mutations must occur remain poorly defined. Recent work has begun to explore these issues, combining phylogenetic analyses, molecular genetics, biochemistry, and mathematical modeling.

A key step in the divergence of two-component genes post-duplication is the establishment of insulated pathways, as extant histidine kinases rarely phosphorylate non-cognate response regulators *in vivo*, even those derived from recent duplication events (Grimshaw et al., 1998; Siryaporn and Goulian, 2008; Skerker et al., 2005). Direct molecular recognition is the primary mechanism by which histidine kinases correctly phosphorylate their cognate response regulators. Phosphoprofiling

experiments *in vitro* demonstrated that histidine kinases will specifically phosphorylate, and dephosphorylate, their cognate response regulators relative to all non-cognate substrates on short, biologically relevant timescales (Skerker et al., 2005). The intrinsic ability of a histidine kinase to discriminate its cognate partner from all non-cognate partners implies the existence of specificity-determining residues in each protein. Such residues presumably must coevolve to maintain the interaction of cognate proteins. Analyses of amino-acid coevolution in large sets of cognate kinase-regulator pairs from across the bacterial kingdom have revealed a small set of putative specificity residues in each protein (Skerker et al., 2008; Weigt et al., 2009). These residues were experimentally shown to dictate protein-protein interaction specificity through the rational reprogramming of two-component signaling proteins (Capra et al., 2010; Skerker et al., 2008). For example, mutating the specificity residues of the histidine kinase EnvZ to match those of RstB, produced a mutant EnvZ that specifically phosphorylated RstA, the cognate regulator of RstB, while abolishing interaction with its usual partner, OmpR.

The mapping of specificity-determining residues in two-component pathways has enabled studies of how specificity evolves post-duplication (Capra et al., 2012a). Phylogenetic and sequence analyses have revealed that specificity residues, which are relatively static in the absence of gene duplication, exhibit a burst of diversification approximately coincident with a pathway duplication event. Typically, both a kinase and regulator diversify, coevolving to retain their interaction while becoming insulated from their duplicated counterparts. Once insulated pathways are established, specificity

residues are again relatively static, thereby preserving interactions between cognate partners.

This process of pathway divergence and insulation can involve changes in one or both pathways produced by a duplication event. Additionally, in some cases, insulation can require changes to yet other pathways (Capra et al., 2012a). For instance, in α-proteobacteria, the NtrB-NtrC pathway was duplicated with subsequent divergence of one copy yielding the extant NtrX-NtrY pathway. Phylogenetic analyses indicated that the emergence of NtrX-NtrY likely produced cross-talk with another, unrelated two-component pathway, the PhoR-PhoB system. Consequently, the α-proteobacterial PhoR and PhoB accumulated substitutions in their specificity residues that retained a PhoR-PhoB interaction while eliminating cross-talk between PhoR and NtrY. Consistent with this model, restoring the ancestral specificity residues to an extant α-proteobacterial PhoR from *Caulobacter crescentus* led to increased cross-talk with NtrY *in vitro* and put *Caulobacter* cells at a selective disadvantage relative to the wild type in conditions that activate PhoR. Collectively, these observations demonstrated that the avoidance of cross-talk is a major selective pressure for two-component pathways, driving the diversification of specificity residues to produce insulated pathways, particularly after gene duplication events.

Although cross-talk is selected against, it is unavoidable immediately after pathway duplication, raising the question of what steps are taken, and in what order, to create a new pathway. Recent mathematical modeling has suggested that changes to specificity residues that eliminate cross-talk should occur first, followed by acquisition of new input/output functionalities, assuming cells must follow neutral or near-neutral

mutational trajectories (Rowland and Deeds, 2014). This work also highlights a major gap in our understanding of two-component pathway evolution, namely how histidine kinases gain new input functions and how response regulators gain new output functions. Domain shuffling likely plays a prominent role, but experimental studies of this process are an important future challenge.

Some non-canonical two-component pathways, particularly those involving so-called hybrid kinases, do not face the same evolutionary pressure to maintain phosphotransfer specificity as do canonical pathways. Hybrid kinases are histidine kinases that phosphotransfer intramolecularly to a response regulator-like receiver domain. The phosphoryl group from the receiver domain can then be passed to a histidine phosphotransferase, or in some cases, enable the kinase to autophosphorylate again and phosphotransfer to a soluble response regulator. Nearly 25% of all histidine kinases are hybrids (Wuichet and Zhulin, 2010) and phosphotransfer profiling experiments have demonstrated that their phosphotransfer specificity is not driven by molecular recognition as their kinase domains alone often phosphorylate many soluble response regulators. Instead, phosphotransfer specificity for hybrid kinases is enforced by spatial proximity; the high effective concentration of the tethered receiver domain ensures intramolecular phosphotransfer (Capra et al., 2012b; Townsend et al., 2013). Consequently, duplicated hybrid kinases are not under the same strong selective pressure to diversify their specificity residues.

Although the evolution of two-component pathways often involves the production of two insulated pathways, there are cases in which components are added to, or integrated with, an existing pathway, yielding novel pathway architectures. A primary example is

the *B. subtilis* sporulation phosphorelay in which five separate kinases, KinA/B/C/D/E, can each initiate a four-step phosphotransfer pathway culminating in phosphorylation of Spo0A (Burbulys et al., 1991). The architecture of this phosphorelay is dictated by the preference of the kinases for phosphorylating Spo0F relative to Spo0A (Grimshaw et al., 1998). Presumably, the *B. subtilis* sporulation phosphorelay evolved from an ancient, canonical two-component system, but how, at a molecular level, did this occur?

One possibility is that an ancestral sporulation pathway involved kinases that directly activated an ancestral Spo0A ortholog with subsequent integration of the two middle components. Such a scenario would have required a change in kinase specificity to prefer the new Spo0F-like regulator over Spo0A. Interestingly, there are extant species, including various *Clostridia* species, that lack Spo0F and Spo0B orthologs and that initiate sporulation through a more canonical two-component pathway (Galperin et al., 2012). For example, in *C. botulinum* and *C. acetobutylicum*, several histidine kinases can directly phosphorylate their respective Spo0A orthologs (Steiner et al., 2011; Wörner et al., 2006). Additionally, the *C. acetobutylicum* kinases can phosphorylate *B. subtilis* Spo0A but not Spo0F, while *B. subtilis* KinA cannot phosphorylate *Clostridium* Spo0A. These observations may imply that *Bacilli* species gained the intermediate components Spo0F and Spo0B. However, it could also be that the phosphorelay was present in a common ancestor of the *Bacilli* and *Clostridia* with subsequent loss of the middle two pathways components in *Clostridia*. Additionally, we note that the *Clostridia* kinases are not obvious homologs of the *Bacilli* kinases KinA-E suggesting that *Clostridia* species may have lost all components except Spo0A and then co-opted other kinases to directly phosphorylate Spo0A.

An alternative possibility for the origin of the sporulation phosphorelay is that it arose from the joining of two previously independent systems, such that the response regulator of one pathway became a phosphodonor for the other histidine kinase, which may have then lost its ability to autophosphorylate. Notably, the histidine phosphotransferase Spo0B, like many other phosphotransferases, structurally resembles a histidine kinase, but has lost the ability to autophosphorylate (Zapf et al., 2000).

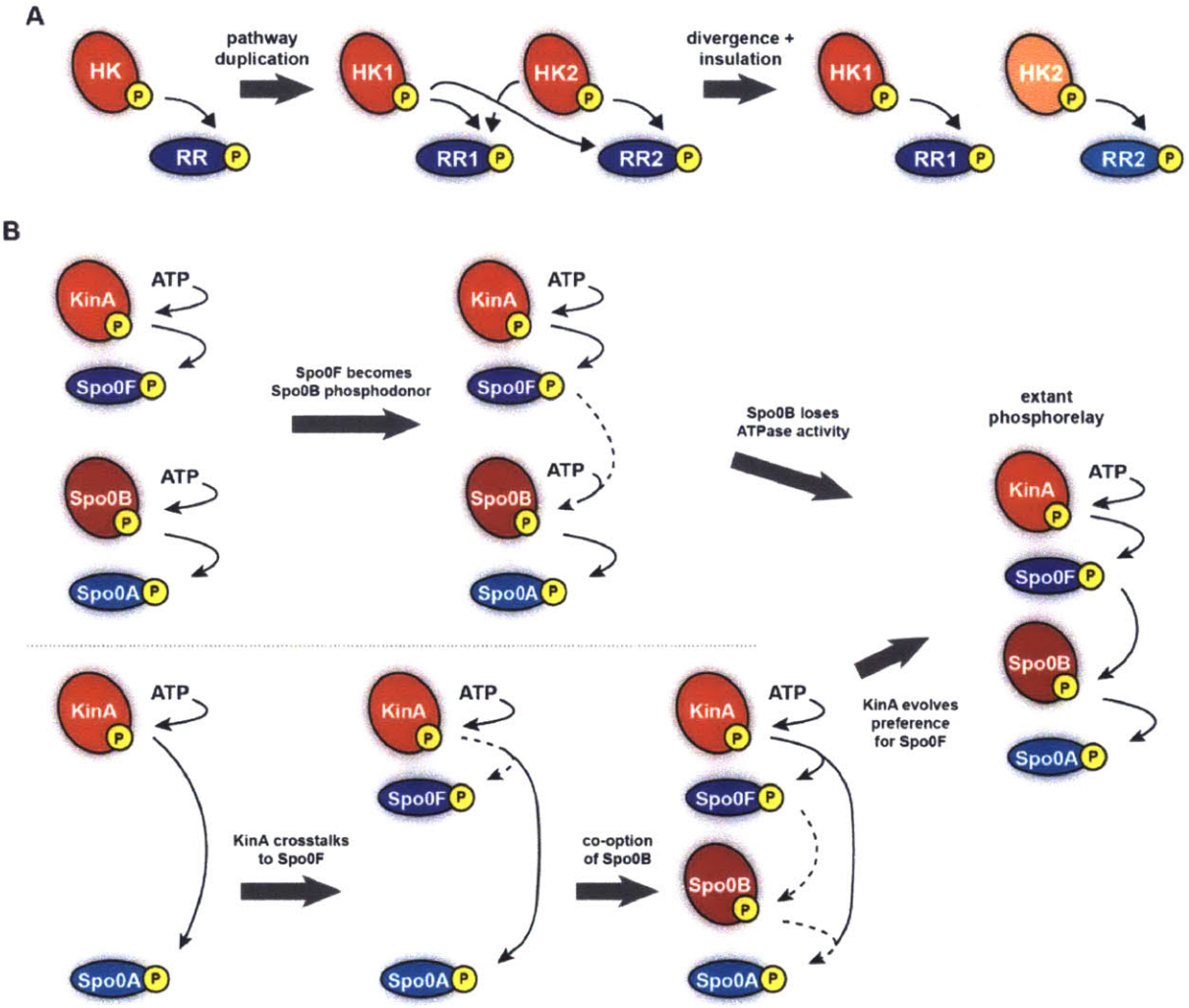

Figure 1.4: Evolution of two-component systems. (a) Canonical two-component systems expand and diversify through gene duplication and subsequent divergence. After a pathway duplication, the specificity residues on the two identical systems diverge, such that each pathway continues to interact while reducing cross-talk between the two systems. (b) Two possible model for the origin of the phosphorelay driving *B. subtilis* sporulation. (top) Two canonical two-component pathways could have merged, with the response regulator of one pathway becoming the phosphodonor to another histidine kinase which then lost autophosphorylation activity. (bottom) KinA could have evolved to cross-talk with an existing response regulator with subsequent co-option of Spo0B as a histidine phosphotransferase and changes in KinA to prefer Spo0F over Spo0A.

There are yet other possible scenarios for how the sporulation phosphorelay arose, and exactly what happened remains uncertain. More in-depth, detailed phylogenetic studies

are needed, along with better characterizations of the pathways controlling Spo0A phosphorylation in various Firmicutes, the clade containing *Bacilli* and *Clostridia*. Reconstructing the origins of the phosphorelay promises to reveal the evolutionary dynamics that shape and influence all two-component pathways, including their connectivities and functions.

The PhoQ-PhoP System

PhoQ-PhoP is a widely studied two-component system in both *E. coli* and *Salmonella enterica* that regulates the response to low Mg^{++} environments, and, in the case of *Salmonella*, the expression of virulence related genes (Groisman, 2001; Kato and Groisman, 2008). In response to stimulus, the histidine kinase PhoQ autophosphorylates and subsequently phosphotransfers to its cognate response regulator, PhoP. In the active phosphorylated state, PhoP acts as a transcription factor and modifies the gene expression of approximately 3% of the genome (Kato and Groisman, 2008). The PhoQ-PhoP pathway is a useful and interesting model two-component system due to it having an experimentally tractable stimulus (Mg^{++}), and because of the many regulatory loops and cascades within the PhoP regulon. As discussed in Chapter II, the regulatory features of the PhoQ-PhoP pathway result in impulse kinetics of PhoP target genes during Mg^{++} starvation (Shin et al., 2006).

I. The PhoP regulon

Given that the PhoQ-PhoP pathway responds to low extracellular Mg^{++}, it is unsurprising that PhoP activates many genes that are necessary for survival in Mg^{++} starvation conditions (Groisman, 2001). PhoP directly activates the expression of the P-type ATPases that serve as Mg^{++} transporters, MgtA (in both *E. coli* and *Salmonella*)

and MgtB (only found in *Salmonella*) (Groisman, 2001; Smith and Maguire, 1998). These Mg^{++} transporters are vital for cell growth in Mg^{++} starvation conditions, as the loss of *phoP*, *mgtA*, or *mgtB* confers growth defects in low Mg^{++} culture (Groisman, 2001; Soncini et al., 1996). Although MgtA and MgtB are share 50% sequence identity, the two Mg^{++} transporters appear to not be entirely redundant and serve different physiological roles. For example, low pH prevents *mgtA* transcription, but does not change levels of MgtB production (Groisman, 2001; Moncrief and Maguire, 1998).

Induction of the PhoQ-PhoP system also helps bacteria resist antimicrobial peptides produced by a wide range of organisms, ranging from other bacteria to higher eukaryotes (Groisman, 2001). In *Salmonella,* the PhoQ-PhoP system responds to antimicrobial peptides by activating the production of proteins that both increase the bacteria's resistance to the peptide, as well as proteins that directly disable the antimicrobial peptide. For example, a protein belonging to the former category is PagP, an outer membrane protein that modifies LPS (Bishop et al., 2000; Groisman, 2001). This modification confers resistance to the human α-helical peptide C18G, and *Salmonella* lacking *pagP* are more sensitive to this peptide (Groisman, 2001; Guo et al., 1998). Futhermore, C18G is cleaved by the PhoP regulated protease PgtE, and overexpression of *pgtE* confers resistance to C18G (Groisman, 2001; Guina et al., 2000). The PhoQ-PhoP system confers resistance to antimicrobial peptides to *E. coli* as well, as *E. coli phoP* mutants have increased sensitivity to peptides magainin 2 and mastoparan (Groisman, 2001; Groisman et al., 1992).

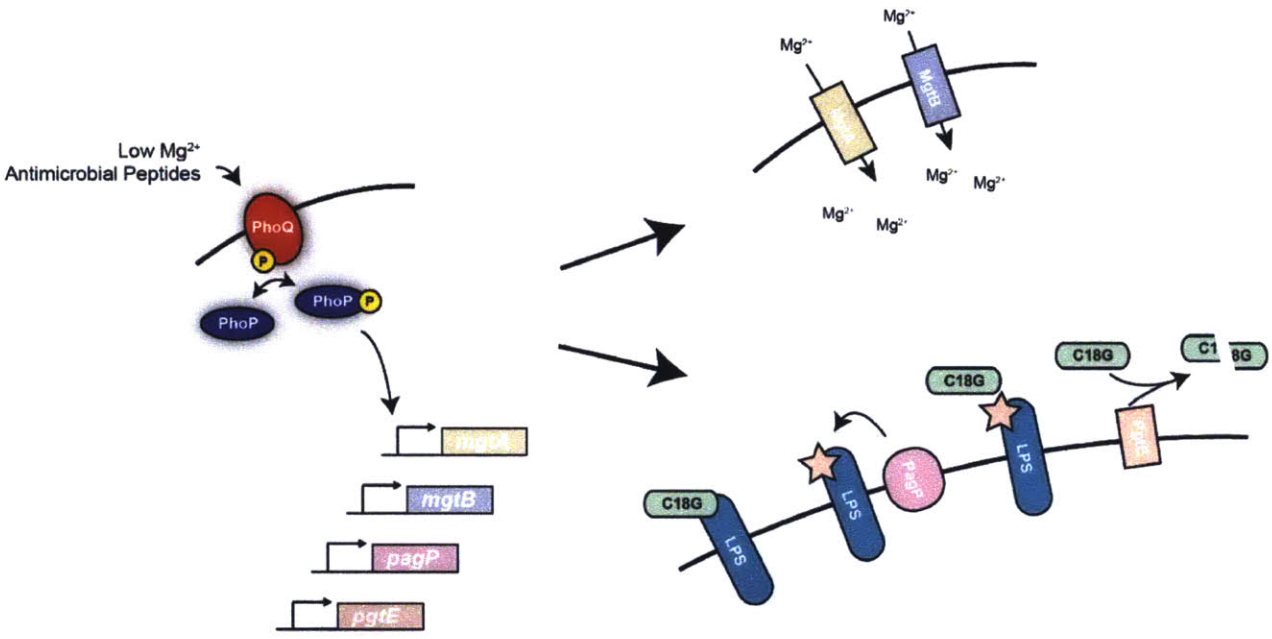

Figure 1.5: PhoQ-PhoP regulates the regulation of Mg^{++} transporters and antimicrobial peptide resistance factors. MgtA and MgtB are transmembrane P-type ATPases that import Mg^{++} into the cell. PagP confers resistance to antimicrobial peptide C18G by modifying LPS to prevent C18G binding. PgtE is a transmembrane protease that cleaves C18G.

The PhoQ-PhoP system is also known for its ability to regulate the output of other two-component systems (Groisman, 2001). In *Salmonella*, the PmrB-PmrA system responds to low pH and extracellular Fe^{3+}, and confers resistance to the antibiotic polymyxin B and Fe^{3+} (Chen and Groisman, 2013; Kato and Groisman, 2008). Once the transmembrane histidine kinase PmrB senses pH or Fe^{3+} changes in the environment, it phosphorylates its cognate response regulator, PmrA, thereby allowing it to activate the PmrA transcriptional regulon. PmrB is bifunctional, and can dephosphorylate PmrA in the absence of stimulus. The PhoQ-PhoP system can regulate levels of PmrA phosphorylation by initiating the production of PmrD. When activated, PhoP increases the transcription of *pmrD*, a gene that encodes a protein that selectively binds to the phosphorylated form of PmrA and prevents dephosphorylation through PmrB. Therefore, when PmrD levels are sufficiently high, phosphorylated PmrA is shielded

from PmrB dependent dephosphorylation and the net level of phosphorylated PmrA is increased (Chen and Groisman, 2013). In other bacteria, more direct cross-regulation exists between the PhoQ-PhoP and PmrB-PmrA systems. In *Yersinia*, phosphorylated PhoP can directly increase activity of the promotors of a subset of the PmrA regulon without the need for an intermediate regulator such as PmrD (Chen and Groisman, 2013; Kato and Groisman, 2008).

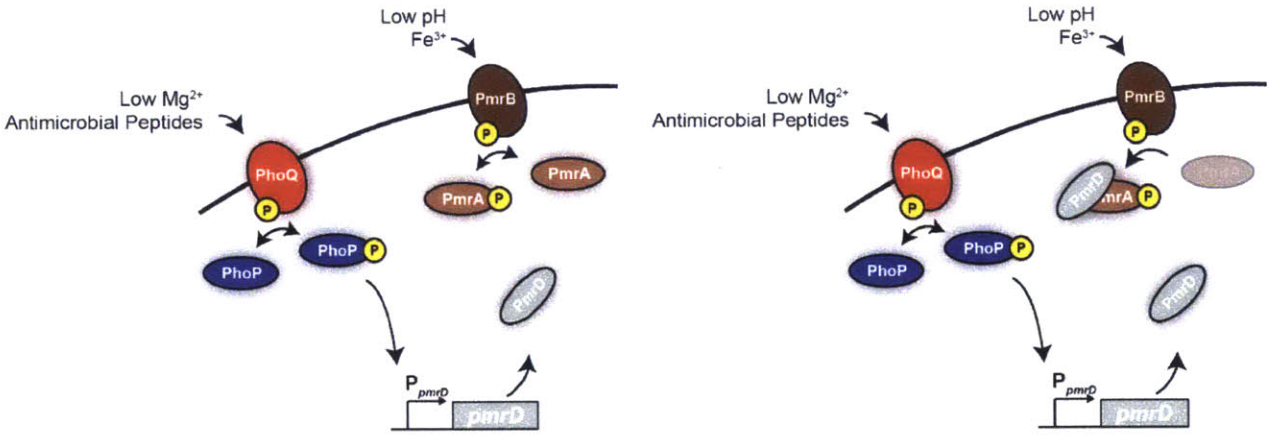

Figure 1.6: PhoQ-PhoP regulates the phosphorylation state of response regulator PmrA. The PmrB-PmrA two-component system responds to changes in extracellular pH and Fe^{3+}. When the PhoQ-PhoP system is activated, it activates the production of PmrD. PmrD selectively binds to the phosphorylated form of PmrA, thereby preventing it from being dephosphorylated by PmrB.

II. PhoQ-PhoP pathway regulation

PhoQ is a canonical histidine kinase that actively phosphorylates and dephosphorylates PhoP depending on the level of extracellular stimulus (Groisman, 2001; Kato and Groisman, 2008). PhoQ has two transmembrane regions flanking a 146 amino acid long periplasmic region, as well as a cytoplasmic region containing the catalytic ATP binding domain as well as the dimerization and histidine phosphotransfer domain. The later domain contains the conserved histidine that is first phosphorylated and subsequently phosphotransfers to PhoP (Castelli et al., 2000; Chamnongpol and Groisman, 2000;

Kato and Groisman, 2008) in response to activating stimuli. Signals known to activate the PhoQ-PhoP system include low extracellular Mg^{++} (García Véscovi et al., 1996), certain antimicrobial peptides (Bader et al., 2005), and low pH (Prost et al., 2007). Because of its experimental tractability, low Mg^{++} is often used as the stimulus for PhoQ when studying the pathway *in vivo*.

PhoP is an OmpR-like response regulator that contains a N-terminal receiver domain and a C-terminal helix-turn-helix DNA binding motif (Kato and Groisman, 2008; Shin and Groisman, 2005). Once phosphorylated, the active PhoP dimerizes and modifies gene expression by directly binding to the gene promoters within its regulon. PhoP promoters in both *Salmonella* and *E. coli* contain a region known as the PhoP box, a specific consensus motif containing (T/G)GTTA-5 bp-(T/G)GTTTA (Kato and Groisman, 2008; Zwir et al., 2005). The PhoP box can be found in either orientation and is most often found 11-13 bp upstream of the -10 region (Kato and Groisman, 2008).

The PhoQ-PhoP system contains a positive feedback loop caused by phosphorylated PhoP enhancing the expression of the *phoPQ* operon (Kato and Groisman, 2008; Miyashiro and Goulian, 2008; Shin et al., 2006). The *phoPQ* operon is transcribed by two promoters; the constitutively active P2 promoter and the PhoP dependent P1 promoter. Because of the existence of the constitutively active P2 promoter, basal levels of PhoQ and PhoP exist in the cell at non-stimulating conditions. Once the system is stimulated, phosphorylated PhoP initiates additional transcription of *phoPQ*, thereby increasing the cellular levels of both PhoQ and PhoP. Despite this positive feedback, the steady state activity level of the PhoQ-PhoP system is similar both with and without the P1 promoter in *Salmonella* and *E. coli* (Miyashiro and Goulian, 2007, 2008; Shin et

al., 2006). However, in *Salmonella*, the positive feedback in the PhoQ-PhoP system has been shown to be a necessary factor in creating an impulse response for PhoP targets when cells transition from a high- to low-Mg^{++} environment (Shin et al., 2006).

Two small membrane proteins directly regulate the activity of the PhoQ-PhoP system, one that represses the system, MgrB, and another that activates the output of the pathway, SafA (Eguchi et al., 2007; Lippa and Goulian, 2009). The role of MgrB, a 47 amino acid peptide, on PhoQ-PhoP regulation was identified by a screen that looked for negative feedback within the PhoQ-PhoP regulon. Single knock-out mutations of highly transcribed PhoP target genes were constructed and subsequently analyzed to determine if the steady state level of the PhoQ-PhoP pathway output was effected. The *mgrB* deletion was the only deletion to impact the pathway output of the PhoQ-PhoP system, and the deletion resulted in increased pathway output for both low and high stimulus conditions. By fusing MgrB to GFP, it was revealed that MgrB localizes to the inner membrane. Furthermore, bacterial two-hybrid studies showed that MgrB and PhoQ interact directly in the periplasm, and that mutations to the periplasmic domain of MgrB disrupt repression of the PhoQ-PhoP system. Therefore, MgrB appears to act by repressing the PhoQ-PhoP pathway at the level of PhoQ, and either represses the PhoQ kinase reactions (either at autophosphorylation or phosphotransfer steps), or stimulates PhoQ's ability to dephosphorylate PhoP (Lippa and Goulian, 2009). Due to the small size of the *mgrB* gene and the highly mutable transmembrane domain, it is difficult to see how many homologous PhoQ-PhoP systems contain a functioning MgrB. However, MgrB has been shown to repress the PhoQ-PhoP system in *E. coli*,

Samonella typhimurium and *Yersinia pestis* in laboratory settings (Lippa and Goulian, 2009).

Recently, MgrB has been shown to have an important role in infection and antibiotic resistance (Cannatelli et al., 2013, 2014; Yigit et al., 2001). *Klebsiella pneumoniae* strains that produce KPC-type carbapenemases (KPC-KP) first appeared in the late 1990s, and can result in difficult to treat infections in humans (Cannatelli et al., 2013). Infections of these strains are typically resistant to most antibiotics and have high mortality rates. Colistin, an antibiotic produced by *Paenibacillus polymyxa*, has been the antibiotic with the most success in treating KPC-KP infections. However, recently discovered KPC-KP variants have been showing resistance to colistin (Bogaerts et al., 2010; Cannatelli et al., 2014). Resistance to colistin can be acquired by a modification of lipopolysaccharide that is positively regulated by the PhoQ-PhoP system (Cannatelli et al., 2013; Cheng et al., 2010; Helander et al., 1996), and a common mechanism for KPC-KP to acquire colistin resistance among clinical isolates is to inactivate MgrB (Cannatelli et al., 2014). It has further been shown that inactivation of *K. pneumoniae mgrB* in laboratory settings leads to the upregulation of PhoP targets, including the *pmrHFIJKLM* operon, a required component in colistin resistance (Cannatelli et al., 2013).

SafA, the transmembrane protein that activates the PhoQ-PhoP system, is transcriptionally regulated by the EvgS-EvgA two-component system (Eguchi et al., 2007). EvgS is a canonical transmembrane histidine kinase that responds to mildly acidic conditions (pH ~5-6.7) and confers acid and drug resistance to *E. coli* (Nishino and Yamaguchi, 2002). At neutral pH in rich media, the EvgS-EvgA system is normally

turned to the OFF state. The *evgS1* allele is constitutively activated, and it also activates the PhoQ-PhoP system at both high and low levels of Mg^{++}. Therefore, it was hypothesized that there existed a link from the EvgS-EvgA system that activates the PhoQ-PhoP system. To find this connection, a screen of EvgA regulated genes was performed to assess their activities on the output of the PhoQ-PhoP system. The only EvgS-EvgA target found to activate PhoQ-PhoP was SafA (Eguchi et al., 2007).

Like MgrB, SafA interacts directly with PhoQ as shown through bacterial two-hybrid assays (Eguchi et al., 2007). SafA has three predicted domains; an N-terminal cytoplasmic domain, a transmembrane domain, and a C-terminal periplasmic domain, and all three regions appear to be somewhat responsible in PhoQ binding (Eguchi et al., 2012). Various SafA truncations were tested for their ability to interact with PhoQ via bacterial two-hybrid assays, and a SafA truncation containing only the transmembrane domain was able to interact with PhoQ at approximately 50% levels relative to the entire SafA protein. However, SafA truncations containing the transmembrane domain as well as either the cytoplasmic or periplasmic domains conferred about 75% interaction relative to whole-length SafA, indicating that either domain increases binding to PhoQ (Eguchi et al., 2012).

Although all three domains of SafA can directly interact with PhoQ, it was unclear which region of SafA was functionally active. NMR analysis shows that SafA interacts directly with the sensory domain of PhoQ in the periplasm (Eguchi et al., 2012). Additionally, abolishing either PhoQ(D179) or SafA(R53), both residues found in the periplasm, disrupt the ability of SafA to positively regulate the PhoQ-PhoP system (Eguchi et al., 2012). This suggests that the interaction between PhoQ and SafA in the periplasm is

essential for complete SafA activity. Furthermore, adding a synthesized version of the C-terminal periplasmic domain of SafA to growing *E. coli* in liquid media is sufficient to stimulate the PhoQ-PhoP system (Eguchi et al., 2012).

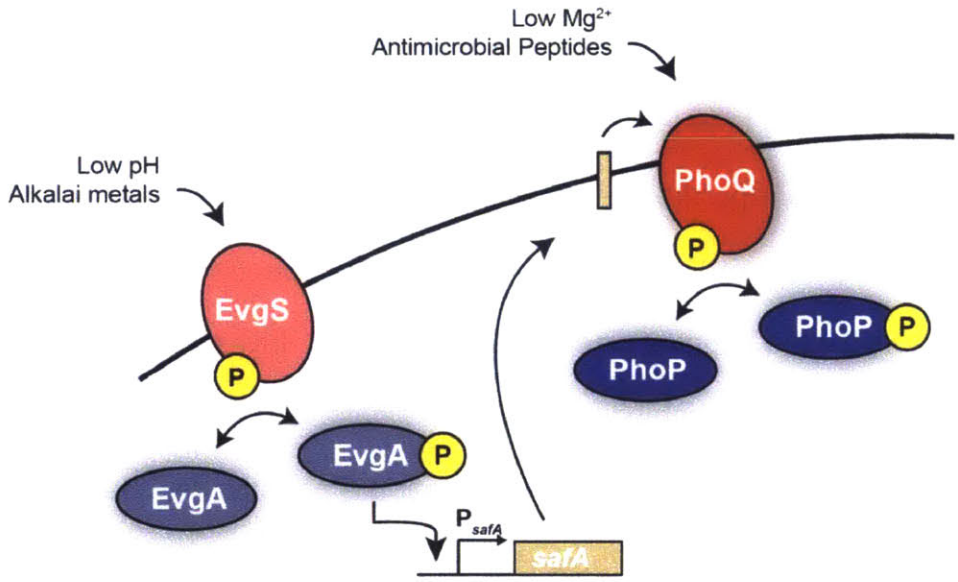

Figure 1.7. SafA connects the EvgS-EvgA and PhoQ-PhoP systems. The histidine kinase EvgS phosphorylates its cognate response regulate when stimulated by low pH and certain alkalai metals. Once phosphorylated, EvgA acts as a transcription factor and initiates the expression of *safA*. The small, transmembrane protein SafA binds to PhoQ in the periplasm and the inner membrane, and increases the output of the PhoQ-PhoP system. SafA stimulates PhoQ directly and decreases its ability to dephosphorylate PhoP.

Because PhoQ is bifunctional, SafA can activate the PhoQ-PhoP system by either stimulating the PhoQ kinase reaction or by inhibiting the PhoQ phosphatase reaction. To differentiate between these two possibilities, the PhoQ-PhoP autophosphorylation, phosphotransfer, and phosphatase reactions were examined *in vitro* both in the presence and absence of the SafA periplasmic domain (Itou et al., 2009). The addition of SafA did not have an effect on the ability of PhoQ to dephosphorylate PhoP, but SafA did increase the rate of PhoQ autophosphorylation, which resulted in higher levels of phosphotransfer to PhoP (Itou et al., 2009). Therefore, it is thought that SafA activates

the PhoQ-PhoP pathway by stimulating the kinase reaction of PhoQ, although this has yet to be shown *in vivo*.

Thesis summary

In this thesis, I discuss how we characterize the induction kinetics of the PhoQ-PhoP pathway in *E. coli*. Using time-lapse microscopy and a fluorescent reporter for a PhoP activated promoter, we replicate the impulse response (previously seen via qRT-PCR) in the PhoQ-PhoP pathway. We identify that the MgrB dependent negative feedback loop is necessary for the impulse kinetics, and that MgrB drives inhibition of the PhoQ-PhoP pathway by selectively inhibiting the PhoQ kinase reaction while permitting the PhoQ phosphatase reaction. We further show that this negative feedback loop greatly diminishes the significance of the PhoQ-PhoP positive feedback loop caused by active PhoP promoting the transcription of the *phoPQ* operon. Next, we examined the effects of SafA on PhoQ-PhoP activation, and find that it does not have a significant effect on PhoQ-PhoP pathway induction kinetics in our experimental conditions. We also analyze the nucleotide binding properties of PhoQ *in vitro*, and present evidence that PhoQ ADP exchange is rapid and that PhoQ can perform multiple rounds of autophosphorylation, contrary to the most recent model of PhoQ-PhoP pathway temporal dynamics. Later, we briefly discuss how the induction kinetics of PhoQ-PhoP vary depending on the environment in which stimulus is introduced, and show that disruptions to the PhoQ-PhoP pathway dynamics can have detrimental effects to fitness. Finally, we present preliminary data on identifying novel membrane regulators of histidine kinases, and preliminary data on the specificity of the *B. subtilis* sporulation phosphorelay.

References

Alm, E., Huang, K., and Arkin, A. (2006). The Evolution of Two-Component Systems in Bacteria Reveals Different Strategies for Niche Adaptation. PLoS Comput Biol *2*, e143.

Ashenberg, O., Rozen-Gagnon, K., Laub, M.T., and Keating, A.E. (2011). Determinants of Homodimerization Specificity in Histidine Kinases. J. Mol. Biol. *413*, 222–235.

Ashenberg, O., Keating, A.E., and Laub, M.T. (2013). Helix bundle loops determine whether histidine kinases autophosphorylate in cis or in trans. J. Mol. Biol. *425*, 1198–1209.

Bader, M.W., Sanowar, S., Daley, M.E., Schneider, A.R., Cho, U., Xu, W., Klevit, R.E., Le Moual, H., and Miller, S.I. (2005). Recognition of antimicrobial peptides by a bacterial sensor kinase. Cell *122*, 461–472.

Batchelor, E., Mock, C.S., Bhan, I., Loewer, A., and Lahav, G. (2008). Recurrent Initiation: A Mechanism for Triggering p53 Pulses in Response to DNA Damage. Mol. Cell *30*, 277–289.

Batchelor, E., Loewer, A., and Lahav, G. (2009). The ups and downs of p53: understanding protein dynamics in single cells. Nat. Rev. Cancer *9*, 371–377.

Batchelor, E., Loewer, A., Mock, C., and Lahav, G. (2011). Stimulus-dependent dynamics of p53 in single cells. Mol. Syst. Biol. *7*, 488.

Bishop, R.E., Gibbons, H.S., Guina, T., Trent, M.S., Miller, S.I., and Raetz, C.R. (2000). Transfer of palmitate from phospholipids to lipid A in outer membranes of gram-negative bacteria. EMBO J. *19*, 5071–5080.

Bogaerts, P., Montesinos, I., Rodriguez-Villalobos, H., Blairon, L., Deplano, A., and Glupczynski, Y. (2010). Emergence of clonally related Klebsiella pneumoniae isolates of sequence type 258 producing KPC-2 carbapenemase in Belgium. J. Antimicrob. Chemother. *65*, 361–362.

Boll, J.M., and Hendrixson, D.R. (2011). A specificity determinant for phosphorylation in a response regulator prevents in vivo cross-talk and modification by acetyl phosphate. Proc. Natl. Acad. Sci. *108*, 20160–20165.

Brandon, L., Dorus, S., Epstein, W., Altendorf, K., and Jung, K. (2000). Modulation of KdpD phosphatase implicated in the physiological expression of the kdp ATPase of Escherichia coli. Mol. Microbiol. *38*, 1086–1092.

Burbulys, D., Trach, K.A., and Hoch, J.A. (1991). Initiation of sporulation in B. subtilis is controlled by a multicomponent phosphorelay. Cell *64*, 545–552.

Cai, S.J., and Inouye, M. (2002). EnvZ-OmpR Interaction and Osmoregulation in Escherichia coli. J. Biol. Chem. *277*, 24155–24161.

Cannatelli, A., D'Andrea, M.M., Giani, T., Pilato, V.D., Arena, F., Ambretti, S., Gaibani, P., and Rossolini, G.M. (2013). In Vivo Emergence of Colistin Resistance in Klebsiella pneumoniae Producing KPC-Type Carbapenemases Mediated by Insertional Inactivation of the PhoQ/PhoP mgrB Regulator. Antimicrob. Agents Chemother. *57*, 5521–5526.

Cannatelli, A., Giani, T., D'Andrea, M.M., Pilato, V.D., Arena, F., Conte, V., Tryfinopoulou, K., Vatopoulos, A., and Rossolini, G.M. (2014). MgrB Inactivation Is a Common Mechanism of Colistin Resistance in KPC-Producing Klebsiella pneumoniae of Clinical Origin. Antimicrob. Agents Chemother. *58*, 5696–5703.

Capra, E.J., and Laub, M.T. (2012). Evolution of two-component signal transduction systems. Annu. Rev. Microbiol. *66*, 325–347.

Capra, E.J., Perchuk, B.S., Lubin, E.A., Ashenberg, O., Skerker, J.M., and Laub, M.T. (2010). Systematic Dissection and Trajectory-Scanning Mutagenesis of the Molecular Interface That Ensures Specificity of Two-Component Signaling Pathways. PLoS Genet *6*, e1001220.

Capra, E.J., Perchuk, B.S., Skerker, J.M., and Laub, M.T. (2012a). Adaptive mutations that prevent crosstalk enable the expansion of paralogous signaling protein families. Cell *150*, 222–232.

Capra, E.J., Perchuk, B.S., Ashenberg, O., Seid, C.A., Snow, H.R., Skerker, J.M., and Laub, M.T. (2012b). Spatial tethering of kinases to their substrates relaxes evolutionary constraints on specificity. Mol. Microbiol. *86*, 1393–1403.

Carmany, D.O., Hollingsworth, K., and McCleary, W.R. (2003). Genetic and Biochemical Studies of Phosphatase Activity of PhoR. J. Bacteriol. *185*, 1112–1115.

Casino, P., Rubio, V., and Marina, A. (2009). Structural Insight into Partner Specificity and Phosphoryl Transfer in Two-Component Signal Transduction. Cell *139*, 325–336.

Castelli, M.E., Véscovi, E.G., and Soncini, F.C. (2000). The Phosphatase Activity Is the Target for Mg2+Regulation of the Sensor Protein PhoQ in Salmonella. J. Biol. Chem. *275*, 22948–22954.

Chamnongpol, S., and Groisman, E.A. (2000). Acetyl phosphate-dependent activation of a mutant PhoP response regulator that functions independently of its cognate sensor kinase. J. Mol. Biol. *300*, 291–305.

Chamnongpol, S., Cromie, M., and Groisman, E.A. (2003). Mg2+ sensing by the Mg2+ sensor PhoQ of Salmonella enterica. J. Mol. Biol. *325*, 795–807.

Chastanet, A., Vitkup, D., Yuan, G.-C., Norman, T.M., Liu, J.S., and Losick, R.M. (2010). Broadly heterogeneous activation of the master regulator for sporulation in Bacillus subtilis. Proc. Natl. Acad. Sci. *107*, 8486–8491.

Chechik, G., Oh, E., Rando, O., Weissman, J., Regev, A., and Koller, D. (2008). Activity motifs reveal principles of timing in transcriptional control of the yeast metabolic network. Nat. Biotechnol. *26*, 1251–1259.

Chen, H.D., and Groisman, E.A. (2013). The Biology of the PmrA/PmrB Two-Component System: The Major Regulator of Lipopolysaccharide Modifications. Annu. Rev. Microbiol. *67*, 83–112.

Cheng, H.-Y., Chen, Y.-F., and Peng, H.-L. (2010). Molecular characterization of the PhoPQ-PmrD-PmrAB mediated pathway regulating polymyxin B resistance in Klebsiella pneumoniae CG43. J. Biomed. Sci. *17*, 60.

Da Re, S.S., Deville-Bonne, D., Tolstykh, T., V ron, M., and Stock, J.B. (1999). Kinetics of CheY phosphorylation by small molecule phosphodonors. FEBS Lett. *457*, 323–326.

Dutta, R., and Inouye, M. (1996). Reverse phosphotransfer from OmpR to EnvZ in a kinase-/phosphatase+ mutant of EnvZ (EnvZ.N347D), a bifunctional signal transducer of Escherichia coli. J. Biol. Chem. *271*, 1424–1429.

Eguchi, Y., Itou, J., Yamane, M., Demizu, R., Yamato, F., Okada, A., Mori, H., Kato, A., and Utsumi, R. (2007). B1500, a small membrane protein, connects the two-component systems EvgS/EvgA and PhoQ/PhoP in Escherichia coli. Proc. Natl. Acad. Sci. *104*, 18712–18717.

Eguchi, Y., Ishii, E., Yamane, M., and Utsumi, R. (2012a). The connector SafA interacts with the multi-sensing domain of PhoQ in Escherichia coli. Mol. Microbiol. *85*, 299–313.

Eguchi, Y., Ishii, E., Yamane, M., and Utsumi, R. (2012b). The connector SafA interacts with the multi-sensing domain of PhoQ in Escherichia coli. Mol. Microbiol. *85*, 299–313.

Fleischer, R., Heermann, R., Jung, K., and Hunke, S. (2007). Purification, reconstitution, and characterization of the CpxRAP envelope stress system of Escherichia coli. J. Biol. Chem. *282*, 8583–8593.

Fujita, M., and Losick, R. (2005). Evidence that entry into sporulation in Bacillus subtilis is governed by a gradual increase in the level and activity of the master regulator Spo0A. Genes Dev. *19*, 2236–2244.

Fujita, M., González-Pastor, J.E., and Losick, R. (2005). High- and Low-Threshold Genes in the Spo0A Regulon of Bacillus subtilis. J. Bacteriol. *187*, 1357–1368.

Galperin, M.Y. (2005). A census of membrane-bound and intracellular signal transduction proteins in bacteria: Bacterial IQ, extroverts and introverts. BMC Microbiol. *5*, 35.

Galperin, M.Y., Mekhedov, S.L., Puigbo, P., Smirnov, S., Wolf, Y.I., and Rigden, D.J. (2012). Genomic determinants of sporulation in Bacilli and Clostridia: towards the minimal set of sporulation-specific genes. Environ. Microbiol. *14*, 2870–2890.

Gao, R., and Stock, A.M. (2009). Biological Insights from Structures of Two-Component Proteins. Annu. Rev. Microbiol. *63*, 133–154.

Gao, R., and Stock, A.M. (2013a). Probing kinase and phosphatase activities of two-component systems in vivo with concentration-dependent phosphorylation profiling. Proc. Natl. Acad. Sci. *110*, 672–677.

Gao, R., and Stock, A.M. (2013b). Evolutionary tuning of protein expression levels of a positively autoregulated two-component system. PLoS Genet. *9*, e1003927.

García Véscovi, E., Soncini, F.C., and Groisman, E.A. (1996). Mg2+ as an extracellular signal: environmental regulation of Salmonella virulence. Cell *84*, 165–174.

Gardino, A.K., and Kern, D. (2007). Functional dynamics of response regulators using NMR relaxation techniques. Methods Enzymol. *423*, 149–165.

Gasch, A.P., Spellman, P.T., Kao, C.M., Carmel-Harel, O., Eisen, M.B., Storz, G., Botstein, D., and Brown, P.O. (2000). Genomic expression programs in the response of yeast cells to environmental changes. Mol. Biol. Cell *11*, 4241–4257.

Grimshaw, C.E., Huang, S., Hanstein, C.G., Strauch, M.A., Burbulys, D., Wang, L., Hoch, J.A., and Whiteley, J.M. (1998). Synergistic Kinetic Interactions between Components of the Phosphorelay Controlling Sporulation in Bacillus subtilis†. Biochemistry (Mosc.) *37*, 1365–1375.

Groban, E.S., Clarke, E.J., Salis, H.M., Miller, S.M., and Voigt, C.A. (2009). Kinetic Buffering of Cross Talk between Bacterial Two-Component Sensors. J. Mol. Biol. *390*, 380–393.

Groisman, E.A. (2001). The Pleiotropic Two-Component Regulatory System PhoP-PhoQ. J. Bacteriol. *183*, 1835–1842.

Groisman, E.A., Heffron, F., and Solomon, F. (1992). Molecular genetic analysis of the Escherichia coli phoP locus. J. Bacteriol. *174*, 486–491.

Guina, T., Yi, E.C., Wang, H., Hackett, M., and Miller, S.I. (2000). A PhoP-regulated outer membrane protease of Salmonella enterica serovar typhimurium promotes resistance to alpha-helical antimicrobial peptides. J. Bacteriol. *182*, 4077–4086.

Guisbert, E., Yura, T., Rhodius, V.A., and Gross, C.A. (2008). Convergence of Molecular, Modeling, and Systems Approaches for an Understanding of the Escherichia coli Heat Shock Response. Microbiol. Mol. Biol. Rev. *72*, 545–554.

Guo, L., Lim, K.B., Poduje, C.M., Daniel, M., Gunn, J.S., Hackett, M., and Miller, S.I. (1998). Lipid A acylation and bacterial resistance against vertebrate antimicrobial peptides. Cell *95*, 189–198.

Helander, I.M., Kato, Y., Kilpeläinen, I., Kostiainen, R., Lindner, B., Nummila, K., Sugiyama, T., and Yokochi, T. (1996). Characterization of Lipopolysaccharides of Polymyxin-Resistant and Polymyxin-Sensitive Klebsiella pneumoniae O3. Eur. J. Biochem. *237*, 272–278.

Hilbert, D.W., and Piggot, P.J. (2004). Compartmentalization of Gene Expression during Bacillus subtilis Spore Formation. Microbiol. Mol. Biol. Rev. *68*, 234–262.

Hsing, W., and Silhavy, T.J. (1997). Function of conserved histidine-243 in phosphatase activity of EnvZ, the sensor for porin osmoregulation in Escherichia coli. J. Bacteriol. *179*, 3729–3735.

Hsing, W., Russo, F.D., Bernd, K.K., and Silhavy, T.J. (1998). Mutations That Alter the Kinase and Phosphatase Activities of the Two-Component Sensor EnvZ. J. Bacteriol. *180*, 4538–4546.

Hutchings, M.I., Hong, H.-J., and Buttner, M.J. (2006). The vancomycin resistance VanRS two-component signal transduction system of Streptomyces coelicolor. Mol. Microbiol. *59*, 923–935.

Huynh, T.N., Noriega, C.E., and Stewart, V. (2010). Conserved mechanism for sensor phosphatase control of two-component signaling revealed in the nitrate sensor NarX. Proc. Natl. Acad. Sci. *107*, 21140–21145.

Igo, M.M., Ninfa, A.J., Stock, J.B., and Silhavy, T.J. (1989). Phosphorylation and dephosphorylation of a bacterial transcriptional activator by a transmembrane receptor. Genes Dev. *3*, 1725–1734.

ITOU, J., EGUCHI, Y., and UTSUMI, R. (2009). Molecular Mechanism of Transcriptional Cascade Initiated by the EvgS/EvgA System in Escherichia coli K-12. Biosci. Biotechnol. Biochem. *73*, 870–878.

Jiang, P., Atkinson, M.R., Srisawat, C., Sun, Q., and Ninfa, A.J. (2000). Functional dissection of the dimerization and enzymatic activities of Escherichia coli nitrogen regulator II and their regulation by the PII protein. Biochemistry (Mosc.) *39*, 13433–13449.

Jong, I.G. de, Veening, J.-W., and Kuipers, O.P. (2010). Heterochronic Phosphorelay Gene Expression as a Source of Heterogeneity in Bacillus subtilis Spore Formation. J. Bacteriol. *192*, 2053–2067.

Kato, A., and Groisman, E.A. (2008). The PhoQ/PhoP Regulatory Network of Salmonella enterica. In Bacterial Signal Transduction: Networks and Drug Targets, R. Utsumi, ed. (Springer New York), pp. 7–21.

Kinoshita, E., Kinoshita-Kikuta, E., and Koike, T. (2009). Separation and detection of large phosphoproteins using Phos-tag SDS-PAGE. Nat. Protoc. *4*, 1513–1521.

Krell, T., Lacal, J., Busch, A., Silva-Jiménez, H., Guazzaroni, M.-E., and Ramos, J.L. (2010). Bacterial Sensor Kinases: Diversity in the Recognition of Environmental Signals. Annu. Rev. Microbiol. *64*, 539–559.

Levine, J.H., and Elowitz, M.B. (2014). Polyphasic feedback enables tunable cellular timers. Curr. Biol. *24*, R994–R995.

Levine, J.H., Fontes, M.E., Dworkin, J., and Elowitz, M.B. (2012). Pulsed Feedback Defers Cellular Differentiation. PLoS Biol *10*, e1001252.

Levine, J.H., Lin, Y., and Elowitz, M.B. (2013). Functional Roles of Pulsing in Genetic Circuits. Science *342*, 1193–1200.

Li, G.-W., Burkhardt, D., Gross, C., and Weissman, J.S. (2014). Quantifying Absolute Protein Synthesis Rates Reveals Principles Underlying Allocation of Cellular Resources. Cell *157*, 624–635.

Lippa, A.M., and Goulian, M. (2009). Feedback inhibition in the PhoQ/PhoP signaling system by a membrane peptide. PLoS Genet. *5*, e1000788.

Litvak, V., Ramsey, S.A., Rust, A.G., Zak, D.E., Kennedy, K.A., Lampano, A.E., Nykter, M., Shmulevich, I., and Aderem, A. (2009). Function of C/EBPδ in a regulatory circuit that discriminates between transient and persistent TLR4-induced signals. Nat. Immunol. *10*, 437–443.

Locke, J.C.W., and Elowitz, M.B. (2009). Using movies to analyse gene circuit dynamics in single cells. Nat. Rev. Microbiol. *7*, 383–392.

López-Maury, L., Marguerat, S., and Bähler, J. (2008). Tuning gene expression to changing environments: from rapid responses to evolutionary adaptation. Nat. Rev. Genet. *9*, 583–593.

Lukat, G.S., McCleary, W.R., Stock, A.M., and Stock, J.B. (1992). Phosphorylation of bacterial response regulator proteins by low molecular weight phospho-donors. Proc. Natl. Acad. Sci. U. S. A. *89*, 718–722.

Mascher, T., Helmann, J.D., and Unden, G. (2006). Stimulus Perception in Bacterial Signal-Transducing Histidine Kinases. Microbiol. Mol. Biol. Rev. *70*, 910–938.

Miyashiro, T., and Goulian, M. (2007). Stimulus-dependent differential regulation in the Escherichia coli PhoQ PhoP system. Proc. Natl. Acad. Sci. U. S. A. *104*, 16305–16310.

Miyashiro, T., and Goulian, M. (2008). High stimulus unmasks positive feedback in an autoregulated bacterial signaling circuit. Proc. Natl. Acad. Sci. U. S. A. *105*, 17457–17462.

Moncrief, M.B.C., and Maguire, M.E. (1998). Magnesium and the Role of mgtC in Growth of Salmonella typhimurium. Infect. Immun. *66*, 3802–3809.

Nishino, K., and Yamaguchi, A. (2002). EvgA of the Two-Component Signal Transduction System Modulates Production of the YhiUV Multidrug Transporter in Escherichia coli. J. Bacteriol. *184*, 2319–2323.

Perego, M. (2001). A new family of aspartyl phosphate phosphatases targeting the sporulation transcription factor Spo0A of Bacillus subtilis. Mol. Microbiol. *42*, 133–143.

Podgornaia, A.I., and Laub, M.T. (2013). Determinants of specificity in two-component signal transduction. Curr. Opin. Microbiol. *16*, 156–162.

Podgornaia, A.I., and Laub, M.T. (2015). Pervasive degeneracy and epistasis in a protein-protein interface. Science *347*, 673–677.

Podgornaia, A.I., Casino, P., Marina, A., and Laub, M.T. (2013). Structural Basis of a Rationally Rewired Protein-Protein Interface Critical to Bacterial Signaling. Structure *21*, 1636–1647.

Prost, L.R., Daley, M.E., Le Sage, V., Bader, M.W., Le Moual, H., Klevit, R.E., and Miller, S.I. (2007). Activation of the bacterial sensor kinase PhoQ by acidic pH. Mol. Cell *26*, 165–174.

Raj, A., and van Oudenaarden, A. (2008). Nature, nurture, or chance: stochastic gene expression and its consequences. Cell *135*, 216–226.

Ram, S., and Goulian, M. (2013). The Architecture of a Prototypical Bacterial Signaling Circuit Enables a Single Point Mutation to Confer Novel Network Properties. PLoS Genet *9*, e1003706.

Ray, J.C.J., and Igoshin, O.A. (2010). Adaptable functionality of transcriptional feedback in bacterial two-component systems. PLoS Comput. Biol. *6*, e1000676.

Rowland, M.A., and Deeds, E.J. (2014). Crosstalk and the evolution of specificity in two-component signaling. Proc. Natl. Acad. Sci. *111*, 5550–5555.

Russo, F.D., and Silhavy, T.J. (1993). The essential tension: opposed reactions in bacterial two-component regulatory systems. Trends Microbiol. *1*, 306–310.

Salazar, M.E., and Laub, M.T. (2015). Temporal and evolutionary dynamics of two-component signaling pathways. Curr. Opin. Microbiol. *24*, 7–14.

Sarkar, M.K., Paul, K., and Blair, D. (2010). Chemotaxis signaling protein CheY binds to the rotor protein FliN to control the direction of flagellar rotation in Escherichia coli. Proc. Natl. Acad. Sci. *107*, 9370–9375.

Shin, D., and Groisman, E.A. (2005). Signal-dependent binding of the response regulators PhoP and PmrA to their target promoters in vivo. J. Biol. Chem. *280*, 4089–4094.

Shin, D., Lee, E.-J., Huang, H., and Groisman, E.A. (2006). A Positive Feedback Loop Promotes Transcription Surge That Jump-Starts Salmonella Virulence Circuit. Science *314*, 1607–1609.

Siryaporn, A., and Goulian, M. (2008). Cross-talk suppression between the CpxA–CpxR and EnvZ–OmpR two-component systems in E. coli. Mol. Microbiol. *70*, 494–506.

Skerker, J.M., Prasol, M.S., Perchuk, B.S., Biondi, E.G., and Laub, M.T. (2005). Two-Component Signal Transduction Pathways Regulating Growth and Cell Cycle Progression in a Bacterium: A System-Level Analysis. PLoS Biol *3*, e334.

Skerker, J.M., Perchuk, B.S., Siryaporn, A., Lubin, E.A., Ashenberg, O., Goulian, M., and Laub, M.T. (2008). Rewiring the Specificity of Two-Component Signal Transduction Systems. Cell *133*, 1043–1054.

Smith, R.L., and Maguire, M.E. (1998). Microbial magnesium transport: unusual transporters searching for identity. Mol. Microbiol. *28*, 217–226.

Soncini, F.C., García Véscovi, E., Solomon, F., and Groisman, E.A. (1996). Molecular basis of the magnesium deprivation response in Salmonella typhimurium: identification of PhoP-regulated genes. J. Bacteriol. *178*, 5092–5099.

Steiner, E., Dago, A.E., Young, D.I., Heap, J.T., Minton, N.P., Hoch, J.A., and Young, M. (2011). Multiple orphan histidine kinases interact directly with Spo0A to control the initiation of endospore formation in Clostridium acetobutylicum. Mol. Microbiol. *80*, 641–654.

Stock, A.M., Robinson, V.L., and Goudreau, P.N. (2000). Two-component signal transduction. Annu. Rev. Biochem. *69*, 183–215.

Szurmant, H., White, R.A., and Hoch, J.A. (2007). Sensor complexes regulating two-component signal transduction. Curr. Opin. Struct. Biol. *17*, 706–715.

Taymaz-Nikerel, H., Cankorur-Cetinkaya, A., and Kirdar, B. (2016). Genome-Wide Transcriptional Response of Saccharomyces cerevisiae to Stress-Induced Perturbations. Front. Bioeng. Biotechnol. *4*.

Timmen, M., Bassler, B.L., and Jung, K. (2006). AI-1 influences the kinase activity but not the phosphatase activity of LuxN of Vibrio harveyi. J. Biol. Chem. *281*, 24398–24404.

Townsend, G.E., Raghavan, V., Zwir, I., and Groisman, E.A. (2013). Intramolecular arrangement of sensor and regulator overcomes relaxed specificity in hybrid two-component systems. Proc. Natl. Acad. Sci. *110*, E161–E169.

T Yura, H Nagai, and Mori, and H. (1993). Regulation of the Heat-Shock Response in Bacteria. Annu. Rev. Microbiol. *47*, 321–350.

Veening, J.-W., Murray, H., and Errington, J. (2009). A mechanism for cell cycle regulation of sporulation initiation in Bacillus subtilis. Genes Dev. *23*, 1959–1970.

Weigt, M., White, R.A., Szurmant, H., Hoch, J.A., and Hwa, T. (2009). Identification of direct residue contacts in protein-protein interaction by message passing. Proc. Natl. Acad. Sci. U. S. A. *106*, 67–72.

Wolfe, A.J. (2005). The acetate switch. Microbiol. Mol. Biol. Rev. MMBR *69*, 12–50.

Wörner, K., Szurmant, H., Chiang, C., and Hoch, J.A. (2006). Phosphorylation and functional analysis of the sporulation initiation factor Spo0A from Clostridium botulinum. Mol. Microbiol. *59*, 1000–1012.

Wuichet, K., and Zhulin, I.B. (2010). Origins and Diversification of a Complex Signal Transduction System in Prokaryotes. Sci. Signal. *3*, ra50–ra50.

Yamamoto, K., and Ishihama, A. (2005). Transcriptional response of Escherichia coli to external zinc. J. Bacteriol. *187*, 6333–6340.

Yeo, W.-S., Zwir, I., Huang, H.V., Shin, D., Kato, A., and Groisman, E.A. (2012). Intrinsic negative feedback governs activation surge in two-component regulatory systems. Mol. Cell *45*, 409–421.

Yigit, H., Queenan, A.M., Anderson, G.J., Domenech-Sanchez, A., Biddle, J.W., Steward, C.D., Alberti, S., Bush, K., and Tenover, F.C. (2001). Novel Carbapenem-Hydrolyzing β-Lactamase, KPC-1, from a Carbapenem-Resistant Strain of Klebsiella pneumoniae. Antimicrob. Agents Chemother. *45*, 1151–1161.

Yosef, N., and Regev, A. (2011). Impulse Control: Temporal Dynamics in Gene Transcription. Cell *144*, 886–896.

Zapf, J., Sen, U., Madhusudan, Hoch, J.A., and Varughese, K.I. (2000). A transient interaction between two phosphorelay proteins trapped in a crystal lattice reveals the mechanism of molecular recognition and phosphotransfer in signal transduction. Structure *8*, 851–862.

Zhao, R., Collins, E.J., Bourret, R.B., and Silversmith, R.E. (2002). Structure and catalytic mechanism of the E. coli chemotaxis phosphatase CheZ. Nat. Struct. Biol. *9*, 570–575.

Zhu, Y., Qin, L., Yoshida, T., and Inouye, M. (2000). Phosphatase activity of histidine kinase EnvZ without kinase catalytic domain. Proc. Natl. Acad. Sci. *97*, 7808–7813.

Zwir, I., Shin, D., Kato, A., Nishino, K., Latifi, T., Solomon, F., Hare, J.M., Huang, H., and Groisman, E.A. (2005). Dissecting the PhoP regulatory network of Escherichia coli and Salmonella enterica. Proc. Natl. Acad. Sci. U. S. A. *102*, 2862–2867.

Chapter II:

The small membrane protein MgrB regulates PhoQ bifunctionality to control PhoP target gene expression

This chapter is being prepared for publication.

Michael E. Salazar[1], Anna I. Podgornaia[1], Michael T. Laub[1,2]

1. Department of Biology
2. Howard Hughes Medical Institute

Massachusetts Institute of Technology

Cambridge, MA 02139, USA

Author Contributions: MES and MTL planned research, MES performed research, AIP performed preliminary experiments, MES and MTL wrote the paper.

Abstract

In *Escherichia coli* and other γ-proteobacteria, the PhoQ-PhoP two-component signaling system responds to low extracellular Mg^{++} and cationic antimicrobial peptides. Upon transition to inducing conditions, the expression of PhoP-dependent genes increases rapidly, but then decays to a new, intermediate steady-state level, a phenomenon referred to as partial adaptation. The molecular basis for this adaptation has been unclear. Here, using time-lapse fluorescence microscopy to examine PhoP-dependent gene expression in individual cells we show that partial adaptation arises through a negative feedback loop involving the small protein MgrB. When cells are shifted to low Mg^{++}, PhoQ engages in multiple rounds of autophosphorylation and phosphotransfer to PhoP, which, in turn, drives the expression of *mgrB*. MgrB then feeds back to inhibit the kinase activity of PhoQ. PhoQ is bifunctional such that, when not active as a kinase, it can stimulate the dephosphorylation of PhoP. Thus, MgrB leads to the inactivation of PhoP and the observed adaptation in PhoP-dependent gene expression. Our results clarify the source of feedback inhibition in the PhoQ-PhoP system and reveal how exogenous factors, such as MgrB, can combine with a canonical two-component signaling pathway to produce complex temporal dynamics in target gene expression.

Introduction

Cells sense and respond to changes in their environments through signal transduction systems. These systems can detect an environmental signal, often using a membrane-bound sensor, and then relay the signal to an intracellular effector such that the cell can enact an appropriate biological response. Two-component signaling pathways are a widely used form of signaling found throughout the bacterial kingdom (Capra and Laub, 2012; Gao and Stock, 2009; Salazar and Laub, 2015). In the canonical two-component system, a sensor histidine kinase in the membrane directly interacts with a ligand or stimulus, triggering autophosphorylation of an intracellular kinase domain, followed by phosphotransfer to a cognate response regulator. Once phosphorylated, the response regulator can initiate a response to the stimulus, often by binding DNA and modulating gene expression. Bacterial genomes typically encode dozens to hundreds of histidine kinases and response regulators.

Although two-component signaling pathways sense and respond to a diverse range of stimuli, these systems share many regulatory features (Goulian, 2010). For most two-component pathways, the sensor histidine kinase is bifunctional, capable of both driving the phosphorylation and dephosphorylation of its cognate response regulator, effectively acting as a kinase and as a phosphatase. Through autophosphorylation and phosphotransfer (which we refer to, for simplicity, as 'kinase' activity) a histidine kinase can activate its cognate response regulator. When not stimulated to autophosphorylate, a bifunctional histidine kinase can stimulate the intrinsic autodephosphorylation activity of the response regulator (Hsing et al., 1998; Huynh et al., 2010; Igo et al., 1989; Russo and Silhavy, 1993), which we refer to as its 'phosphatase' activity.

Many two-component signaling pathways also have feedback loops, both negative and positive. Active, phosphorylated response regulators will often promote the transcription of themselves and their cognate kinases, whereas some activate the expression of factors that downregulate pathway output (Gao and Stock, 2013a; Lippa and Goulian, 2009; Ray and Igoshin, 2010; Salazar and Laub, 2015; Shin et al., 2006). The cross-regulation of different two-component systems has also been observed in which a downstream target of one pathway modulates the phosphorylation state or activity of another pathway (Chen and Groisman, 2013; Eguchi et al., 2007, 2012). Precisely how these feedback loops combine and effect the signaling dynamics of two-component-based pathways remains largely unexplored.

Although two-component signaling pathways are often thought of as binary systems that switch between an OFF and ON state, there is increasing evidence that these systems can produce complex output responses. In several cases, target gene expression exhibits an 'impulse' or partial adaptation, in which, after a stimulus is detected, expression increases to a maximal level and then subsequently decreases to a new steady-state level intermediate that of the initial and maximal levels (Gao and Stock, 2013b; Hutchings et al., 2006; Shin et al., 2006; Yamamoto and Ishihama, 2005). Even more complex dynamics have been observed for the phosphorelay governing sporulation in *Bacillus subtilis* where Spo0A target genes can exhibit a series of pulses in expression (Levine et al., 2012).

The PhoQ-PhoP pathway is a well-studied two-component signaling system found throughout γ-proteobacteria, including *Escherichia coli* and *Salmonella* species. PhoQ, a transmembrane histidine kinase, can be stimulated by exposure to low extracellular

Mg^{++}, certain cationic antimicrobial peptides, and pH fluctuations (Bader et al., 2005; Groisman, 2001). Once stimulated, PhoQ autophosphorylates and then transfers the phosphoryl group to PhoP, its cognate response regulator, which can then stimulate expression of its target genes. One PhoP target is the small (47 amino acids), transmembrane protein MgrB, which can feedback to inhibit PhoQ through an unknown mechanism (Lippa and Goulian, 2009). SafA is another small (65 amino acids), transmembrane protein that directly interacts with PhoQ, although it seems to promote PhoQ activation (Eguchi et al., 2007, 2012). The *phoPQ* operon is regulated by two promoters: P1 is activated by PhoP~P whereas P2 is constitutive (Miyashiro and Goulian, 2007a; Shin et al., 2006).

Previous work with *Salmonella* found that some PhoP target genes exhibit partial adaptation, as measured by qRT-PCR, following exposure to a stimulus (Shin et al., 2006). But how the various components and feedback loops of the PhoQ-PhoP system combine to produce the observed partial adaptation in PhoP target gene expression is unclear. One recent model proposed a mechanism intrinsic to PhoQ (Yeo et al., 2012). In this model, activated PhoQ binds ATP and autophosphorylates, with ADP then remaining locked in the nucleotide binding pocket of PhoQ due to a very slow PhoQ:ADP dissociation rate. The autophosphorylated PhoQ can phosphotransfer once to PhoP, but then is trapped with ADP, preventing subsequent autophosphorylation and promoting the phosphatase activity of PhoQ leading to an inactivation of PhoP. This model predicts that the partial adaptation of PhoP target gene expression is intrinsic to PhoQ. However, as noted, the small protein MgrB is also thought to feedback negatively on PhoQ and thus may contribute to partial adaptation.

To clarify the source of partial adaptation in PhoP target gene expression, we used time-lapse fluorescence microscopy to examine individual *E. coli* cells responding to extracellular Mg^{++} limitation. Our results support a model in which Mg^{++} limitation switches PhoQ from being primarily in the phosphatase state to the kinase state. Individual PhoQ molecules then engage in multiple rounds of autophosphorylation and phosphotransfer, driving the accumulation of PhoP~P and target gene expression, including *phoPQ* and *mgrB*. As MgrB accumulates, it binds to PhoQ and inhibits the kinase reaction while permitting the phosphatase reaction. PhoQ then stimulates the dephosphorylation of PhoP, leading to a decrease in target protein expression and the partial adaptation observed. Importantly, cells lacking *mgrB* no longer exhibit partial adaptation. We conclude that the MgrB-dependent negative feedback loop plays a crucial role in establishing the temporal dynamics of PhoQ-PhoP signaling.

Results

Time-lapse microscopy reveals partial adaptation of the PhoQ-PhoP system

To study how various regulatory features and feedback loops impact the PhoQ-PhoP pathway and affect the temporal dynamics of PhoP-dependent transcription, we monitored expression of a PhoP target gene in single cells using time-lapse fluorescence microscopy (Fig. 2.1A-B). We used a reporter construct in which the *mgrB* promoter, one of the strongest PhoP-dependent promoters in *E. coli* (Miyashiro and Goulian, 2007a, 2008), was fused to the gene encoding yellow fluorescent protein (YFP) on the chromosome. The reporter strain also harbored a constitutively active promoter, P_{tetA}, driving the expression of cyan fluorescent protein (CFP), which reports on general protein expression. We used the ratio of the two fluorescent reporters, YFP:CFP, to assess PhoP~P activity in individual cells. Cells containing these reporters were grown as shaking cultures in minimal medium containing high levels of Mg^{++} (50 mM, unless otherwise specified), which we refer to as the OFF state for the PhoQ-PhoP system, and then subsequently transferred to agarose pads made with minimum medium containing low concentrations of Mg^{++} (typically 0.01 mM, unless indicated otherwise), referred to as the ON state. Cells continued growing and dividing throughout our time-lapse experiments (Fig. 2.1B).

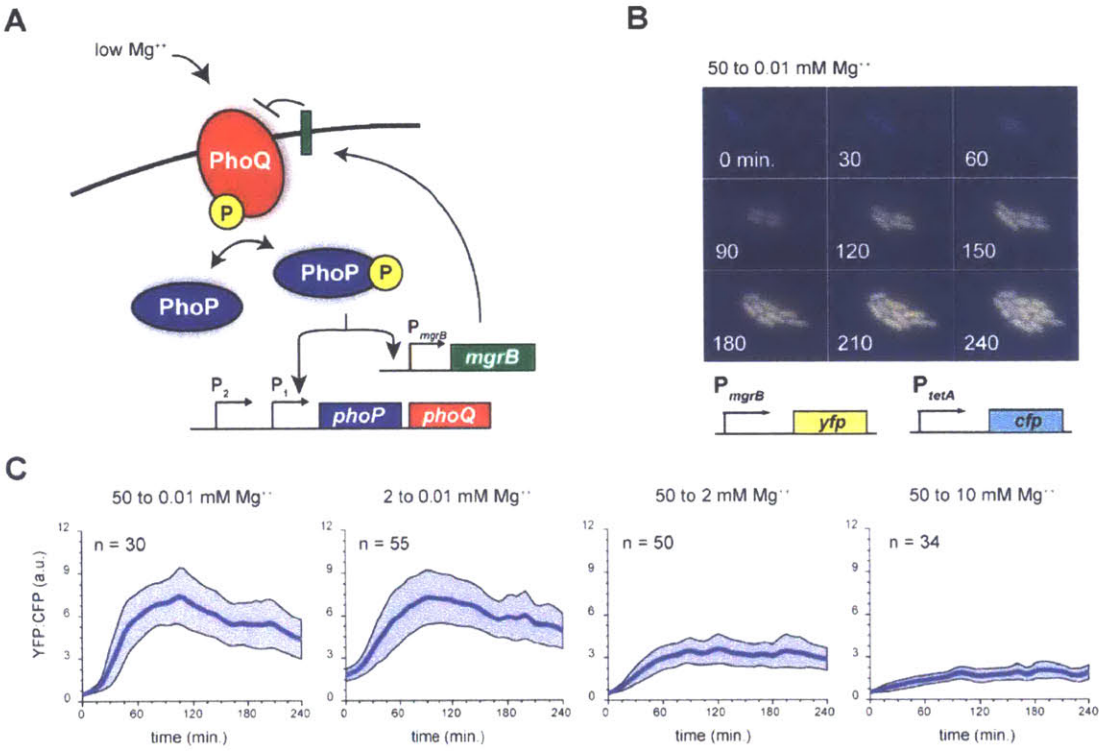

Figure 2.1. Partial adaptation in PhoP target gene expression following a shift to low extracellular Mg^{++} in *E. coli*.
(A) Schematic of the PhoQ-PhoP pathway. PhoQ, a transmembrane histidine kinase, can be stimulated by low extracellular Mg^{++} to autophosphorylate and then phosphotransfer to PhoP. PhoQ is bifunctional and can, when not stimulated, promote PhoP dephosphorylation. Active, phosphorylated PhoP drives the transcription of *mgrB*, which encodes a small, transmembrane protein that binds to PhoQ and suppresses output from the PhoQ-PhoP system. The *phoPQ* operon is transcriptionally regulated by two promoters: P_1 is activated by phosphorylated PhoP, and P_2 is constitutively expressed.
(B) Time-lapse fluorescence microscopy of PhoP-dependent gene expression. YFP (yellow) is driven by P_{mgrB}, and CFP (blue) is expressed from P_{tetA}. Cells were grown in M9 with 50 mM Mg^{++} and then washed and placed on agarose pads made of M9 with 0.01 mM Mg^{++}. Cells were imaged every 5 min; images from every 30 min are shown.
(C) Quantification of PhoP activity following the shifts in extracellular Mg^{++} concentration noted above each panel. Thick lines represent the mean YFP:CFP ratio and the shaded region indicates the mean +/- one standard deviation.

When cells transitioned from high to low extracellular Mg^{++}, *i.e.* from OFF to ON, the YFP:CFP ratio rapidly increased above the baseline (Fig. 2.1C, Appendix 1). The YFP:CFP ratio increased monotonically for the first 80 minutes post-shift, but then subsequently decreased, approaching a new steady-state level after approximately 200 minutes that was intermediate between the initial and maximal expression levels. The

vast majority of cells imaged on agarose pads exhibited the same general YFP:CFP dynamics, including the partial adaptation to an intermediate YFP:CFP level after ~240 minutes, with relatively modest variability in individual temporal profiles (Appendix 1). Replicate populations also exhibited similar dynamics (Appendix 1). This partial adaptation is similar to that observed previously in the mRNA level of a PhoP target gene in cultured *Salmonella* cells (Shin et al., 2006).

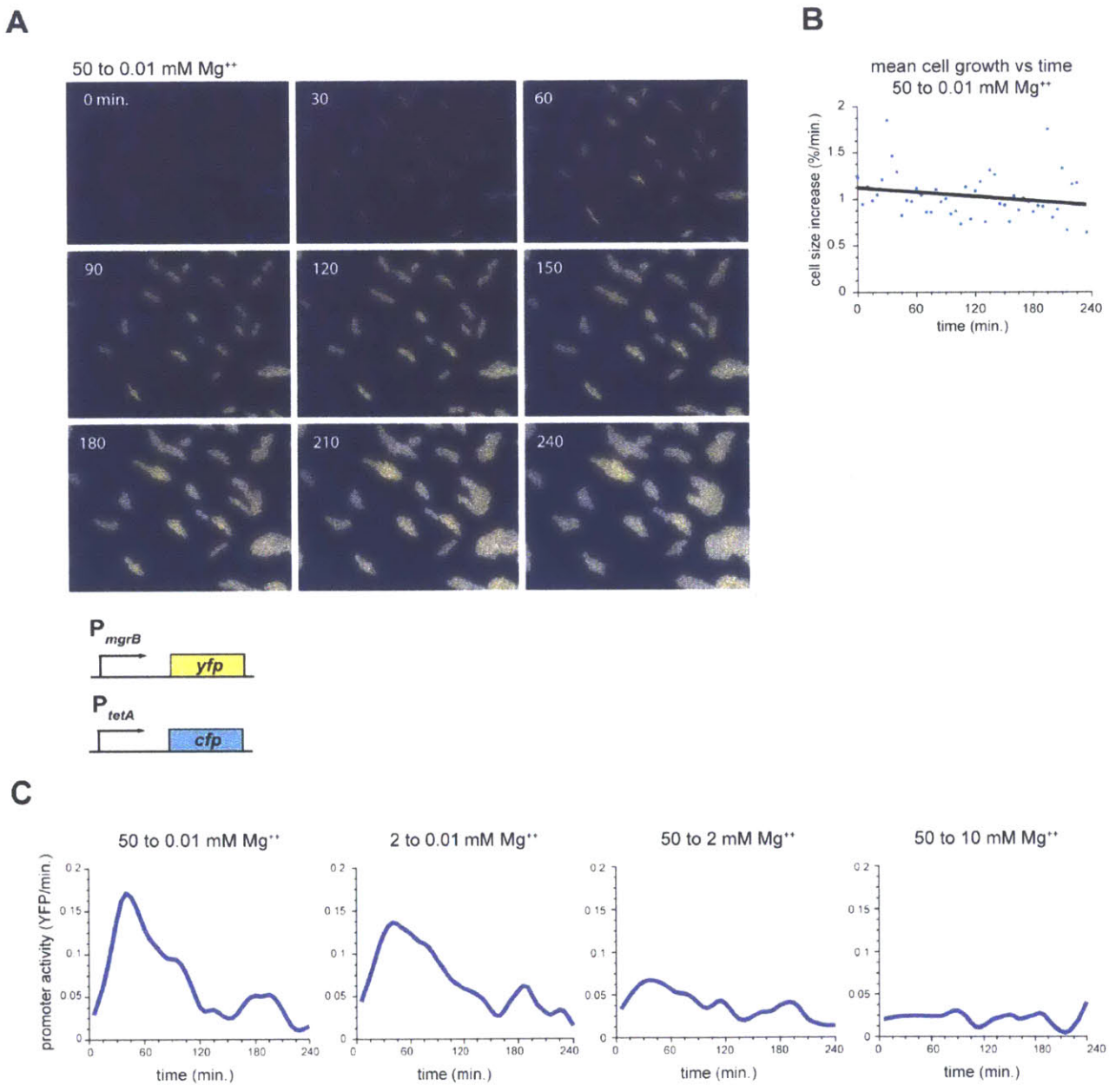

Figure 2.2. Time-lapse fluorescence microscopy reveals the temporal dynamics of the *E. coli* PhoQ-PhoP system.

(A) Whole frame view of time-lapse fluorescence microscopy of PhoP-dependent gene expression. YFP (yellow) is driven by P_{mgrB}, and CFP (blue) is expressed from P_{tetA}. Cells were grown in M9 with 50 mM Mg^{++} and then washed and placed on agarose pads made of M9 with 0.01 mM Mg^{++}. Cells were imaged every 5 min; images from every 30 min are shown.

(B) Mean cell growth (% growth / min.) for wild-type cells at each time point. Line represents the linear best fit. Cells were grown in M9 with 50 mM Mg^{++} and then imaged on M9 agarose pads with 0.01 mM Mg^{++}. These data were used to calculate the dilution rate, as required for assessing promoter activity (Methods).

(C) Plots of promoter activity following the same shifts in extracellular Mg^{++} used in Figure 1C.

Although YFP levels did not peak until ~80 min after shifting cells to medium with low Mg^{++}, the *mgrB* promoter responds within minutes. To gauge promoter activity, we calculated the approximate slope of the YFP:CFP profile as a function of time, taking into account dilution from cell growth, as done previously (Levine et al., 2012) (Fig. 2.2). The promoter activity increased within minutes with the largest value occurring ~40 minutes after cells were shifted from high to low Mg^{++} (Fig. 2.2C). Given that the maturation time for YFP is ~15-20 minutes (Iizuka et al., 2011; Miyashiro and Goulian, 2007b), we infer that cells respond within minutes to the change in extracellular Mg^{++}.

Partial adaptation of the PhoQ-PhoP system also occurred after other changes in stimulus levels (Fig. 2.1C, Appendix 1). Cells shifted from 2 to 0.01 mM extracellular Mg^{++} started at a higher initial YFP:CFP ratio, as expected, but still showed a partial adaptation and reached the same steady-state as cells shifted from 50 to 0.01 mM. Cells shifted from 50 to 2 mM extracellular Mg^{++} exhibited a slower initial increase in the YFP:CFP ratio and reached a lower maximum than when shifted to 0.01 mM Mg^{++}, and did not show significant partial adaptation after the maximum was reached, suggesting that strong activation of the PhoQ-PhoP system is necessary for a full impulse response.

A partial adaptation of the PhoQ-PhoP system did not occur for cells shifted from 50 to 10 mM extracellular Mg^{++} (Fig. 2.1C, Appendix 1). These cells exhibited a much smaller increase in the YFP:CFP ratio than when shifted to 0.01 mM Mg^{++}, and reached a new steady-state without any apparent adaptation or non-monotonic behavior in the YFP:CFP ratio suggesting that the partial adaptation occurs following major shifts in extracellular Mg^{++} levels. Finally, to confirm that all of the dynamics documented here depend on PhoQ-PhoP and are not a non-specific effect of shifting cells to medium with lower extracellular Mg^{++}, we examined the YFP:CFP ratio in Δ*phoQ* cells (Fig. 2.3). In this case no significant increase in the YFP:CFP ratio was observed after a shift to low Mg^{++} conditions. To confirm that there was no change in YFP:CFP ratio in Δ*phoQ* cells below the detection limit for our exposure settings, we also examined these Δ*phoQ* cells with 500 msec (instead of the usual 100 msec) exposure time (Fig. 2.3, right). Again, we saw no change in YFP:CFP ratio.

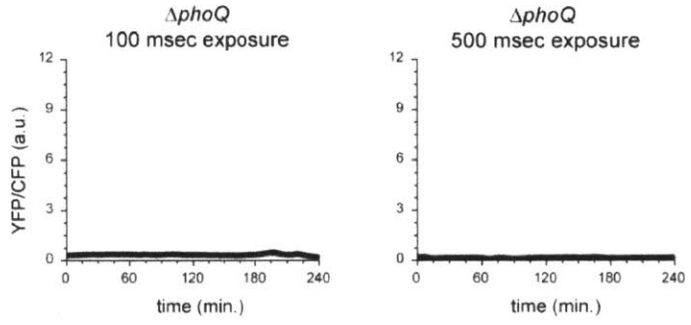

Figure 2.3. The activation of P_{mgrB} is PhoQ dependent.

Quantification of PhoP activity following a shift in the extracellular Mg^{++} concentration, as noted above each panel. Cells harbored the P_{mgrB}-*yfp* reporter and a Δ*phoQ* mutation. The left and right panels represent data from two independent experiments with exposure times 100 msec and 500 msec, respectively.

An MgrB-dependent negative feedback loop is necessary for partial adaptation

We hypothesized that partial adaptation results from the induction of MgrB (note that the P_{mgrB} reporter is integrated on the *E. coli* chromosome without disrupting the native *mgrB* locus). MgrB was previously shown to negatively regulate PhoP-dependent gene expression at steady-state (Lippa and Goulian, 2009), but how it affects the temporal dynamics of PhoQ-PhoP signaling was unknown. To test its role, we deleted *mgrB* from the fluorescent reporter strain used for time-lapse microscopy and then shifted cells from high (50 mM) to low (0.01 mM) extracellular Mg^{++} and again imaged individual cells on agarose pads. These Δ*mgrB* cells retained signal responsiveness, again exhibiting a rapid induction of YFP within ~20 minutes, but they reached substantially higher YFP:CFP levels and no longer displayed the partial adaptation seen in wild-type cells (Fig. 2.4A, Appendix I). As with wild-type cells, individual Δ*mgrB* cells exhibited modest variability around an average temporal profile (Appendix I), and the lack of partial adaptation was observed in experimental replicates (Fig. 2.4B, Appendix I). Using data from independent replicates for both wild-type and Δ*mgrB* cells, we found that the ratio of the final YFP:CFP value to the maximal YFP:CFP value was significantly different between the two strains, with a ratio of 0.58 +/- 0.067 (n = 5) for the wild type and 0.87 +/- 0.021 (n = 3) for Δ*mgrB* ($p = 0.00042$, Student's two-tailed t-test). These findings support the notion that MgrB represses the expression of PhoP-dependent targets (Lippa and Goulian, 2009), and indicate that an MgrB-mediated negative feedback loop is necessary for the partial adaptation of the PhoQ-PhoP system in *E. coli*. To rule out the possibility that partial adaptation was not observed in Δ*mgrB* cells simply because YFP levels were higher than the wild-type cells throughout the experiment and so

possibly saturated, we also examined Δ*mgrB* cells following a shift from 50 mM Mg^{++} to an intermediate (10 mM) level of Mg^{++} (Fig. 2.4C). In this case the Δ*mgrB* cells reached a steady-state YFP level comparable to that seen for wild-type cells shifted to 0.01 mM Mg^{++}, but still lacked partial adaptation.

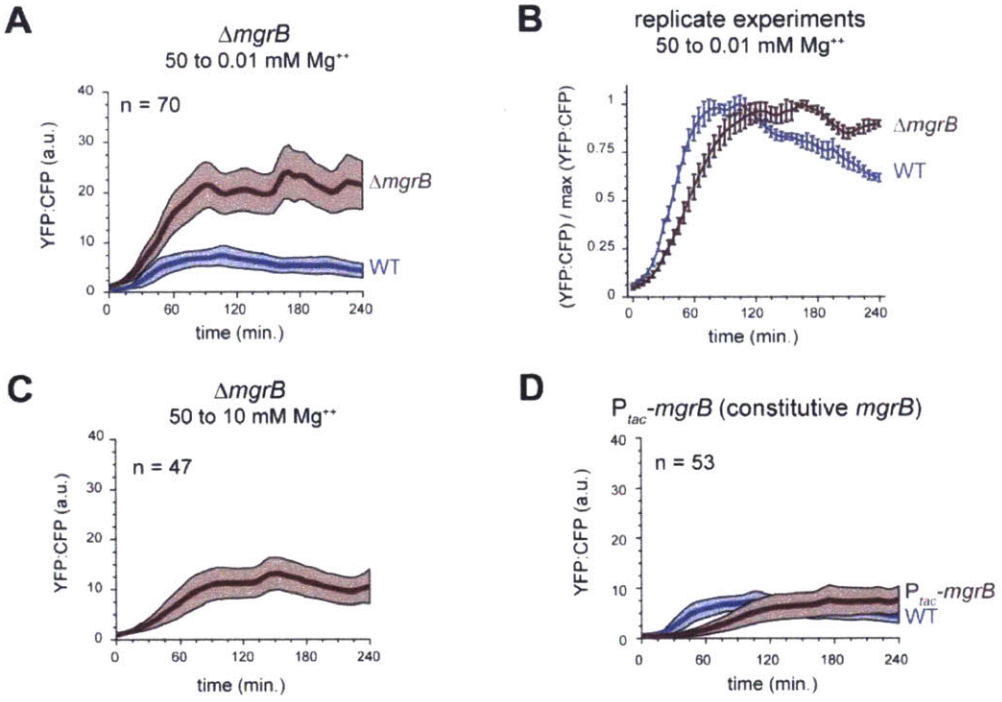

Figure 2.4. An MgrB-dependent negative feedback loop is necessary to drive partial adaptation by inhibiting the PhoQ kinase reaction.

(A, C, D) Quantification of PhoP-dependent expression in the mutant strains indicated. The wild-type profile from Fig. 1 is shown for comparison in panels A and D. Cells were grown in 50 mM Mg^{++} M9 culture and then shifted to M9 agarose pads containing (A) 0.01 mM Mg^{++}, (C) 10 mM Mg^{++}, or (D) 0.01 mM Mg^{++} + 0.25 mM IPTG.

(B) The mean and standard error YFP:CFP ratio for experimental replicates for wild-type (n = 5) and Δ*mgrB* (n = 3) cells grown in 50 mM Mg^{++} M9 culture then shifted to M9 agorse pads containing 0.01 mM Mg^{++}.

Collectively, our data support the following model. When cells are grown in a high Mg^{++} environment, the balance of PhoQ kinase and phosphatase activities is such that most PhoP exists in the unphosphorylated state. When Mg^{++} levels drop substantially, the proportion of PhoQ molecules in a kinase state increases, resulting in a rapid increase

in PhoP~P, which promotes the production of MgrB and other PhoP targets. As MgrB accumulates, it binds PhoQ and either promotes phosphatase activity or inhibits kinase activity, thereby causing a partial decrease in PhoP~P levels. A new steady state is reached when the rate of MgrB production is balanced by the rate of YFP degradation and dilution.

This model predicts that if MgrB were constitutively produced, cells should also no longer exhibit the same partial adaptation seen when *mgrB* transcription is regulated by PhoP~P. To test this prediction, we constructed a strain containing an IPTG-inducible P_{tac}-*mgrB* construct in place of the native, PhoP-dependent, *mgrB* locus. When cells grown in minimal medium with 0.25 mM IPTG were shifted from high to low extracellular Mg^{++}, the PhoP-dependent YFP reporter did not exhibit any obvious partial adaptation (Fig. 2.4D, Appendix I). Cells were, however, still signal responsive, indicating that the number of PhoQ molecules in a kinase state still increases following a shift to lower Mg^{++} conditions. The post-shift, steady-state YFP:CFP ratio was higher when *mgrB* was produced constitutively than in wild-type cells, likely reflecting differences in the strength of the P_{tac} and P_{mgrB} promoters.

MgrB inhibits the kinase activity of PhoQ

We next sought to determine whether MgrB reduces PhoP~P levels by inhibiting the PhoQ kinase reaction (by disrupting autophosphorylation or phosphotransfer) or by stimulating PhoQ phosphatase activity. To distinguish between these two possibilities, we sought to examine the induction kinetics of a strain producing PhoQ(T281R), a variant that should have little to no activity as a phosphatase for PhoP~P, but that retains its ability to phosphorylate PhoP (Miyashiro and Goulian, 2008; Ram and

Goulian, 2013). If MgrB promotes the phosphatase activity of PhoQ, deleting *mgrB* should have no effect on cells producing PhoQ(T281R). Conversely, if MgrB inhibits the kinase activity of PhoQ, deleting *mgrB* should effect signaling in cells producing PhoQ(T281R).

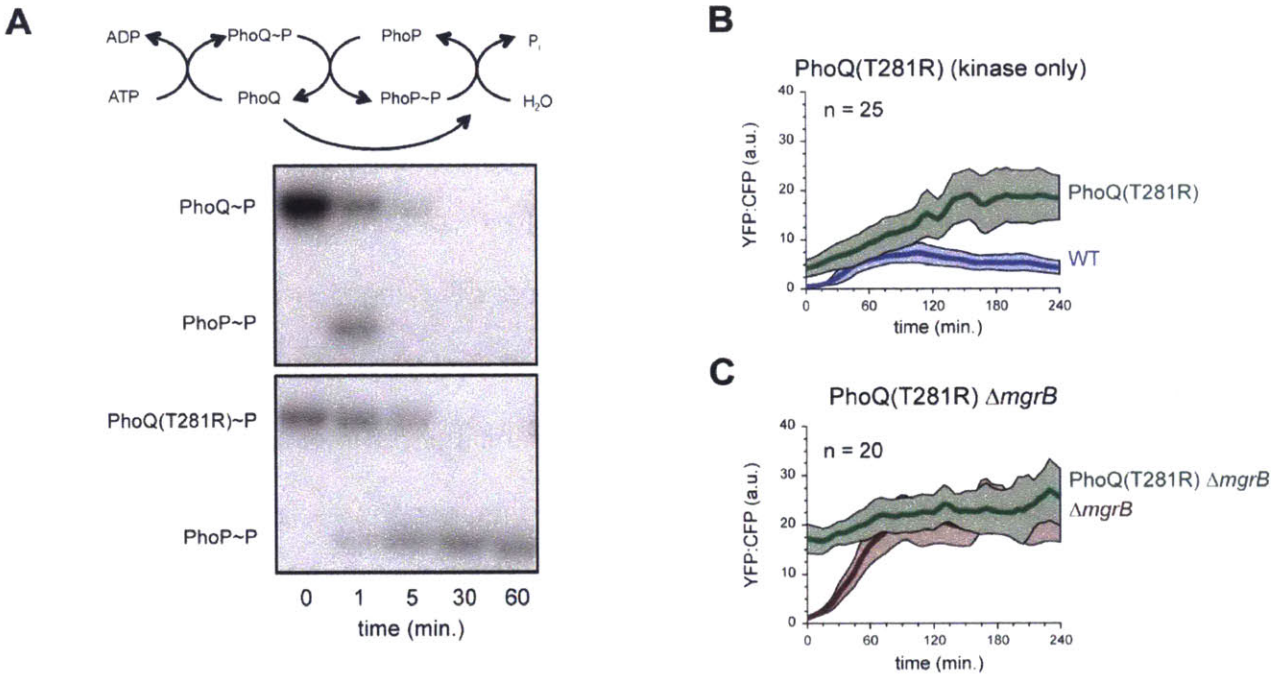

Figure 2.5. MgrB inhibits the PhoQ kinase activity to drive partial adaptation.

(A) (Top) Diagram summarizing the phosphotransfer events that occur in the PhoQ-PhoP system. (Middle, Bottom) Phosphotransfer from autophosphorylated PhoQ or PhoQ(T281R) to PhoP.

(B-C) Quantification of PhoP-dependent expression in the mutant strains indicated. The wild-type profile from Fig. 1 is shown for comparison in panel B and Δ*mgrB* from Fig. 4 is shown in panel C for comparison. Cells were grown in 50 mM Mg^{++} M9 culture and then shifted to M9 agarose pads containing 0.01 mM Mg^{++}. (C) PhoQ(T281R) (green), (D) PhoQ(T281R) + Δ*mgrB* (green).

We first confirmed that the T281R substitution in PhoQ selectively ablates its phosphatase activity *in vitro* (Fig. 2.5A). We purified the cytoplasmic portion of wild-type PhoQ and a variant harboring the T281R substitution. Each construct was autophosphorylated with [γ-^{32}P]-ATP for 1 hour and then incubated with PhoP. Wild-type PhoQ rapidly transferred radiolabelled phosphoryl groups to PhoP, leading initially to a

decrease in PhoQ~P levels and a concomitant increase in PhoP~P. At longer time points, the phosphorylated PhoP band disappeared. This dephosphorylation of PhoP~P is dependent on PhoQ phosphatase activity as PhoP~P alone is relatively stable against hydrolysis (Miyashiro and Goulian, 2008). Note that this apparent adaptation *in vitro* arises because ATP is not regenerated or maintained over the course of the reaction, so PhoQ ends up bound to ADP and in a phosphatase state. Like the wild-type construct, PhoQ(T281R) was also capable of autophosphorylating and transferring phosphoryl groups to PhoP, but, in contrast to the wild-type protein, it could not efficiently dephosphorylate PhoP, manifesting in the retention of PhoP~P at later time points. These data are consistent with prior studies on PhoQ (Miyashiro and Goulian, 2008) and indicate that the PhoQ(T281R) variant retains kinase activity but lacks phosphatase activity.

We then engineered a strain harboring the P_{mgrB}-*yfp* reporter to produce PhoQ(T281R) from the native *phoQ* locus in an otherwise wild-type background and used time-lapse microscopy to examine PhoP~P activity in individual cells, as above (Fig. 2.5B, Appendix I). In this strain, there were already higher levels of YFP, compared to the wild type, before cells were switched from high to low extracellular Mg^{++} growth conditions. The expression of YFP was induced further by the switch to low Mg^{++}, but, unlike in wild-type cells, YFP levels did not decrease after reaching their maximum. This finding indicates that the ability of PhoQ to dephosphorylate PhoP~P is necessary for partial adaptation. Additionally, because PhoP~P target gene expression was elevated in the initial, high Mg^{++} environment, we conclude that the PhoQ phosphatase reaction is also required to completely shut off PhoP in high Mg^{++} conditions.

Although these results indicate that PhoQ must harbor phosphatase activity for partial adaptation to occur, they do not reveal whether MgrB promotes PhoQ phosphatase activity or inhibits PhoQ kinase activity. To address this issue, we examined expression dynamics in a strain producing PhoQ(T281R) and lacking *mgrB* (Fig. 2.5C, Appendix I). In this strain, PhoP~P target gene expression at t = 0 minutes was very high, increasing further after shifting cells to medium with low Mg^{++}. Importantly, because PhoP~P target gene expression was higher in PhoQ(T281R) Δ*mgrB* cells relative to the PhoQ(T281R) single mutant, we conclude that MgrB normally inhibits the kinase activity of PhoQ. If MgrB had promoted the phosphatase activity of PhoQ, we would have expected no effect of deleting *mgrB* in a strain producing PhoQ(T281R), which lacks phosphatase activity.

Taken together, our data support a model in which regulated changes in PhoQ bifunctionality drive the temporal dynamics of PhoP target gene induction. When cells are growing in a high Mg^{++} environment, PhoQ exists primarily in the phosphatase state, preventing the accumulation of PhoP~P and its target genes. Any residual kinase activity is further blocked by low levels of MgrB. Upon Mg^{++} limitation or starvation, the kinase activity of PhoQ increases significantly, driving PhoP phosphorylation. The increase in PhoP~P then drives MgrB production, which feeds back to inhibit the PhoQ kinase reaction while allowing PhoQ to continue acting as a phosphatase, producing the partial adaptation observed.

MgrB masks the effects of a PhoP-dependent positive feedback loop

While PhoP~P initiates a negative feedback loop by promoting *mgrB* expression, it also drives a positive feedback loop by promoting expression of the *phoPQ* operon from one

of its two promoters (Fig. 2.1A). The P2 promoter is constitutively active whereas P1 contains a PhoP binding site that allows PhoP~P to boost the expression of the *phoPQ* operon (Miyashiro and Goulian, 2008). To verify positive autoregulation, we monitored expression of *phoPQ* in individual cells using a P_{phoPQ}-*yfp* reporter integrated on the chromosome (Fig. 2.6A, Appendix I). As with P_{mgrB}-*yfp*, expression of the P_{phoPQ}-*yfp* reporter peaked approximately 60-80 minutes after a shift from high to low Mg^{++} conditions and then subsequently decayed to a new steady state. This partial adaptation mirrored that seen with the P_{mgrB} reporter and is consistent with the *phoPQ* promoter being directly regulated by PhoP~P. As with the P_{mgrB} reporter, the partial adaptation was dependent on *mgrB* (Fig. 2.6B-C, Appendix I). The magnitude of YFP levels for the *phoPQ* reporter were lower than for *mgrB*, consistent with prior studies (Miyashiro and Goulian, 2007a).

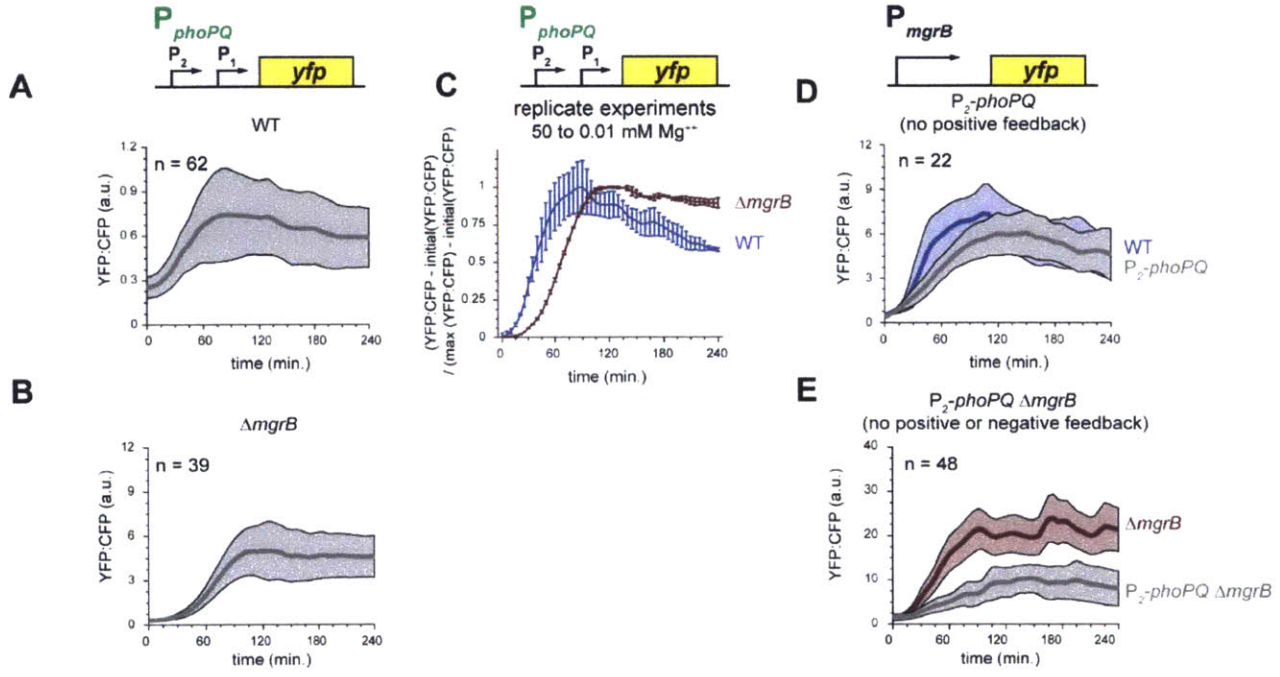

Figure 2.6. MgrB suppresses the effects of a PhoQ-PhoP positive feedback loop.

(A-B) Quantification of PhoP activity using a P_{phoPQ}-*yfp* reporter in otherwise WT (A) or Δ*mgrB* cells (B), presented as in Figure 1. Cells were grown in M9 with 50 mM Mg^{++} and then shifted to agarose pads made of M9 with 0.01 mM Mg^{++}. (C) The mean and standard error YFP:CFP ratio for experimental replicates for wild-type (n = 2) and Δ*mgrB* (n = 2) cells grown in 50 mM Mg^{++} M9 culture then shifted to M9 agorse pads containing 0.01 mM Mg^{++}. (D-E) Quantification of PhoP activity using a P_{mgrB}-*yfp* reporter in a strain harboring a mutation in the PhoP binding site in promoter P1 for *phoPQ* and otherwise wild type (D) or also harboring a Δ*mgrB* mutation (E). The wild-type profile from Fig. 2.1 and the Δ*mgrB* profile from Fig. 2.4 are shown for comparison in panels D and E, respectively.

To assess how the positive transcriptional feedback loop contributes to the kinetics of PhoP-dependent gene expression, we compared a wild-type strain harboring the P_{mgrB}-*yfp* reporter to a strain in which the PhoP binding site upstream of *phoPQ* was eliminated (Miyashiro and Goulian, 2008). There were subtle differences in the timing and maximal level of YFP:CFP between the wild-type and promoter mutant strains, but the dynamics of the P_{mgrB}-*yfp* reporter were generally similar for these two strains (Fig. 2.6D, Appendix I). This result is consistent with other studies which have shown that the PhoQ-PhoP positive feedback loop has subtle effects on the output of the pathway (Miyashiro and Goulian, 2008). We also examined the role of MgrB in a strain lacking the positive feedback loop (Fig. 2.6E, Appendix I). As in wild-type cells, deleting *mgrB* in a strain lacking the PhoP binding site upstream of *phoPQ* eliminated partial adaptation and led to substantially higher levels of YFP induction throughout a time-lapse experiment. Taken together, our results indicate that the induction of MgrB normally limits PhoP activity by (i) inhibiting PhoQ kinase activity and (ii) suppressing a positive feedback loop that would otherwise drive the accumulation of PhoQ and PhoP and produce a stronger induction of PhoP-dependent genes.

SafA does not contribute substantially to partial adaptation

SafA is another small membrane protein that directly interacts with PhoQ (Eguchi et al., 2007, 2012). Unlike MgrB, SafA is thought to positively regulate the PhoQ-PhoP system

(Fig. 2.7A). Expression of *safA* depends on the EvgS-EvgA two-component system, not PhoQ-PhoP. Because PhoQ-PhoP does not regulate the expression of *safA*, we initially assumed it would be expressed at a constant level, and, therefore, would not affect the partial adaptation of PhoP target genes.

To test this assumption, we engineered a strain in which the *safA* promoter drives YFP, and the *tetA* promoter constitutively drives CFP. Using this strain, we followed the same approach as with the P_{mgrB}-*yfp* reporter strain; we grew cells in liquid medium with high Mg^{++} and transferred them to agarose pads with low Mg^{++} for time-lapse microscopy. Although the YFP:CFP ratio changed modestly throughout the course of the experiment, it never reached a level appreciably above background noise (Fig. 2.7A-B). These results suggest that SafA does not accumulate to significant levels upon shift from shaking culture to agarose pads

To test whether *safA* contributes to the temporal dynamics of PhoQ-PhoP target genes, we deleted *safA* from the P_{mgrB}-*yfp* reporter strain and examined the YFP:CFP ratio by time-lapse microscopy as cells transitioned from high to low Mg^{++} (Fig. 2.7B, Appendix I). The Δ*safA* cells did not appear substantially different from the wild-type reporter strain, indicating that SafA has relatively small effects, if any, on the PhoQ-PhoP pathway in these conditions, particularly compared to MgrB. A double deletion of *safA* and *mgrB* also behaved similarly to the single *mgrB* deletion supporting the notion that *safA* has little to no effect on PhoQ-PhoP signaling in the conditions tested here (Fig. 2.7D, Appendix I).

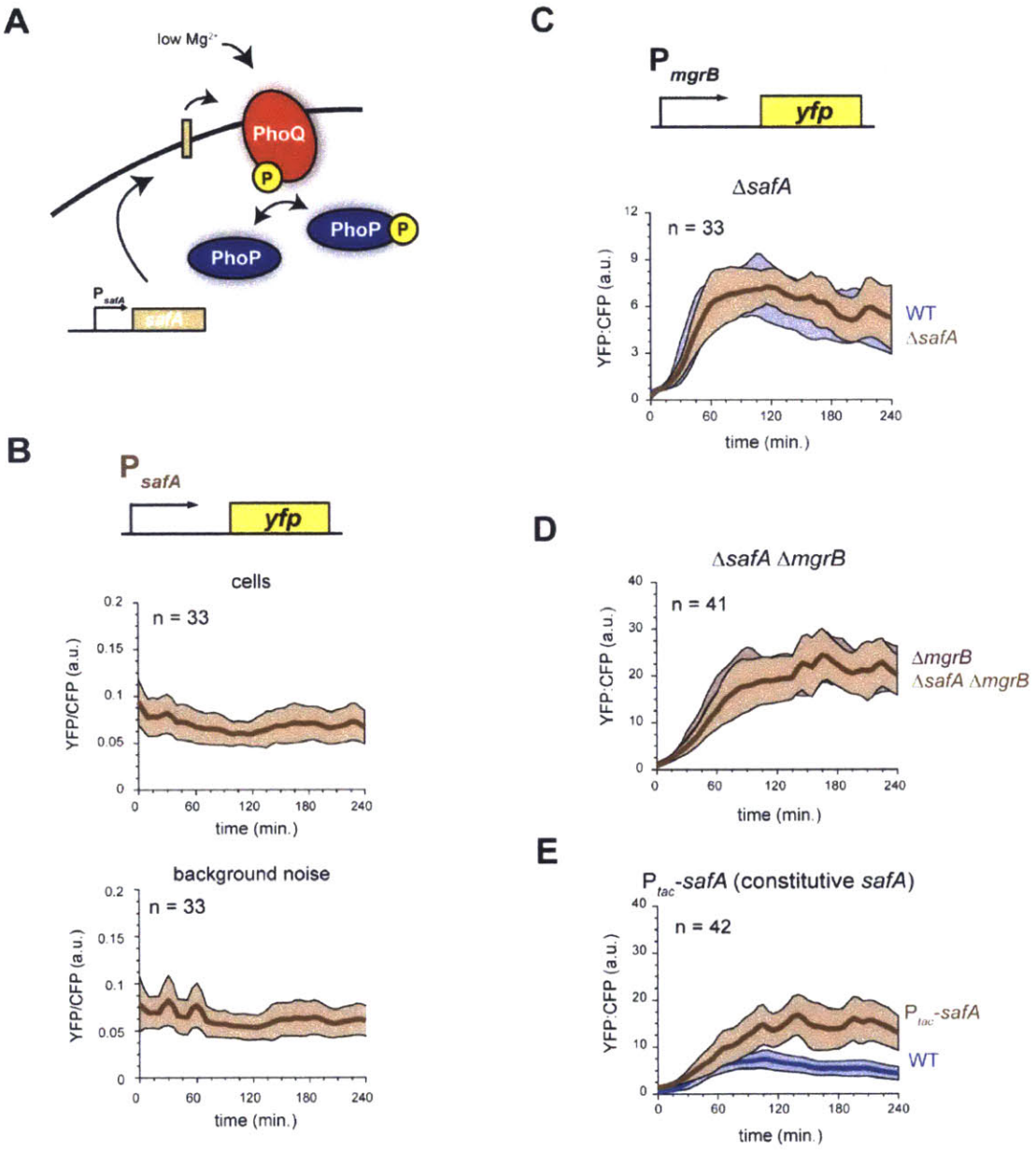

Figure 2.7. SafA does not substantially contribute to PhoP activity or pathway adaptation following a change in extracellular Mg^{++}.

(A) Schematic of the effect of SafA on the PhoQ-PhoP system. *safA* encodes a small membrane protein that binds PhoQ and stimulates output from the PhoQ-PhoP system.

(B) Quantification of P_{safA} activity. YFP is produced from the *safA* promoter and CFP is produced from a constitutive *tetA* promoter. (Top) Cells were grown in M9 culture with 50 mM Mg^{++} and then imaged on M9 agarose pads with 0.01 mM Mg^{++}. (Bottom) Background YFP:CFP signal of time-lapse microscopy for experiment in panel A.

(C-E) Quantification of PhoP activity using a P_{mgrB}-*yfp* reporter in a Δ*safA* (B), Δ*safA* Δ*mgrB* (C), or P_{tac}-*safA* (D) strain with the WT or Δ*mgrB* profiles shown for comparison. In each case, cells were grown in M9 with 50 mM Mg^{++} and then shifted to M9 agarose pads with 0.01 mM Mg^{++}.

Although SafA expressed from its native promoter did not affect PhoQ-PhoP target expression kinetics in our conditions, cells engineered to constitutively produce SafA from a P_{tac} promoter showed significantly higher induction of the P_{mgrB}-*yfp* reporter (Fig. 2.7E, Appendix I). In these cells, expression of the P_{mgrB}-*yfp* reporter increased steadily until reaching a maximum much later than wild-type after the shift to low Mg^{++} conditions. This maximal level was approximately two-fold higher than that reached in the wild-type strain. These data are consistent with SafA being an activator of the PhoQ-PhoP system. Furthermore, SafA does not appear to disrupt the interaction between MgrB and PhoQ, because the YFP:CFP ratio for the SafA overexpression experiment does not activate as quickly as the double deletion of *mgrB* and *safA*. Finally, our results are consistent with *in vitro* studies showing that SafA promotes PhoQ kinase activity rather than inhibiting phosphatase activity (Ishii et al., 2013). Deleting *safA* had essentially no effect on the initial levels of the PhoP-dependent reporter when PhoQ is primarily in a phosphatase state, and constitutive expression of SafA only boosted expression after cells were shifted to a condition where PhoQ is predominantly a kinase.

PhoQ performs multiple rounds of autophosphorylation *in vitro*

Our results favor a model in which partial adaptation depends primarily on a negative feedback loop in which PhoP~P drives production of the small protein MgrB, which inhibits PhoQ kinase activity. However, incubating PhoQ and PhoP with ATP *in vitro* can also produce an apparent partial adaptation even without MgrB (Fig. 2.5A). This

observation led to an alternative model in which adaptation stems from an "intrinsic" negative feedback loop functioning independent of MgrB (Yeo et al., 2012). This model posits that ADP has very slow association and dissociation rates for PhoQ so that after an initial round of autophosphorylation and phosphotransfer, PhoQ would become locked in an ADP-bound state, promoting PhoP~P dephosphorylation and preventing subsequent rounds of autophosphorylation and phosphotransfer.

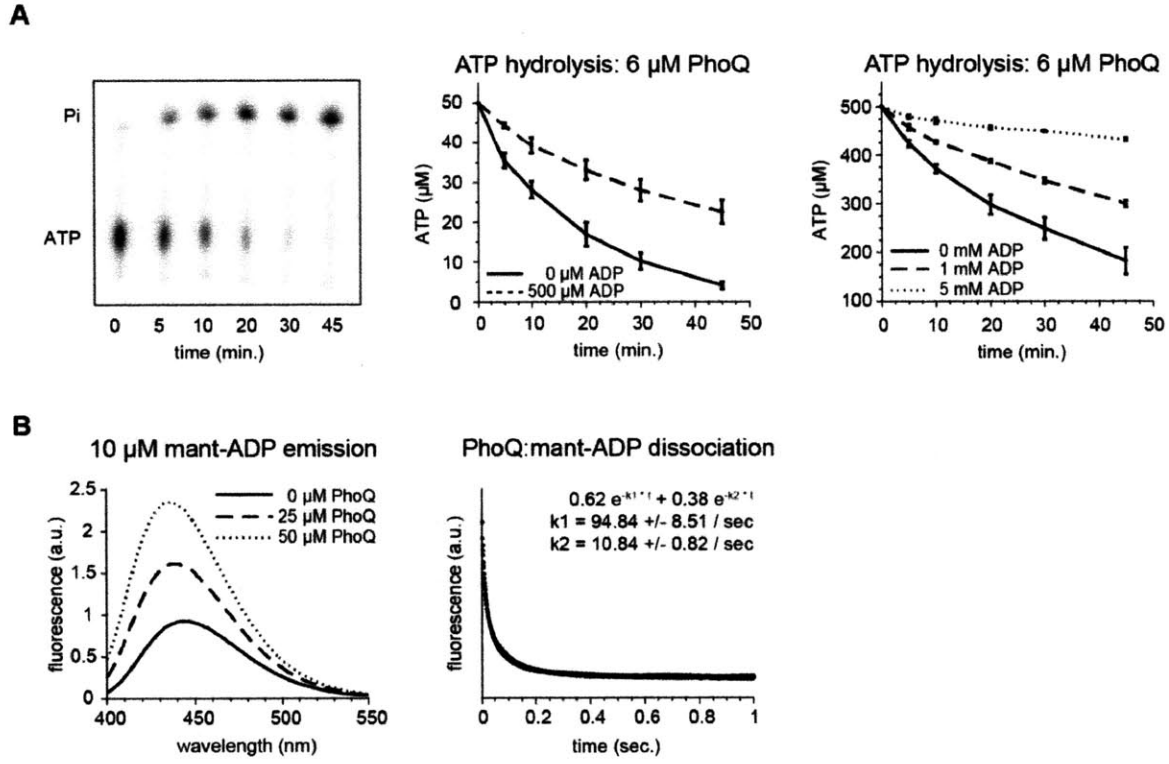

Figure 2.8. The ADP produced by PhoQ autophosphorylation is readily exchanged and does not inactivate PhoQ.

(A) (Left) Time course of 50 μM ATP hydrolysis by 6 μM PhoQ, as measured by thin-layer chromatography. (Middle) Mean and standard error of PhoQ mediated 50 μM ATP hydrolysis in the absence or presence of 500 μM ADP (n = 2). (Right) Mean and standard error of PhoQ mediated 500 μM ATP hydrolysis in the presence of 0, 1, or 5 mM ADP (n = 3).

(B) (Left) Steady-state emission spectra following 356 nm excitation for 10 μM mant-ADP incubated with 0, 25, or 50 μM PhoQ. (Right) Plot of fluorescence (> 400 nm) over time after mixing 10 μM mant-ADP and 50 μM PhoQ with 50 mM ADP. The decrease in fluorescence from three traces was fit to a double exponential decay curve with time constants 94.84 +/- 8.51 / sec and 10.87 +/- 0.82 / sec.

To test whether PhoQ is limited to one cycle of autophosphorylation and phosphotransfer, we first monitored the amount of ATP hydrolyzed by PhoQ *in vitro* using thin-layer chromatography (Fig. 2.8A). For these experiments, we use a His_6-MBP-tagged PhoQ construct lacking its transmembrane domains, hereafter referred to as PhoQ for simplicity; as shown above, this construct harbors both kinase and phosphatase activities (Fig. 2.5A). After 45 minutes, 6 μM PhoQ had hydrolyzed ~50 μM ATP to completion (Fig. 2.5A middle) and ~ 300 of 500 uM ATP (Fig 2.5A right), indicating that individual PhoQ molecules must be performing multiple rounds of ATP-dependent autophosphorylation, with hydrolysis of the His~P presumably occurring after each round as no PhoP was added to this reaction. This result implies that ADP likely does not remain in the nucleotide binding pocket of PhoQ after autophosphorylation to permanently inhibit subsequent ATP hydrolysis reactions. Additionally, we found that PhoQ autophosphorylation was inhibited significantly by adding free ADP to the reaction, indicating that ADP that is not the result of PhoQ mediated ATP hydrolysis can directly bind to the PhoQ nucleotide binding pocket.

We also sought to directly measure the dissociation rate of PhoQ and ADP using the fluorescent nucleotide mant-ADP (Fig. 2.8B). First, to confirm that PhoQ binds this ADP derivative, we measured the emission spectrum (following excitation at 356 nm) of 10 μM mant-ADP incubated with or without PhoQ. In the presence of 25 μM PhoQ, the intensity of the fluorescence from mant-ADP increased, and the center of mass of the emission spectrum shifted downward. The fluorescence intensity and center of mass changed further in the presence of 50 μM PhoQ indicating that the K_D of PhoQ and mant-ADP is relatively high, consistent with previous estimates for the K_D for PhoQ and

ADP of 80-100 μM (Yeo et al., 2012). To directly measure the PhoQ:mant-ADP dissociation rate, 50 μM PhoQ and 10 μM mant-ADP were incubated at room temperature for 1 hr and then mixed at a 1:1 ratio with 50 mM ADP. Fluorescence was monitored over time, with the decrease in signal resulting from dissociation of mant-ADP. The decrease observed fit a double exponential decay curve, suggesting that there are two dissociation rates for PhoQ and mant-ADP, possibly reflecting the dimeric nature of PhoQ. Both time constants (93.13 and 10.75 /sec) are relatively fast, indicating that the dissociation of ADP from PhoQ is rapid and such that PhoQ likely does not become trapped with ADP after autophosphorylation.

We conclude that a standard *in vitro* phosphotransfer reaction containing PhoQ and PhoP undergoes multiple rounds of autophosphorylation and phosphotransfer, with bands corresponding to both proteins visible by autoradiography. As the initial amount of phosphorylated PhoQ depletes, PhoQ-ADP also accumulates, leading to PhoP dephosphorylation and an apparent partial (or even complete) adaptation (Fig. 2.5). Similar behavior has been seen with a wide range of two-component signaling proteins *in vitro* as standard reactions do not replenish labeled ATP (Skerker et al., 2005). Furthermore, because the phosphatase rate of phosphorylated PhoP by PhoQ is faster than the rate of PhoQ autophosphorylation *in vitro*, it is not expected that the phosphorylated PhoP band should be observed for large lengths of time (Sanowar and Le Moual, 2005). In total, our data indicate that partial adaptation in the PhoQ-PhoP system is not due to a slow dissociation rate between PhoQ and ADP, but due to MgrB.

Discussion

E. coli, like many γ-proteobacteria, relies on the PhoQ-PhoP signaling pathway to respond to low extracellular Mg^{++}, changes in pH, and certain antimicrobial peptides. Our data support the following model (Fig. 2.1A and Fig. 2.9). In the absence of a stimulus, most PhoQ molecules in the cell are likely in a phosphatase state. In cells shifted rapidly from high to low extracellular Mg^{++}, most PhoQ molecules switch to the kinase state, enabling autophosphorylation of the conserved histidine residue and the creation of a high-energy phosphoramidate that can engage in phosphotransfer with PhoP (Gao and Stock, 2009). Individual PhoQ molecules likely engage in multiple rounds of autophosphorylation of phosphotransfer leading to the accumulation of a substantial pool of phosphorylated PhoP that can stimulate the expression of target genes. Many PhoP target genes help cells respond to the initial stimulus, either affecting Mg^{++} homeostasis or cell envelope composition (Kato and Groisman, 2008).

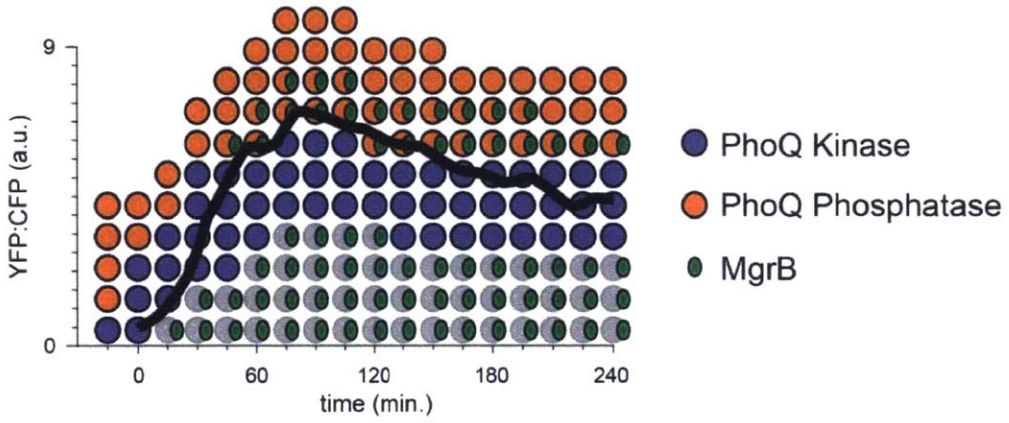

Figure 2.9. Model of PhoQ-PhoP temporal dynamics.

The amount of PhoQ in the kinase and phosphatase states (blue and orange circles) and MgrB (green oval) as a function of time after a shift to low Mg^{++} conditions is summarized. Faded blue circles represent PhoQ in the kinases state inhibited by MgrB. The black line represents the mean output from the PhoP-dependent *mgrB* promoter following a shift from 50 to 0.01 mM Mg^{++} (see Figure 2.1).

Active PhoP also initiates two feedback loops, one positive and one negative. By binding the P1 promoter, PhoP~P increases expression of *phoQ* and *phoP*. The additional PhoQ molecules produced are presumably biased to being in a kinase state if cells are still experiencing low Mg^{++} conditions, leading to increased PhoP activation. Concomitantly however, PhoP also drives expression of *mgrB*, which can feedback and inhibit the kinase activity of PhoQ. These MgrB-inhibited PhoQ molecules can continue to act as phosphatases for phosphorylated PhoP. This negative feedback therefore limits the output of the system and leads to a partial adaptation of PhoP target proteins such that they reach a final steady-state intermediate between the initial and maximal values, approximately 2 hrs after the initial transition in growth conditions. The temporal dynamics of PhoP-dependent gene expression is ultimately a product of the properties of individual components in the system, particularly the bifunctional nature of PhoQ, as well as the feedback loops created by PhoP directly regulating itself, *phoQ*, and *mgrB*.

Histidine kinase bifunctionality and the mechanism of inhibition by MgrB

Most histidine kinases are likely bifunctional, acting effectively as kinases and phosphatases for their cognate response regulators. For PhoQ the phosphatase activity is likely important in the absence of a stimulus to prevent the inappropriate activation of PhoP and its target genes, as was previously reported for the EnvZ-OmpR and CpxA-CpxR two-component systems (Siryaporn and Goulian, 2008). Consistent with this notion, we found that in cells lacking PhoQ phosphatase activity, the expression of our P_{mgrB} reporter was significantly higher even before cells were shifted to low extracellular Mg^{++}. Phosphatase activity and bifunctionality may also prevent bimodality in pathway

output, possibly because histidine kinases lacking bifunctionality are inefficient at turning off their cognate regulator after a stimulus is no longer present (Ram and Goulian, 2013).

Our results indicate that the bifunctionality of PhoQ is also critical to generating the non-monotonic temporal dynamics of PhoP target gene expression. Cells in which the phosphatase activity of PhoQ was selectively ablated, by producing PhoQ(T281R), did not show a partial adaptation in PhoP-dependent gene expression as in wild-type cells. Importantly, combining the PhoQ(T281R) mutant with an *mgrB* deletion led to even higher levels of PhoP target gene expression compared to either mutation alone. This result implies that MgrB inhibits the kinase activity of PhoQ rather than promoting the phosphatase activity. If MgrB worked by suppressing phosphatase activity, deleting it would have had little to no effect, in terms of PhoP activity, on cells producing PhoQ(T281R). Precisely how MgrB inhibits the kinase activity of PhoQ is not clear yet. Formally, MgrB could be inhibiting the autophosphorylation reaction or phosphotransfer to PhoP, or both. We favor the former possibility given that MgrB resides in the inner membrane and is thought to interact with PhoQ via their periplasmic domains (Lippa and Goulian, 2009). MgrB may stabilize or promote a conformation of the periplasmic domain of PhoQ that locks the cytoplasmic domains in a configuration incompatible with autophosphorylation.

Whether other histidine kinases are regulated by small proteins like MgrB remains to be shown. However, there is increasing evidence that many bacteria encode large numbers of small proteins that are often missed by conventional annotation methods

(Storz et al., 2014). Many of these proteins localize to the membrane where they could be regulating bifunctional histidine kinases.

Positive autoregulation

Many two-component signaling pathways are subject to positive transcriptional autoregulation (Goulian, 2010), but the function and importance of such feedback remains uncertain. Positive autoregulation for PhoQ-PhoP has only modest effects on the dynamics and steady-state behavior of PhoP target gene expression, at least in the presence of MgrB (Miyashiro and Goulian, 2008; Shin et al., 2006) (Fig. 2.6). However, the elimination of positive autoregulation had a much more substantial effect on cells lacking *mgrB* (Fig. 2.6D). Thus, at least for PhoQ-PhoP, the presence of MgrB effectively masks some of the effects of positive transcriptional autoregulation. In other two-component pathways lacking a negative regulator like MgrB, autoregulation may have a more substantial effect on signaling output. Indeed, recent work on the PhoR-PhoB system in *E. coli* demonstrated that positive autoregulation was critical to tuning PhoR-PhoB levels in phosphate-replete and phosphate-deplete conditions (Gao and Stock, 2013a).

Concluding remarks

Although two-component signaling pathways are often thought of as binary devices that are ON or OFF, there are more and more cases of complex temporal dynamics associated with these pathways. Partial adaptation like that seen for PhoQ-PhoP has been documented in other cases (Hutchings et al., 2006; Yamamoto and Ishihama, 2005). And, as noted earlier, some pathways such as the phosphorelay controlling

sporulation in *B. subtilis* exhibits multiple pulses. The physiological benefit, if any, of such non-monotonic responses to input stimuli remains uncertain. For *B. subtilis* sporulation, pulses were suggested to be part of a mechanism for setting a 'timer' that works over multiple cell cycles to defer sporulation (Levine et al., 2012). And in *Salmonella*, the partial adaptation observed for PhoP-dependent gene expression was suggested to be critical for virulence (Shin et al., 2006). However, assessing the role of temporal dynamics is difficult as mutations that eliminate specific features of a signaling pathway's dynamic response may also affect steady-state behavior or the integrated output. Nevertheless, complex outputs from two-component signaling pathways appear quite common suggesting that the temporal dynamics of these systems may help cells fine-tune their responses to a range of environmental stimuli.

Experimental Procedures

Growth conditions

All cells used in microscopy experiments were grown overnight in M9 minimal media (1x M9 salts, 100 μM $CaCl_2$, 0.2% glucose, 0.1% casamino acids) with 2 mM $MgSO_4$. Cultures were then back diluted into M9 at the desired concentration of $MgSO_4$ and grown for ~ 2-3 hours until cells were in mid-exponential phase. Cells transferred to 0.01 or 2 mM Mg^{++} for imagining were then pelleted at 8,000 rpm for 2 minutes and resuspended in phosphate buffer solution (PBS) three times to wash away extracellular Mg^{++}, while cells transferred to 10 mM Mg^{++} were imaged without washing. Cells were placed on ~ 80 μL agarose pads for microscopy (see the 'Time-lapse microscopy' below for details). Cells were grown at 37°C with shaking. Cells resistant to kanamycin were selected using 30 μg/ml in liquid culture and 50 μg/ml on agar plates.

Strain construction

Strains used are listed in Table S1. Strains generated for time-lapse microscopy were created starting from TIM210 (P_{mgrB} reporter) and TIM148 (P_{phoPQ} reporter). *mgrB, phoQ,* and *evgS* deletions were generated by P1 phage transduction from AML58 (*mgrB*) or the Keio knockout collection (*phoQ*) (Baba et al., 2006). The *safA* deletion was created by amplifying the FRT:*kan*:FRT segment from pKD13 with primers that had overlapping regions to the start and end of the *safA* coding region, and integrating the amplified DNA into the chromosome using λ Red-mediated recombination (Datsenko and Wanner, 2000). The *phoQ*(T281R) allele was transduced into reporter strains using P1 phage transduction from ML2205. To create ML2288, the strain lacking PhoQ-PhoP

positive autoregulation, the P_2-*phoPQ* promoter mutation was amplified from TIM45 and fused to the *kan* resistance cassette using single-overlap-extension PCR. This DNA fragment was integrated into TIM210 using λ Red-mediated recombination. Strains containing the IPTG inducible *mgrB* and *safA* were created by integrating the genes into pEXT20 (CGSC #12325) between the SacI and HindIII restriction sites. The promoter and gene segments were amplified and fused to the kanamycin resistance cassette from pKD13 and integrated into the chromosome using λ Red-mediated recombination. When constructing strains that had more than one of the modifications listed above, P1 phage transduction was used to transfer the mutations between strains. Strains created using P1 phage transduction that no longer contain kanamycin resistance were subjected to FLP-FRT recombination with standard protocols using pCP20 (Datsenko and Wanner, 2000). To create the reporter strain for the *safA* promoter, the 500 bp region upstream of *safA* was fused to the 5' end of *yfp* and integrated into pCAH63 (Haldimann and Wanner, 2001). The resulting plasmid was then integrated into the chromosome using standard protocols (Haldimann and Wanner, 2001), and transduced into TIM210 using P1 phage transduction.

Protein purification

Protein expression and purification were carried out as previously described (Skerker et al., 2005, 2008). Only the cytoplasmic portion (residues 238-486) of PhoQ and PhoQ(T281R) were used. The PhoQ(T281R) substitution was constructed using round-the-horn mutagenesis (Podgornaia and Laub, 2015).

In vitro phosphotransfer assays

To examine phosphotransfer kinetics from PhoQ to PhoP, PhoQ constructs were first autophosphorylated as above for 1 hr in HKEDG buffer (10mM HEPES-KOH pH 8.0, 50 mM KCl, 10% glycerol, 0.1 mM EDTA, 1 mM DTT) with 5 mM $MgCl_2$, 0.5 mM ATP, and ~2.5 μCi [γ^{32}P]-ATP from a stock at ~6000 Ci/mmol (Perkin Elmer) in a volume of 5 μL. Experiments were performed at 30°C. 5 μL PhoP in HKEDG with 5mM $MgCl_2$ was then added to the PhoQ autophosphorylation reaction to give a final concentration of 1 μM PhoQ (or PhoQ(T281R)) and 8 μM PhoP. Reactions were stopped as before by the addition of 4X loading buffer (500 mM Tris-HCl pH 6.8, 8% SDS, 40% glycerol, 400mM β-mercaptoethanol). Samples were analyzed by SDS-PAGE and phosphoimaging.

PhoQ:mant-ADP binding

Emission spectra were measured using a PTI QM-2000-4SE spectrofluorimeter (PTI). Binding of 10 μM mant-ADP (ThermoFisher) to PhoQ was assayed by changes in fluorescence emission in the range of 400-550 nm with excitation at 356 nm. PhoQ and mant-ADP were co-incubated in HKEDG with 5 mM $MgCl_2$. Experiments were performed at room temperature.

PhoQ and mant-ADP dissociation kinetics were measured using a KinTek Stopped-Flow Model SF-300X. 10 μM mant-ADP and 50 μM PhoQ were co-incubated in HKEDG with 5 mM $MgCl_2$, and then mixed with an equal volume of 50 mM ADP at room temperature to prevent rebinding between mant-ADP and PhoQ. 356 nm was used for the excitation wavelength and a 400 nm long-pass filter was used to detect signal.

Decreases in fluorescence signal from three experiments was fitted to a double exponential curve.

Time-lapse microscopy

A Zeiss Observer Z1 microscope with a 100x/1.4 oil immersion objective and an LED-based Colibri illumination system were used for phase and fluorescence microscopy. Cells were placed on M9-glucose +1.5% low-melting agarose pads with the indicated level of $MgSO_4$, after being pelleted at 8000 rpm for 2 minutes and resuspended in PBS three times to wash away excess Mg^{++}. Images were taken every 5 minutes with an exposure time of 100 msec (for the P_{mgrB} reporter) or 500 msec (for the P_{phoPQ} and P_{safA} reporters, as well as the P_{mgrB} reporter in cells lacking *phoQ*) for each fluorescence channel. The temperature of the pad was maintained at 30°C using the Zeiss Temp Module S1 and Heating Insert P S1, and automatic focusing was performed with the Zeiss Definite Tracking module. Timepoints that appeared out of focus were removed from the analysis. Segmentation and individual cell tracking were performed with MicrobeTracker (Sliusarenko et al., 2011) on a Linux platform. Only one daughter cell per division was tracked to avoid redundancy and bias, and only cells that continued replicating through the entire movie and were correctly identified by the MicrobeTracker alg4ecoli segmentation algorithm were analyzed. Approximately 95% of cells continuing growing and replicating throughout a typical time-lapse experiment. Total fluorescence and fluorescence density per cell were calculated from the YFP and CFP channels for each cell in each frame. Expression level of a given reporter is reported as a ratio of YFP to CFP density. The Lowess smoothing function in MATLAB was used to smooth fluorescence densities and YFP:CFP ratios. Cell size over time was also analyzed

through MicrobeTracker. Background noise of P_{safA} reporter time-lapse microscopy experiment was measured by loading mismatched fields between YFP and Phase channels (Fig. 2.7).

Promoter activity, P, was calculated as described previously (Levine et al., 2012). Briefly, $\frac{d(\frac{YFP}{CFP})}{dt} = P - \gamma(\frac{YFP}{CFP})$, where $\gamma = 1 - \frac{100}{100+(mean\ cell\ size\ increase(\%))}$ is the dilution factor, as determined by increase in cell size.

Thin-layer chromatography

6 μM PhoQ and the indicated amount of ATP and ADP (plus 2.5 μCi [γ^{32}P]-ATP) were incubated together at 37°C in HKEDG buffer with 5 mM $MgCl_2$. At the appropriate time points, the reactions were stopped with an equal volume of stop buffer (8 mM urea, 20 mM TrisCl, pH 7.5, 5mM EDTA). 2 μL of each stopped reaction was placed on a PEI-cellulose TLC plate. After the samples dried, the TLC plate was first run with water only to wash away urea buffer. After the plate was then dried again, it was run with 0.75 M KH_2PO_4 (pH 4.2) to separate ATP and P_i. The plates were then analyzed by phosphorimaging.

Table 1. Strains used

Strain	Genotype	Source
TIM210	*ΔlacZYA* attλ::[P_{mgrB}-YFP] attHK::[P_{tetA}-CFP]	(Miyashiro and Goulian, 2007a)
AML58	*ΔmgrB*::FRT:*kan*:FRT	(Lippa and Goulian, 2009)
ML2281	*ΔlacZYA* attλ::[P_{mgrB}-YFP] attHK::[P_{tetA}-CFP] *ΔmgrB*	This work

ML2205	*phoQ*(T281R):FRT:*kan*:FRT	(Podgornaia and Laub, 2015)
ML2583	*ΔlacZYA* attλ::[P_{mgrB}-YFP] attHK::[P_{tetA}-CFP] *phoQ*(T281R)	This work
ML2584	*ΔlacZYA* attλ::[P_{mgrB}-YFP] attHK::[P_{tetA}-CFP] *phoQ*(T281R) ΔmgrB	This work
TIM45	Δ(P_2P_1-*phoPQ*) Φ(P_{mgrB}-*yfp*) *attλ*::[P_2-*phoPQ*] *attHK*::[P_{tetA}-*cfp*]	(Miyashiro and Goulian, 2008)
ML2288	*ΔlacZYA* attλ::[P_{mgrB}-YFP] attHK::[P_{tetA}-CFP] FRT:*kan*:FRT:P_2-*phoPQ*	This work
ML2289	*ΔlacZYA* attλ::[P_{mgrB}-YFP] attHK::[P_{tetA}-CFP] P_2-*phoPQ*	This work
ML2290	*ΔlacZYA* attλ::[P_{mgrB}-YFP] attHK::[P_{tetA}-CFP] *ΔmgrB* P_2-*phoPQ*	This work
ML2282	*ΔlacZYA* attλ::[P_{mgrB}-YFP] attHK::[P_{tetA}-CFP] Δ*mgrB*::(FRT:*kan*:FRT:P_{tac} -*mgrB*)	This work
ML2585	*ΔsafA*::FRT:*kan*:FRT	This work
ML2586	*ΔlacZYA* attλ::[P_{mgrB}-YFP] attHK::[P_{tetA}-CFP] *ΔsafA*::FRT:*kan*:FRT	This work
ML2587	*ΔsafA*::(FRT:*kan*:FRT:P_{tac}-*safA*)	This work
ML2588	*ΔlacZYA* attλ::[P_{mgrB}-YFP] attHK::[P_{tetA}-CFP] *ΔsafA*::(FRT:*kan*:FRT:P_{tac}-*safA*)	This work
ML2589	*ΔlacZYA* attλ::[P_{mgrB}-YFP] attHK::[P_{tetA}-CFP] Δ*mgrB* *ΔsafA*::FRT:*kan*:FRT	This work
ML2590	*ΔlacZYA* attλ::[P_{mgrB}-YFP] attHK::[P_{tetA}-CFP] *phoQ*(T281R) *ΔsafA*::FRT:*kan*:FRT	This work
ML2592	Dh5α attλ::[pCAH63 P_{safA}-YFP]	This work
ML2593	*ΔlacZYA* attλ::[pCAH63 P_{safA}-YFP] attHK::[P_{tetA}-CFP]	This work
ML2276	*ΔlacZYA* attλ::[P_{mgrB}-YFP] attHK::[P_{tetA}-CFP] ΔphoQ::(FRT:*kan*:FRT)	This work

TIM148	attλ::[pTM79 Δ*cat* (P_{phoPQ}-YFP)] attHK::[*pTM27Δkan*]	(Miyashiro and Goulian, 2007a)
ML2641	attλ::[pTM79 Δcat (PphoPQ-YFP)] attHK::[pTM27Δkan] Δ*mgrB*::FRT:*kan*:FRT	This work
ML1988	Δ*phoQ789*::*kan*	(Baba et al., 2006)

Acknowledgements

We thank the members of the Laub lab, as well as V. Baytshtok, A. Amor, and A. Olivares for advice and assistance with mant-ADP experiments. We also thank M. Goulian for providing strains used in this work.

References

Baba, T., Ara, T., Hasegawa, M., Takai, Y., Okumura, Y., Baba, M., Datsenko, K.A., Tomita, M., Wanner, B.L., and Mori, H. (2006). Construction of Escherichia coli K-12 in-frame, single-gene knockout mutants: the Keio collection. Mol. Syst. Biol. *2*, 2006.0008.

Bader, M.W., Sanowar, S., Daley, M.E., Schneider, A.R., Cho, U., Xu, W., Klevit, R.E., Le Moual, H., and Miller, S.I. (2005). Recognition of antimicrobial peptides by a bacterial sensor kinase. Cell *122*, 461–472.

Capra, E.J., and Laub, M.T. (2012). Evolution of two-component signal transduction systems. Annu. Rev. Microbiol. *66*, 325–347.

Chen, H.D., and Groisman, E.A. (2013). The Biology of the PmrA/PmrB Two-Component System: The Major Regulator of Lipopolysaccharide Modifications. Annu. Rev. Microbiol. *67*, 83–112.

Datsenko, K.A., and Wanner, B.L. (2000). One-step inactivation of chromosomal genes in Escherichia coli K-12 using PCR products. Proc. Natl. Acad. Sci. U. S. A. *97*, 6640–6645.

Eguchi, Y., Itou, J., Yamane, M., Demizu, R., Yamato, F., Okada, A., Mori, H., Kato, A., and Utsumi, R. (2007). B1500, a small membrane protein, connects the two-component systems EvgS/EvgA and PhoQ/PhoP in Escherichia coli. Proc. Natl. Acad. Sci. *104*, 18712–18717.

Eguchi, Y., Ishii, E., Yamane, M., and Utsumi, R. (2012). The connector SafA interacts with the multi-sensing domain of PhoQ in Escherichia coli. Mol. Microbiol. *85*, 299–313.

Gao, R., and Stock, A.M. (2009). Biological Insights from Structures of Two-Component Proteins. Annu. Rev. Microbiol. *63*, 133–154.

Gao, R., and Stock, A.M. (2013a). Evolutionary tuning of protein expression levels of a positively autoregulated two-component system. PLoS Genet. *9*, e1003927.

Gao, R., and Stock, A.M. (2013b). Probing kinase and phosphatase activities of two-component systems in vivo with concentration-dependent phosphorylation profiling. Proc. Natl. Acad. Sci. *110*, 672–677.

Goulian, M. (2010). Two-component signaling circuit structure and properties. Curr. Opin. Microbiol. *13*, 184–189.

Groisman, E.A. (2001). The Pleiotropic Two-Component Regulatory System PhoP-PhoQ. J. Bacteriol. *183*, 1835–1842.

Haldimann, A., and Wanner, B.L. (2001). Conditional-Replication, Integration, Excision, and Retrieval Plasmid-Host Systems for Gene Structure-Function Studies of Bacteria. J. Bacteriol. *183*, 6384–6393.

Hsing, W., Russo, F.D., Bernd, K.K., and Silhavy, T.J. (1998). Mutations That Alter the Kinase and Phosphatase Activities of the Two-Component Sensor EnvZ. J. Bacteriol. *180*, 4538–4546.

Hutchings, M.I., Hong, H.-J., and Buttner, M.J. (2006). The vancomycin resistance VanRS two-component signal transduction system of Streptomyces coelicolor. Mol. Microbiol. *59*, 923–935.

Huynh, T.N., Noriega, C.E., and Stewart, V. (2010). Conserved mechanism for sensor phosphatase control of two-component signaling revealed in the nitrate sensor NarX. Proc. Natl. Acad. Sci. *107*, 21140–21145.

Igo, M.M., Ninfa, A.J., Stock, J.B., and Silhavy, T.J. (1989). Phosphorylation and dephosphorylation of a bacterial transcriptional activator by a transmembrane receptor. Genes Dev. *3*, 1725–1734.

Iizuka, R., Yamagishi-Shirasaki, M., and Funatsu, T. (2011). Kinetic study of de novo chromophore maturation of fluorescent proteins. Anal. Biochem. *414*, 173–178.

ISHII, E., EGUCHI, Y., and UTSUMI, R. (2013). Mechanism of Activation of PhoQ/PhoP Two-Component Signal Transduction by SafA, an Auxiliary Protein of PhoQ Histidine Kinase in Escherichia coli. Biosci. Biotechnol. Biochem. *77*, 814–819.

Kato, A., and Groisman, E.A. (2008). The PhoQ/PhoP Regulatory Network of Salmonella enterica. In Bacterial Signal Transduction: Networks and Drug Targets, R. Utsumi, ed. (Springer New York), pp. 7–21.

Levine, J.H., Fontes, M.E., Dworkin, J., and Elowitz, M.B. (2012). Pulsed Feedback Defers Cellular Differentiation. PLoS Biol *10*, e1001252.

Lippa, A.M., and Goulian, M. (2009). Feedback inhibition in the PhoQ/PhoP signaling system by a membrane peptide. PLoS Genet. *5*, e1000788.

Miyashiro, T., and Goulian, M. (2007a). Stimulus-dependent differential regulation in the Escherichia coli PhoQ PhoP system. Proc. Natl. Acad. Sci. U. S. A. *104*, 16305–16310.

Miyashiro, T., and Goulian, M. (2007b). [22] - Single-Cell Analysis of Gene Expression by Fluorescence Microscopy. In Methods in Enzymology, B.R.C. and A.C. Melvin I. Simon, ed. (Academic Press), pp. 458–475.

Miyashiro, T., and Goulian, M. (2008). High stimulus unmasks positive feedback in an autoregulated bacterial signaling circuit. Proc. Natl. Acad. Sci. U. S. A. *105*, 17457–17462.

Podgornaia, A.I., and Laub, M.T. (2015). Pervasive degeneracy and epistasis in a protein-protein interface. Science *347*, 673–677.

Ram, S., and Goulian, M. (2013). The Architecture of a Prototypical Bacterial Signaling Circuit Enables a Single Point Mutation to Confer Novel Network Properties. PLoS Genet *9*, e1003706.

Ray, J.C.J., and Igoshin, O.A. (2010). Adaptable functionality of transcriptional feedback in bacterial two-component systems. PLoS Comput. Biol. *6*, e1000676.

Russo, F.D., and Silhavy, T.J. (1993). The essential tension: opposed reactions in bacterial two-component regulatory systems. Trends Microbiol. *1*, 306–310.

Salazar, M.E., and Laub, M.T. (2015). Temporal and evolutionary dynamics of two-component signaling pathways. Curr. Opin. Microbiol. *24*, 7–14.

Sanowar, S., and Le Moual, H. (2005). Functional reconstitution of the Salmonella typhimurium PhoQ histidine kinase sensor in proteoliposomes. Biochem. J. *390*, 769–776.

Shin, D., Lee, E.-J., Huang, H., and Groisman, E.A. (2006). A Positive Feedback Loop Promotes Transcription Surge That Jump-Starts Salmonella Virulence Circuit. Science *314*, 1607–1609.

Siryaporn, A., and Goulian, M. (2008). Cross-talk suppression between the CpxA–CpxR and EnvZ–OmpR two-component systems in E. coli. Mol. Microbiol. *70*, 494–506.

Skerker, J.M., Prasol, M.S., Perchuk, B.S., Biondi, E.G., and Laub, M.T. (2005). Two-Component Signal Transduction Pathways Regulating Growth and Cell Cycle Progression in a Bacterium: A System-Level Analysis. PLoS Biol *3*, e334.

Skerker, J.M., Perchuk, B.S., Siryaporn, A., Lubin, E.A., Ashenberg, O., Goulian, M., and Laub, M.T. (2008). Rewiring the Specificity of Two-Component Signal Transduction Systems. Cell *133*, 1043–1054.

Sliusarenko, O., Heinritz, J., Emonet, T., and Jacobs-Wagner, C. (2011). High-throughput, subpixel precision analysis of bacterial morphogenesis and intracellular spatio-temporal dynamics. Mol. Microbiol. *80*, 612–627.

Storz, G., Wolf, Y.I., and Ramamurthi, K.S. (2014). Small proteins can no longer be ignored. Annu. Rev. Biochem. *83*, 753–777.

Yamamoto, K., and Ishihama, A. (2005). Transcriptional response of Escherichia coli to external zinc. J. Bacteriol. *187*, 6333–6340.

Yeo, W.-S., Zwir, I., Huang, H.V., Shin, D., Kato, A., and Groisman, E.A. (2012). Intrinsic Negative Feedback Governs Activation Surge in Two-Component Regulatory Systems. Mol. Cell *45*, 409–421.

Appendix I:

Time-lapse microscopy

Results

Here, we present single cell YFP:CFP expression and replicate experiments for the time-lapse microscopy data presented in Chapter II.

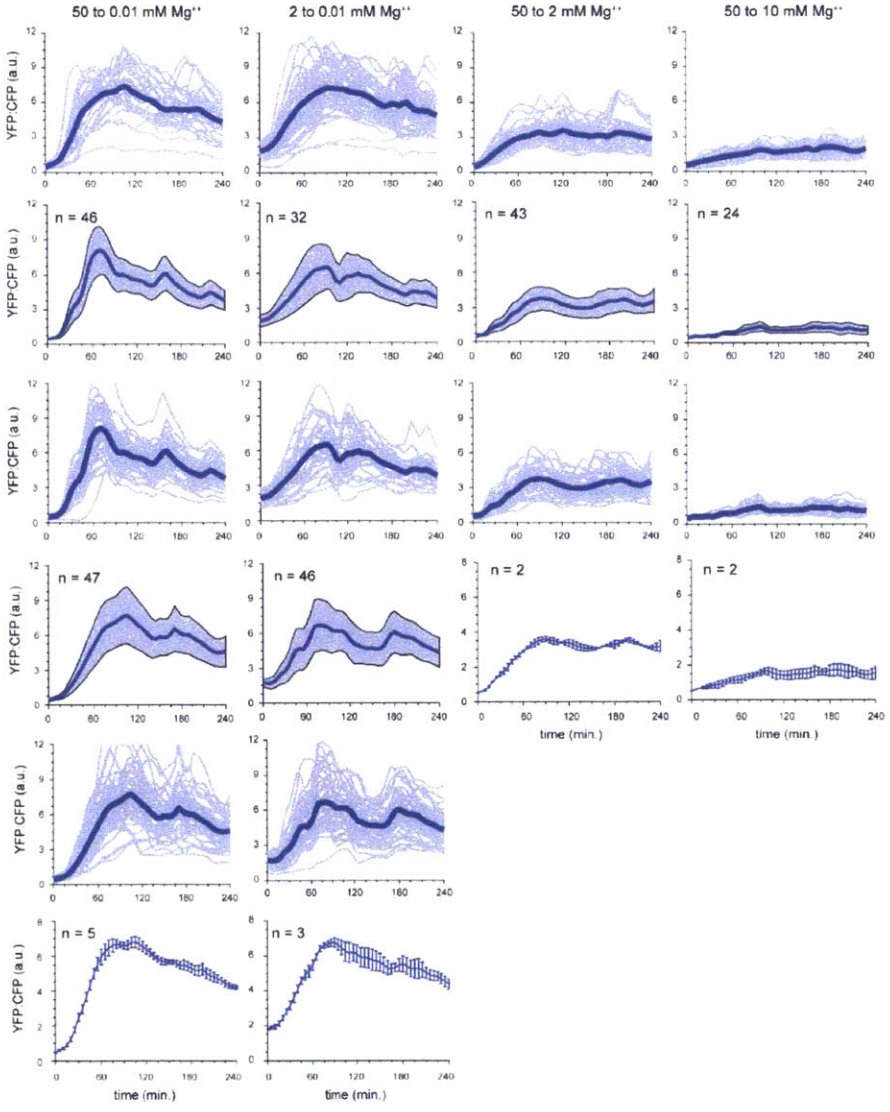

Figure Appendix I.1. Related to Fig 2.1

Quantification of PhoP activity following the shifts in extracellular Mg^{++} concentration noted above each panel. Thick lines represent the mean YFP:CFP ratio and the shaded region indicates the mean +/- one standard deviation. The top panels indicate the individual traces (light blue lines) used to calculate the mean and standard deviation in Fig. 2.1. The middle rows were generated from the imaging of an independent population of cells with the individual traces shown in the corresponding panels below. The final row is the average (+/- SEM) of the mean YFP:CFP ratios from multiple independent experiments.

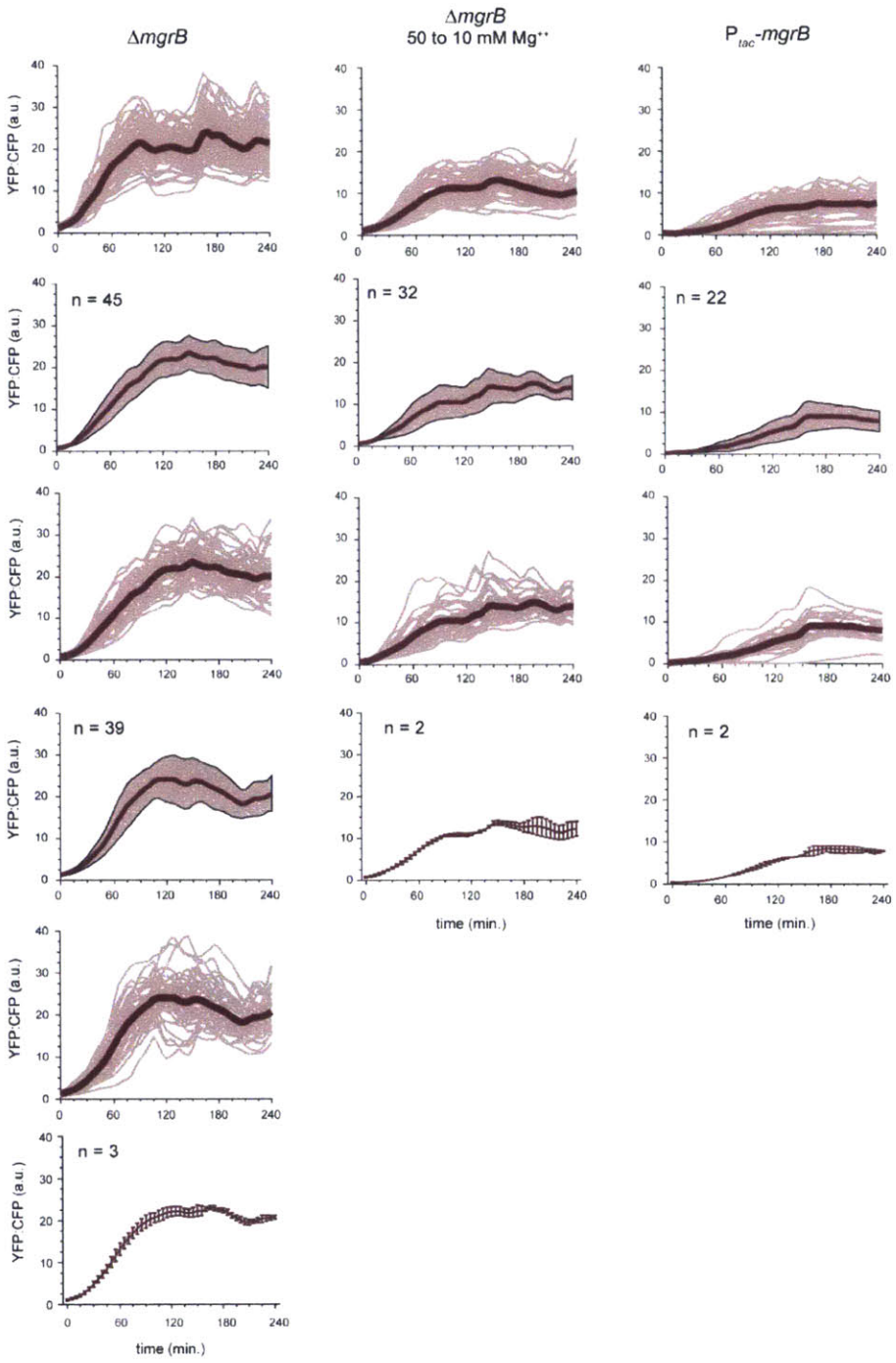

Figure Appendix I.2. Related to Fig 2.4

Quantification of PhoP activity following the shifts in extracellular Mg^{++} concentration from (left) 50 to 0.01 mM, (middle) 50 to 10 mM, (right) 50 to 0.01 mM + 0.25 mM IPTG. Thick lines represent the mean YFP:CFP ratio and the shaded region indicates the mean +/- one standard deviation. The top panels indicate the individual traces (light red lines) used to calculate the mean and standard deviation in Fig. 2.4. The middle rows were generated from the imaging of an independent population of cells with the individual traces shown in the corresponding panels below. The final row is the average (+/- SEM) of the mean YFP:CFP ratios from multiple independent experiments.

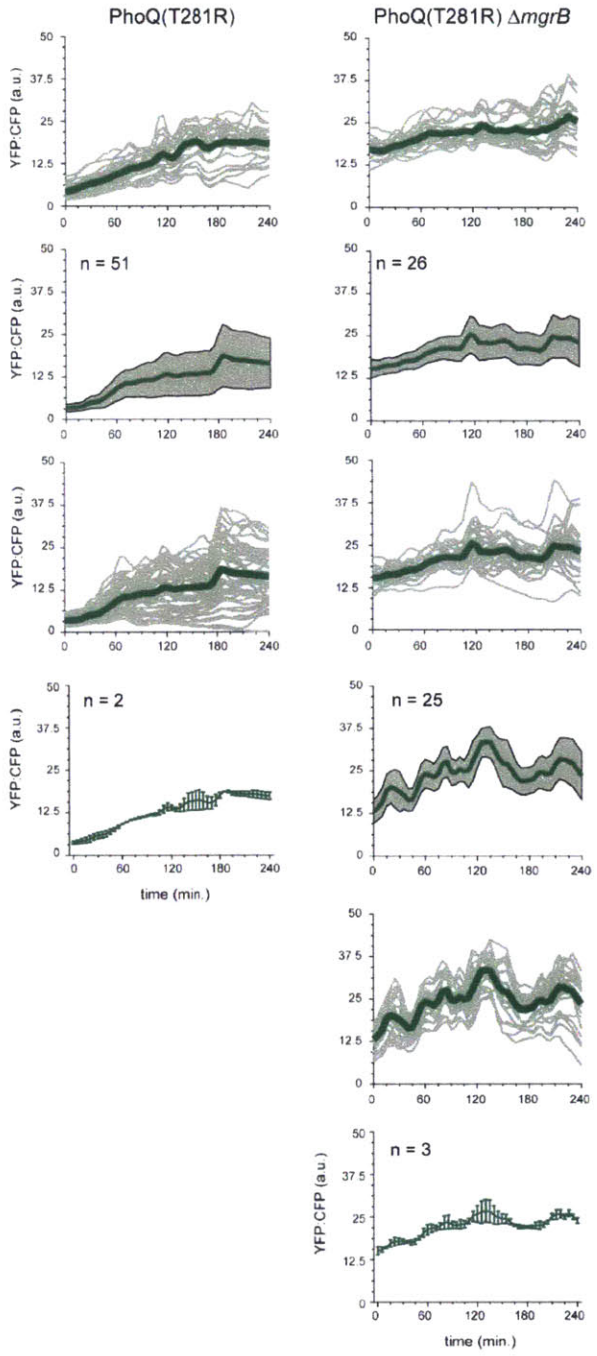

Figure Appendix I.3. Related to Fig 2.5

Quantification of PhoP activity following the shifts in extracellular Mg^{++} concentration from 50 to 0.01 mM. Thick lines represent the mean YFP:CFP ratio and the shaded region indicates the mean +/- one standard deviation. The top panels indicate the individual traces (light green lines) used to calculate the mean and standard deviation in Fig. 2.5. The middle rows were generated from the imaging of an independent population of cells with the individual traces shown in the corresponding panels below. The final row is the average (+/- SEM) of the mean YFP:CFP ratios from multiple independent experiments.

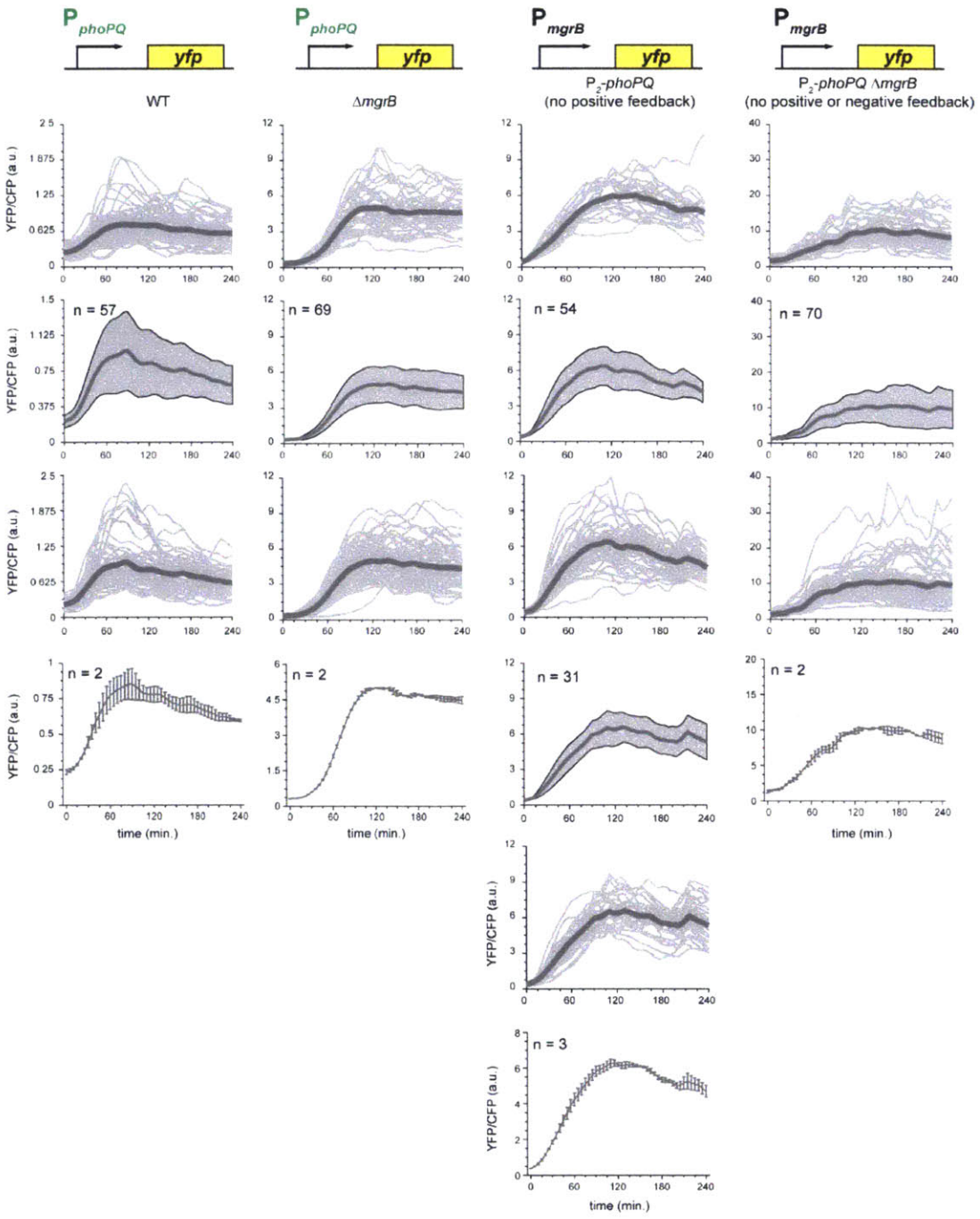

Figure Appendix I.4. Related to Fig 2.6

Quantification of PhoP activity following the shifts in extracellular Mg^{++} concentration from 50 to 0.01 mM. Thick lines represent the mean YFP:CFP ratio and the shaded region indicates the mean +/- one standard deviation. The top panels indicate the individual traces (light grey lines) used to calculate the mean and standard deviation in Fig. 2.6 The middle rows were generated from the imaging of an independent population of cells with the individual traces shown in the corresponding panels below. The final row is the average (+/- SEM) of the mean YFP:CFP ratios from multiple independent experiments.

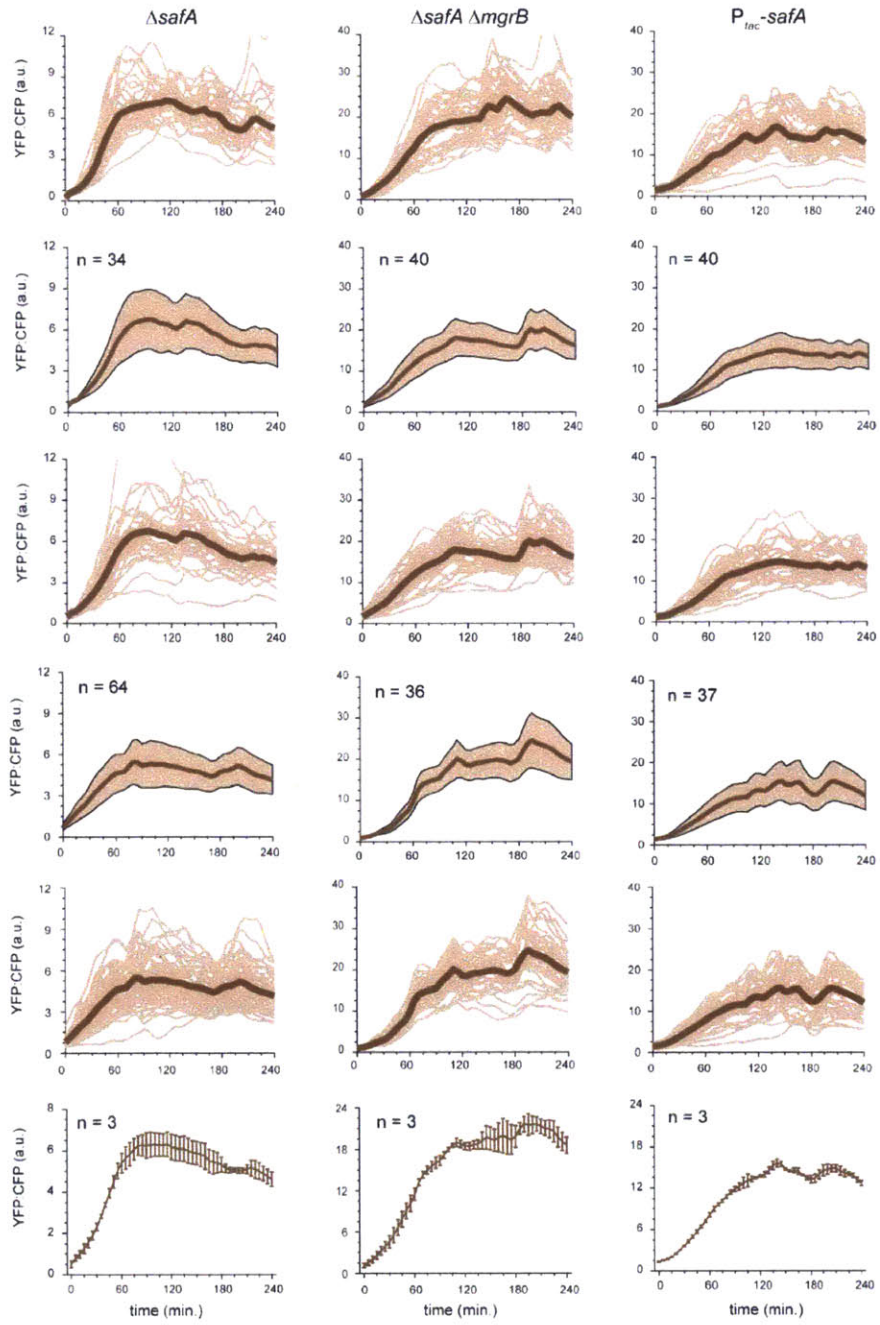

Figure Appendix I.5. Related to Fig 2.7

Quantification of PhoP activity following the shifts in extracellular Mg^{++} concentration from 50 to 0.01 mM. Thick lines represent the mean YFP:CFP ratio and the shaded region indicates the mean +/- one standard deviation. The top panels indicate the individual traces (light tan lines) used to calculate the mean and standard deviation in Fig. 2.7 The middle rows were generated from the imaging of an independent population of cells with the individual traces shown in the corresponding panels below. The final row is the average (+/- SEM) of the mean YFP:CFP ratios from multiple independent experiments.

Appendix II:

PhoQ-PhoP induction in liquid culture

Background

In the previous chapter, we discuss the roles of PhoQ bifunctionality, the *mgrB* negative feedback loop, the *phoPQ* positive feedback loop, and SafA on the induction kinetics of the PhoQ-PhoP system. We performed these experiments through time-lapse fluorescence microscopy. Cells were grown in repressive conditions for the PhoQ-PhoP system (50 mM Mg^{++} M9) and imaged on agarose pads of inducing conditions (typically 0.01 mM Mg^{++} M9). To supplement these results, we wanted to explore how cell growth conditions can influence the PhoQ-PhoP induction kinetics. In this appendix, we briefly characterize the induction kinetics of the PhoQ-PhoP system of cells growing in liquid culture.

Results

MgrB alters the sensitivity of PhoQ to Mg^{++} limitation

In addition to suppressing output from the PhoQ-PhoP pathway and influencing the network activation kinetics, we found that MgrB also influences the apparent sensitivity of PhoQ to extracellular Mg^{++} (Fig. Appendix II.1A). To examine signal sensitivity, we measured steady-state PhoP target gene expression levels (grown for ~3 hours in culture) in M9 liquid media at various concentrations of extracellular Mg^{++} ranging from 0.032 to 100 mM. For the wild type, the concentration of extracellular Mg^{++} that resulted in 50% maximal PhoP-dependent gene expression was 2.1 mM (Fig. Appendix II.1A) (Miyashiro and Goulian, 2007). In contrast, the Δ*mgrB* strain exhibited higher sensitivity, with the 50% maximal point occurring at 5.4 mM Mg^{++}, *i.e.* induction of PhoP dependent gene expression required less Mg^{++} starvation in the Δ*mgrB* strain. Conversely, cells

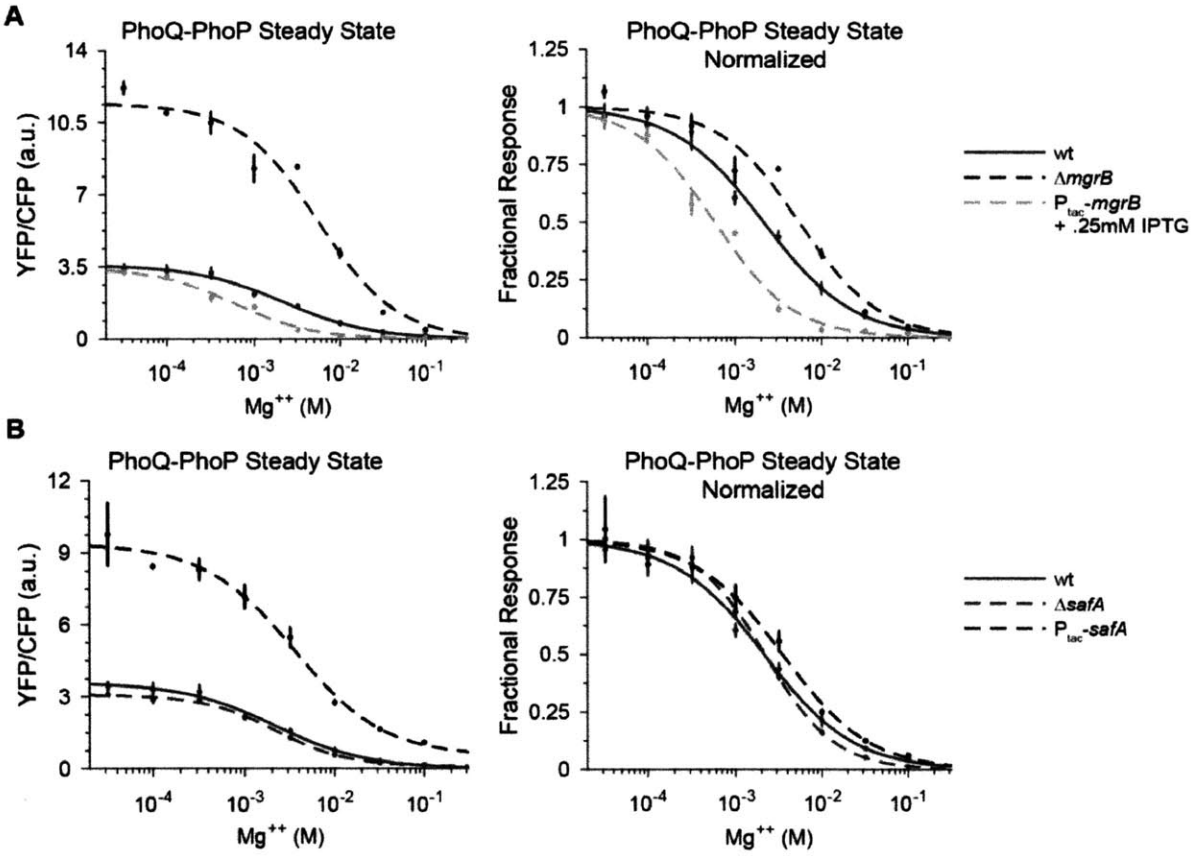

C

Strain	$[Mg^{++}]_{50\%}$ (mM)
WT	2.1
Δ*mgrB*	5.4
P_{tac}-*mgrB*	0.6
Δ*safA*	2.2
P_{tac}-*safA*	3.5

Figure Appendix II.1: Steady state response of PhoQ-PhoP network variants grown in M9 liquid culture with varying concentrations of Mg^{++}. All strains contain P_{mgrB}-*yfp* and P_{tetA}-*cfp*. **A.** Steady state PhoQ-PhoP network response of wild-type, Δ*mgrB*, and P_{tac}-*mgrB* (+ 0.25 mM IPTG) cells in varying concentrations of Mg^{++}, pre and post normalization. **B.** Steady state PhoQ-PhoP network response of wild-type, Δ*safA*, and P_{tac}-*safA* cells in varying concentrations of Mg^{++}, pre- and post-normalization. **C.** Table containing the Mg^{++} concentration required to produce 50% maximal YFP:CFP ratio for various PhoQ-PhoP network variants.

constitutively producing *mgrB* exhibited lower sensitivity to Mg^{++} limitation compared to the wild type, with a half maximal induction occurring at 0.6 mM extracellular Mg^{++}. Thus, not only does MgrB limit the maximal level of PhoP~P activity, it also lowers the

range of Mg^{++} sensitivity for PhoQ. Unlike MgrB, deleting or constitutively expressing *safA* did not have any substantial effect on PhoQ sensitivity to extracellular Mg^{++} limitation (Fig. Appendix II.1B).

PhoQ-PhoP partial adaptation is growth condition dependent

To test whether adaptation is also observed in bulk cultures shifted from high to low extracellular Mg^{++}, we grew cells harboring the P_{mgrB}-*yfp* reporter in 50 mM Mg^{++} and then washed and resuspended cells in 0.10 mM (diluting the culture 1:1 with fresh medium after each doubling to prevent entry into stationary phase). Samples of cells were taken at various times after the initial shift and imaged on agarose pads, as above. Cells exhibited an increase in the YFP:CFP ratio until a steady state was reached after ~2 hours (Fig. Appendix II.2A(i.)). However, unlike cells analyzed by time-lapse microscopy on agarose pads, the YFP:CFP ratio did not overshoot the steady state. Furthermore, the induction rate of the YFP:CFP ratio is much slower in liquid culture than on agarose pads. As discussed in Chapter 2, a strong activation of the PhoQ-PhoP system is required for an impulse response (Fig. 2.1), and the system is likely not sufficiently induced in liquid culture to elicit the impulse response. Because the partial adaptation observed by time-lapse microscopy is PhoQ dependent (Chapter 2), these data suggest that PhoQ responds differently to extracellular Mg^{++} in shaking culture and on agarose pads. Cells lacking *mgrB* exhibit similar dynamics to wild-type cells in these conditions, but the YFP:CFP ratio increases to a higher steady state (Fig. Appendix II.2A(ii.)). Furthermore, cells lacking the positive feedback loop also displayed similar dynamics, but had a slightly lower steady state than wild type cells (Fig. Appendix II.2A(iii.)). Partial adaptation for the PhoQ-PhoP network has been observed in liquid

culture in *Salmonella*, which indicates that the kinetics of PhoQ-PhoP network activation are significantly different across species (Shin et al., 2006).

It has been previously shown that in extreme Mg^{++} starvation condition, the positive feedback loop plays a much larger role in determining the level of the PhoQ-PhoP network output than in less extreme starvation conditions (Miyashiro and Goulian, 2008). To replicate these data, we grew cells in 50 mM Mg^{++} liquid culture until early log

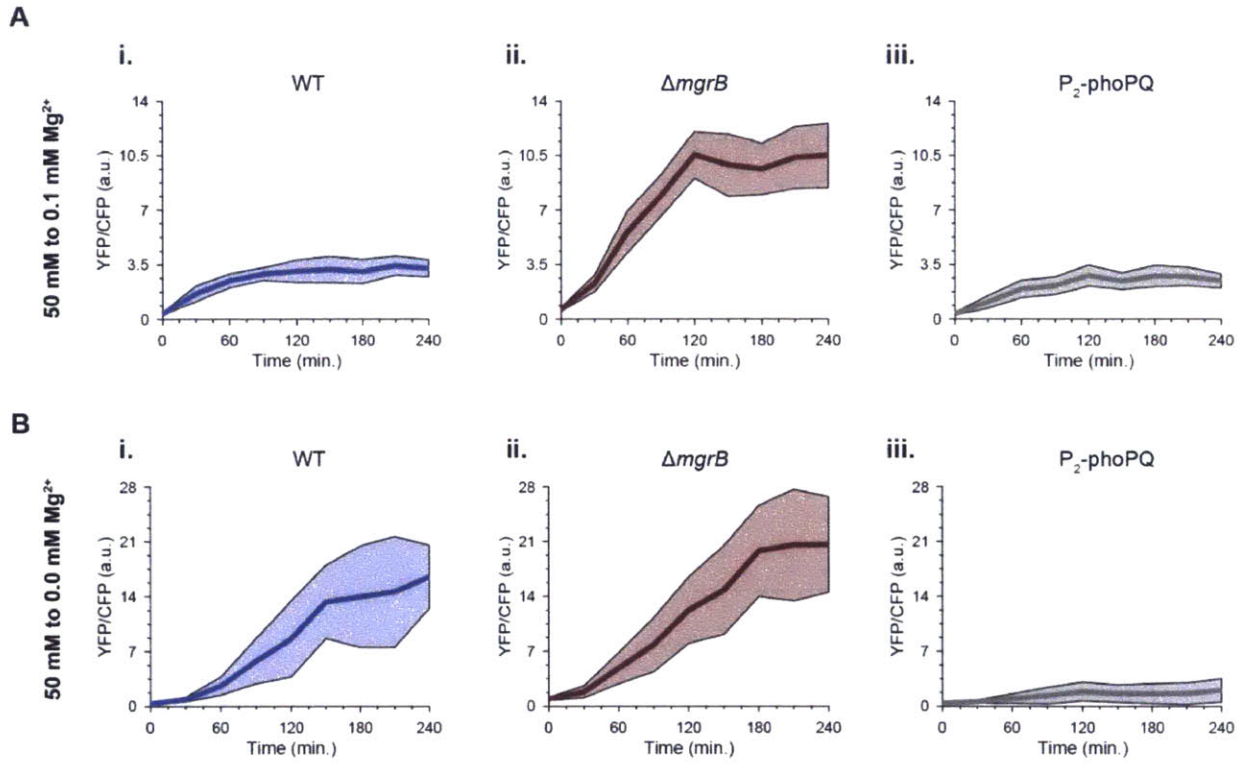

Figure Appendix II.2: PhoQ-PhoP network activation in liquid M9 culture. All strains contain P_{mgrB}-*yfp* and P_{tetA}-*cfp*. Cells were grown in 50 mM Mg^{++} M9 to exponential phase and transferred to **A.** 0.1 mM Mg^{++}, or **B.** 0 mM Mg^{++}. Thick line represents mean YFP:CFP ratio, and shaded region indicates mean +/- one standard deviation.

phase as before, but then transferred the cells to 0 mM Mg^{++} M9 liquid media after washing to remove residual Mg^{++}. At various time-points, the cells were fixed and imaged to assess PhoQ-PhoP network activity. In agreement with previously reported results, extreme levels of Mg^{++} starvation leads to a dramatic increase in YFP:CFP

activity in wild-type cells (Fig. Appendix II.2B(i.)), but does not lead to nearly as high YFP:CFP levels in cells containing P_{2}-*phoPQ* in place of the native promoter (Fig. Appendix II.2B(iii.)) (Miyashiro and Goulian, 2008). Interestingly, in these extreme Mg^{++} starved conditions, there is a significantly smaller difference between the YFP:CFP ratios in wild-type and Δ*mgrB* cells compared to cells grown in 0.1 mM Mg^{++} (Fig. Appendix II.2A,B). Therefore, at extreme Mg^{++} starvation conditions, these data suggest that MgrB becomes less effective at modulating the PhoQ kinase to phosphatase ratio, therefore allowing the positive feedback loop to have a more dramatic effect on the temporal dynamics of the PhoQ-PhoP system.

PhoQ-PhoP induction kinetics confer growth advantage

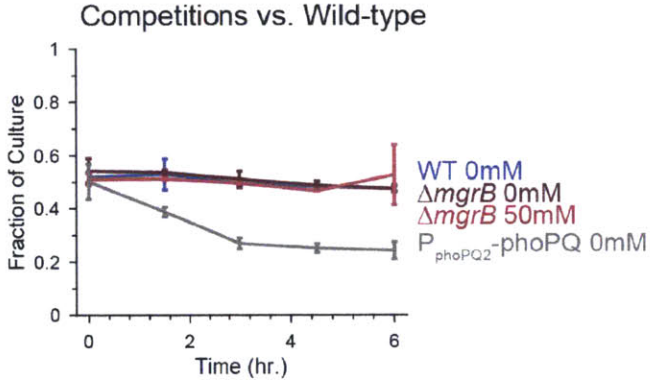

Figure Appendix II.3: Competitions between PhoQ-PhoP network mutants versus wild-type in M9 liquid culture. PhoQ-PhoP network mutants and wild-type cells were grown in 50 mM Mg^{++} M9 to exponential phase, and were mixed in equal numbers in either 0 mM or 50 mM Mg^{++} M9 liquid culture. Cells were fixed at indicated time-points and counted via fluorescence microscopy.

After characterizing the temporal dynamics of the PhoQ-PhoP signaling pathway, we wanted to determine if the tight control of PhoP~P target gene expression contributed to fitness and survival during growth in various concentrations of Mg^{++}. To this end, we grew wild-type cells competitively with either Δ*mgrB* or P_{phoPQ2}-*phoPQ* cells. Each strain was cultured independently in high Mg^{++} liquid culture to mid-exponential phase, and

then mixed 50:50 in M9 medium containing 0 mM Mg^{++}. The competing strains were labeled with different fluorescent markers and then counted at various time points after mixing (Fig. Appendix II.3). As a control, wild-type PhoPQ cells were competed against each other (with two separate fluorescent markers), and each subpopulation remained at approximately 50% of the total culture. When wild-type cells competed with Δ*mgrB*, neither strain grew significantly more than the other, suggesting that neither has a growth advantage in Mg^{++} starved conditions. Because Δ*mgrB* are less efficient at turning the PhoQ-PhoP system to the OFF state at high Mg^{++} levels, we also competed Δ*mgrB* and wild-type cells at 50 mM Mg^{++}. Once again, neither strain grew significantly more than the other, suggesting that the advantage MgrB confers to cells occurs in situations other than Mg^{++} stress in liquid culture. However, wild-type cells significantly outcompete cells lacking the positive transcriptional autoregulation, P_2-*phoPQ*. This suggests that rapid activation of the PhoQ-PhoP regulon may be important in Mg^{++} limited conditions.

Discussion

Here, we characterized the induction kinetics of the PhoQ-PhoP system for cells growing in liquid culture. Interestingly, the induction kinetics were slow and did not display the partial adaptation observed in cells growing on agarose pads during time-lapse microscopy. These data suggest that there are other stimuli regulating the activity of PhoQ (and MgrB-PhoQ complex) in addition to extracellular Mg^{++} that differ between growth in liquid and growth on agarose. There are many differences between the two growth conditions that could possibly differentially regulate PhoQ activity, including different oxygenation levels and different concentrations of intercellular signaling

molecules. Because there are already other known factors aside from Mg^{++} that can stimulate PhoQ-PhoP (Groisman, 2001; Kato and Groisman, 2008), it is not surprising that different growth conditions produces different induction kinetics for the PhoQ-PhoP system. Future work can be done to more thoroughly understand the differences in PhoQ-PhoP network activation in different growth conditions.

Experimental Procedures

Steady state PhoQ-PhoP network activity

Overnight cell cultures grown in 2 mM Mg^{++} M9-glu were washed in PBS and back diluted 1600X in M9 media with various Mg^{++} concentrations. After ~3 hrs of growth at 37°C, cells were fixed using paraformaldehyde. Cells were placed on 1.5% agarose pads for imaging using a Zeiss Observer Z1 microscope with a 100x/1.4 oil immersion objective and an LED-based Colibri illumination system. Florescence exposure time was increased to 500 msec for both YFP and CFP channels. YFP and CFP signal densities were calculated using MicrobeTracker, and best fit sigmoid for YFP:CFP steady states were determined by MATLAB.

PhoQ-PhoP network induction time course

Cells were grown overnight in 2 mM Mg^{++} M9-glu and back diluted 1:200 in 50 mM Mg^{++} M9 for ~ 3 hrs. Excess Mg^{++} was washed away by pelleting cells at 8000 rpm for 2 minutes and resuspending in PBS three times. Cells were pelleted a final time and resuspended in 0 mM or 0.1 mM Mg^{++} M9, as indicated. For cells resuspended in 0.1 mM Mg^{++} M9, cells were back diluted 1:1 every 45 minutes to maintain an OD_{600} value of approximately 0.1-0.3. At the indicated time-points, cells were fixed using

paraformaldehyde and imaged using a Zeiss Observer Z1 microscope with a 100x/1.4 oil immersion objective and an LED-based Colibri illumination system. Florescence exposure time was increased to 100 msec for both YFP and CFP channels. YFP and CFP signal densities were calculated using MicrobeTracker, and best fit sigmoid for YFP:CFP steady states were determined by MATLAB.

Competitions

Competing strains were grown overnight in separate cultures of 10mM Mg^{++} M9-glu. The following morning, both cultures were diluted 10x in 50mM Mg^{++} M9-glu. After ~1hr, cells were first pelleted at 8000 rpm for 2 minutes and then washed thrice in PBS. Cells were resuspended in 0 mM or 50 mM Mg^{++} M9-glu following the final PBS wash. The OD of the resuspended cultures were measured, and then cells of each competing strain were transferred to the competition medium of 0 mM or 50 mM Mg^{++} M9-glu in equal number such that the final OD = 0.1. Cells then grew at 37 degrees C with shaking at fixed with paraformaldehyde at the indicated time points. The number of cells for each competing strain was determined via microscopy using a Zeiss Observer Z1 microscope with a 100x/1.4 oil immersion objective and an LED-based Colibri illumination system.

References

Groisman, E.A. (2001). The Pleiotropic Two-Component Regulatory System PhoP-PhoQ. J. Bacteriol. *183*, 1835–1842.

Kato, A., and Groisman, E.A. (2008). The PhoQ/PhoP Regulatory Network of Salmonella enterica. In Bacterial Signal Transduction: Networks and Drug Targets, R. Utsumi, ed. (Springer New York), pp. 7–21.

Miyashiro, T., and Goulian, M. (2007). Stimulus-dependent differential regulation in the Escherichia coli PhoQ PhoP system. Proc. Natl. Acad. Sci. U. S. A. *104*, 16305–16310.

Miyashiro, T., and Goulian, M. (2008). High stimulus unmasks positive feedback in an autoregulated bacterial signaling circuit. Proc. Natl. Acad. Sci. U. S. A. *105*, 17457–17462.

Shin, D., Lee, E.-J., Huang, H., and Groisman, E.A. (2006). A Positive Feedback Loop Promotes Transcription Surge That Jump-Starts Salmonella Virulence Circuit. Science *314*, 1607–1609.

Chapter III:

Conclusions and future directions

Concluding Remarks

In the previous chapter, I discuss how I characterized the temporal dynamics of *E. coli* PhoQ-PhoP induction. Two-component systems are frequently used by bacteria to sense and respond to changes in their environments (Capra and Laub, 2012; Stock et al., 2000). After recognizing environmental stimuli, histidine kinases autophosphorylate and phosphotransfer to their cognate response regulators, which activates them to affect the appropriate responses to the environmental signals. Recent work has shown that the kinetics of two-component system activation are complex, and the systems do not always simply transition from an OFF state to a fully ON state in a monotonic fashion (Salazar and Laub, 2015). Some two-component systems undergo an impulse response during activation, in which the output of the network increases from a near zero level to a high maximum, but then partially adapts until a new steady state is reached. Instead, other systems exhibit a series of pulses in their output during exposure to a constant level of stimulus, in which the network's output successively increases and decreases until the stimulus is removed from the system.

The PhoQ-PhoP system was previously shown to perform an impulse response during activation in *Salmonella* (Shin et al., 2006). After cells detect low extracellular Mg^{++}, the expression of PhoP target genes rapidly increases. Once a maximal level of PhoP target gene expression is reached, target gene expression subsequently decreases, or partially adapts, and approaches a new steady state level of expression. In this work, I discuss how these kinetics are the result of multiple levels of feedback and regulatory features in the PhoQ-PhoP system, including a negative feedback loop involving a small

transmembrane protein, a positive transcriptional feedback loop on the *phoPQ* operon, and the ability of PhoQ to act as both a kinase and as a phosphatase on PhoP.

Before cells transition to a Mg^{++} starved environment, the PhoQ-PhoP system exists in the OFF state (Groisman, 2001; Kato and Groisman, 2008). PhoQ prevents the accumulation of PhoP~P by acting primarily as a phosphatase. The *phoPQ* operon is transcribed at basal levels by the constitutively active P2 promoter. After cells are exposed to low extracellular Mg^{++}, the relative fraction of the PhoQ molecules in the kinase state increases, resulting in a net increase in the level of PhoP~P. The newly activated PhoP~P further increases the transcription of the *phoPQ* operon by activating the P1 promoter. This positive feedback increases the level of PhoP (and PhoP~P), which further accelerates the transcription of the PhoP regulon. PhoP~P also activates the transcription of *mgrB*, a gene encoding a small, transmembrane protein that interacts directly with PhoQ in the transmembrane and periplasmic regions (Lippa and Goulian, 2009). MgrB modulates the relative proportion of PhoQ molecules in the kinase and phosphatase states by inhibiting the PhoQ kinase reaction while permitting the PhoQ phosphatase reaction. This modulation in PhoQ bifunctionality causes a decrease in PhoP~P levels, and therefore reduces transcription of PhoP target genes. When cells are growing on agarose pads with low Mg^{++}, this decrease in PhoP~P levels results in a decrease in PhoQ-PhoP network activity until a new steady state is reached.

This work helps contribute to our understanding of how the temporal dynamics of gene expression are regulated at the molecular level. However, due to the huge diversity in signal transduction networks in bacteria and higher organisms, more work needs to be done to more fully understand how genetic circuits integrate to form the wide range of

induction kinetics that exist in nature. Below, I have outlined approaches to study a more complex two-component network, how to identify additional regulators of known two-component systems, and more questions that could be explored about the PhoQ-PhoP system.

Future Directions

Specificity and Evolution of the *Bacilli* Sporulation Phosphorelay

As discussed in Chapter I, some two-component systems have evolved into larger phosphorelays, involving multiple steps of phosphotransfer between the initial histidine kinase and the final response regulator (Capra and Laub, 2012; Salazar and Laub, 2015). Some of these more complex phosphorelays utilize so-called hybrid histidine kinases, in which an intramolecular phosphotransfer event occurs in the histidine kinase before the phosphoryl group is transferred to its cognate response regulator through an intermediate phosphotransferase. Other phosphorelays, including the phosphorelay regulating the initiation of sporulation in *B. subtilis*, involve several layers of intermolecular phosphotransfer between the initial kinase and the final response regulator.

When *B. subtilis* is exposed to sporulation inducing conditions, five histidine kinases, KinA-E, autophosphorylate and phosphotransfer to the response regulator Spo0F. Spo0F does not contain an effector domain and only serves to transfer the phosphoryl group to the phosphotransferase Spo0B, which ultimately phosphorylates the response regulator Spo0A. Once phosphorylated, Spo0A serves as an active transcription factor to initiate sporulation. This network architecture appears to be shared between all

sporulating *Bacilli*. However, in the closely related *Clostridia* class of sporulating bacteria, Spo0F and Spo0B are not found in the genomes of certain species and histidine kinases appear to directly phosphorylate Spo0A (Galperin et al., 2012; Steiner et al., 2011).

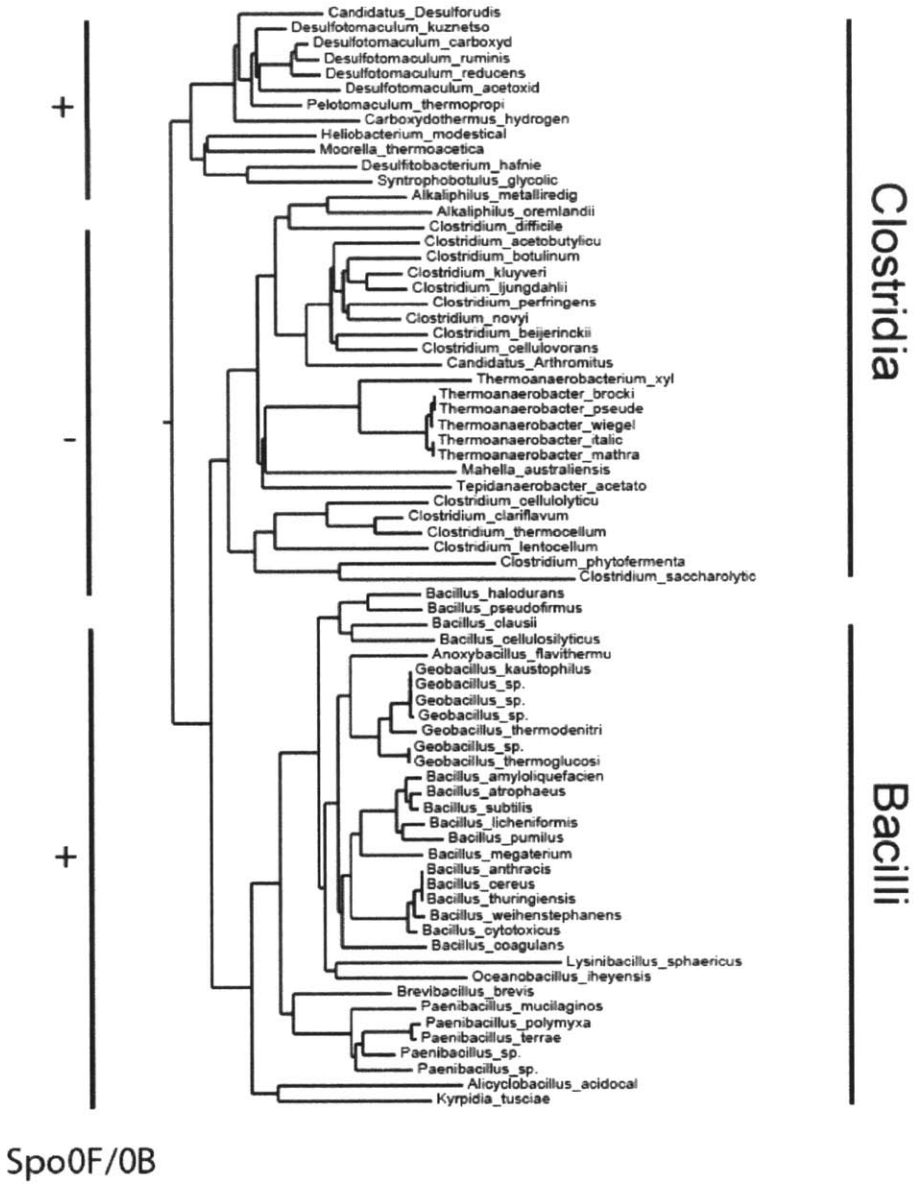

Figure 3.1: Hierarchical cluster of Spo0A sequences in sporulating *Bacilli* and *Clostridia*. Nearest neighbor clustering of Spo0A orthologue sequences. The presence or absence of Spo0F and Spo0B are marked on the left side of the cluster.

It is still unclear how the sporulation phosphorelay in both *Bacilli* and *Clostridia* evolved to their current states. Preliminary results suggest that the four component phosphorelay is a relatively ancient architecture for regulating the initiation of sporulation and that a subset of *Clostridia* subsequently lost their genomic copies of Spo0F and Spo0B (Fig. 3.1). Clustering analysis of sporulating *Bacilli* and *Clostridia* Spo0A sequences reveals three distinct clusters; one cluster comprised entirely of *Bacilli* (all of which contain Spo0F and Spo0B orthologues), another cluster containing *Clostridia* whose genomes do not contain Spo0F and Spo0B orthologues, and a final cluster, the outgroup, containing *Clostridia* species where some of the genomes do contain Spo0F and Spo0B orthologues. Because the outgroup is composed of bacteria containing supposedly functional four component sporulation phosphorelays, these data suggests that the sporulation phosphorelays in some *Clostridia* reverted to a smaller two-component system. However, these findings should be viewed as preliminary, because the existence of a four component phosphorelay has not yet been experimentally verified in the *Clostridia* outgroup, and more computational work needs to be performed to support the validity of this hierarchical clustering for the sporulation phosphorelay and confirm the existence or absense of Spo0B and Spo0F orthologues in *Clostridia* species.

In *B. subtilis*, the KinA-E (the kinases regulating the initiation of sporulation) cannot directly phosphotransfer to Spo0A (Burbulys et al., 1991). Therefore, in order to accommodate for the loss of Spo0F and Spo0B, mutations on either the *Clostridia* sporulation kinases or Spo0A may have occurred to create direct kinase to Spo0A phosphotransfer. Because two of the Clostridia sporulation kinases, Cac0903/3319,

directly phosphotransfer to *Bacillus* and *Clostridia* Spo0A, it is likely that mutations on the *Clostridia* kinases allowed for direct phosphotransfer to Spo0A (Steiner et al., 2011). To test this hypothesis, I rewired the specificity residues of *B. subtilis* KinA to match those of Cac3319 (Skerker et al., 2008). The fully rewired KinA, as well as several mutational intermediates, were able to directly phosphotransfer to Spo0A (Fig. 3.2), supporting the hypothesis that mutations in the sporulating kinases compensated for the loss of Spo0F and Spo0A in *Clostridia.*

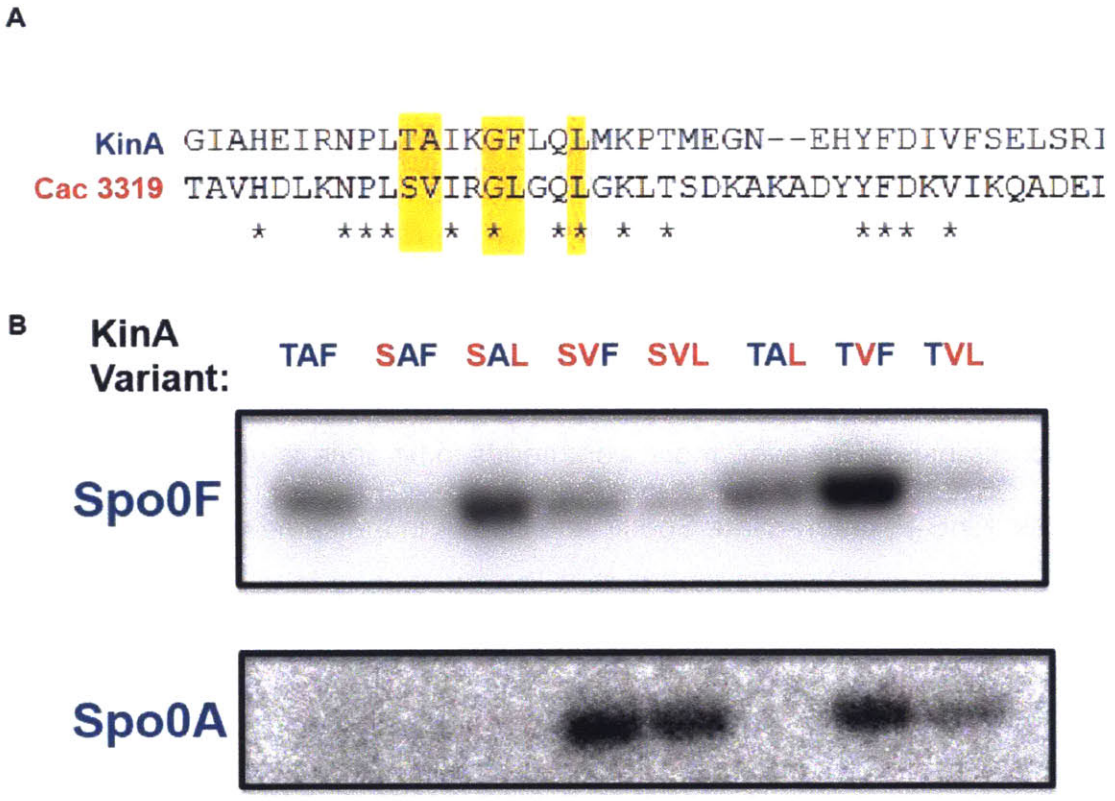

Figure 3.2: Rewiring of *B. subtilis* KinA with Cac3319 specificity residues. **A.** Partial sequence alignment of the DHp domains of KinA and Cac3319 with specificity residues highlighted. **B**. Cac3319 specificity residues numbers 1, 2, and 4 were partially and completely grafted onto KinA. KinA specificity mutants were incubated with *B. subtilis* Spo0F for 1 hour to assess for phosphotransfer activity.

Two-component systems can also be rewired by mutating specificity residues of one response regulator to match those of one from another system. In order to understand

how *B. subtilis* KinA-E recognize Spo0F and avoid Spo0A, I mutated specificity residues of Spo0A to match the specificity residues of Spo0F, the response regulator directly phosphorylated by KinA-E (Fig. 3.3). There are four specificity residue positions with different residues on Spo0F and Spo0A. When a quadruple mutant of Spo0A(N12Q, E14G, L15I, Y21V) is made such that the mutant contains all specificity residues of Spo0F, KinA is able to directly phosphorylate the mutant *in vitro*. However, a triple mutant of Spo0A containing only three Spo0F specificity residues (E14G, L15I, Y21V) is phosphorylated by KinA with greater efficiency than the quadruple mutant. This triple Spo0A specificity mutant is functional at wild-type levels *in vivo*, and can rescue 5% of sporulation in the absence of Spo0F and Spo0B, suggesting that this Spo0A triple mutant is being directly activated by KinA and that the *B. subtilis* four component phosphorelay can be reduced to a more canonical two-component system *in vivo*. These data also indicate that KinA recognizes specific residues on Spo0F that permit direct phosphotransfer. However, more work needs to be done to understand if the other kinases, KinB-E, differentiate Spo0F and Spo0A in the same manner.

Presumably, the Spo0A(E14G, L15I, Y21V) variant can be used to study the kinetics of sporulation initiation. As discussed in Chapter I, the phosphorylation level of Spo0A pulses several times before sporulation begins. Although this phenomenon has been well documented (Levine et al., 2012), the molecular mechanism generating Spo0A~P pulsing remains unclear. It has been hypothesized that the pulsing is caused by feedback loops that feed into the network by regulating the phosphorylation state of Spo0F and Spo0B. Using the Spo0A(E14G, L15I, Y21V) allele could test this

hypothesis, because the hypothesis predicts that pulsing would not be observed in the absence of either Spo0F or Spo0B.

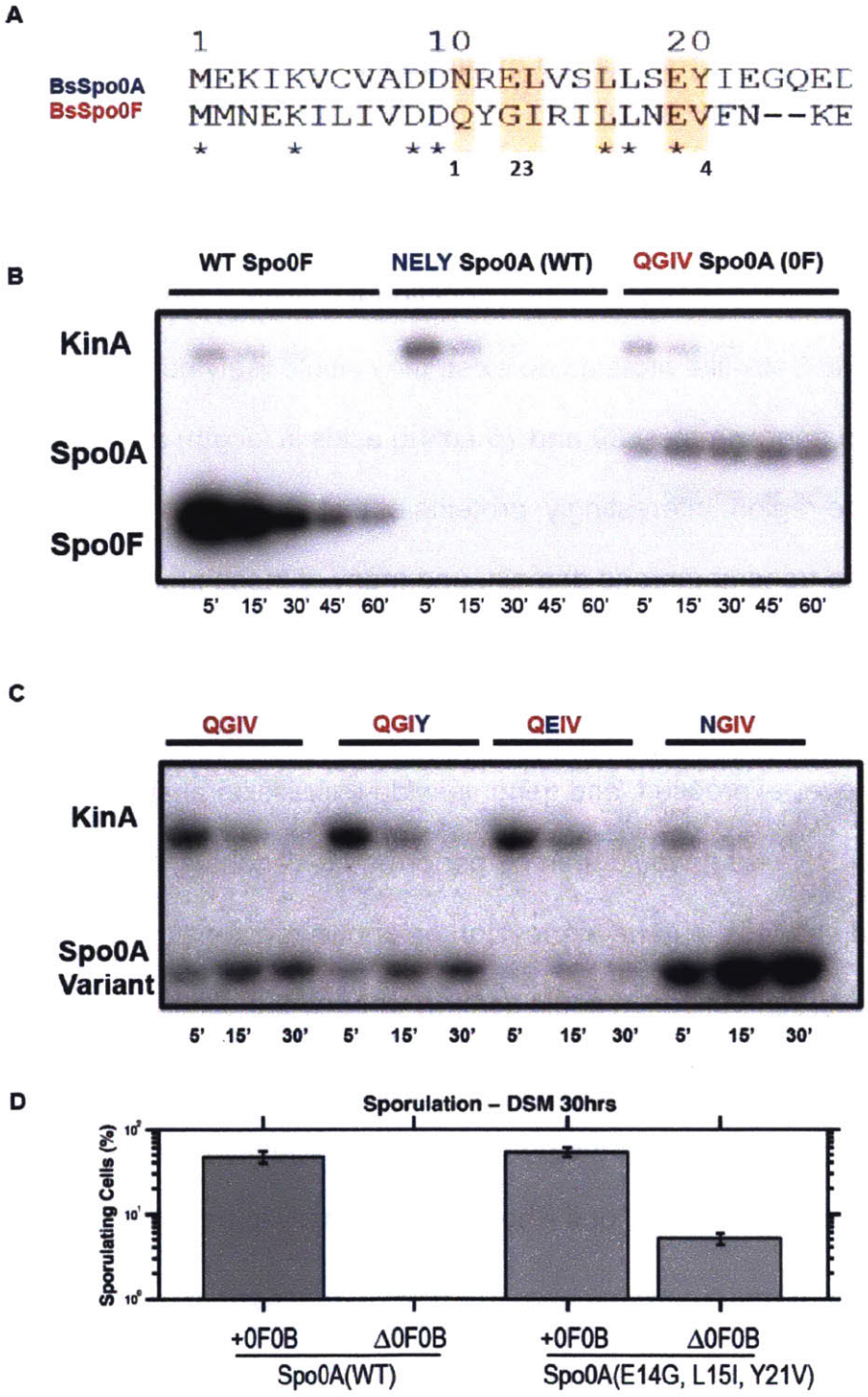

Figure 3.3: Rewiring of *B. subtilis* Spo0A with Spo0F specificity residues. A. Partial sequence alignment of Spo0A and Spo0F with specificity residues highlighted. **B.** Phosphotransfer of KinA to Spo0F, Spo0A, and Spo0A mutated to contain Spo0F specificity residues. **C.** Phosphotransfer of KinA to Spo0A mutants with three of the four Spo0F specificity residues. **D.** Sporulation efficiency of Spo0A(WT) and Spo0A(E14G, L15I, Y21V) with and without Spo0F and Spo0B.

Small Transmembrane Regulators of Histidine Kinases

Currently, MgrB and SafA are the only known transmembrane small protein regulators of histidine kinases, and both are only known to regulate PhoQ. Presumably, there exist other similar proteins that regulate the bifunctional activity of other histidine kinases. If other MgrB- and SafA-like proteins do exist, they would likely be characterized by being short (between approximately 30 and 75 amino acids in length) and having a single transmembrane region. Interestingly, proteins of that size are enriched for having a single predicted transmembrane domain, and many of these proteins are uncharacterized (Fig. 3.4). These uncharacterized small membrane proteins could be tested for their effects on two-component systems. To do this, a candidate protein would be deleted or over-expressed, and genome wide expression analysis (such as microarrays or RNA-seq) would then be performed in various growth conditions. If there were detected changes in gene expression on known regulons of two-component systems, then further validation could confirm whether the candidate protein was an MgrB- or SafA-like regulator of that system. These experiments would help us understand whether small transmembrane proteins regulating histidine kinases is a common regulatory technique, or if PhoQ is an anomaly in being regulated by MgrB and SafA.

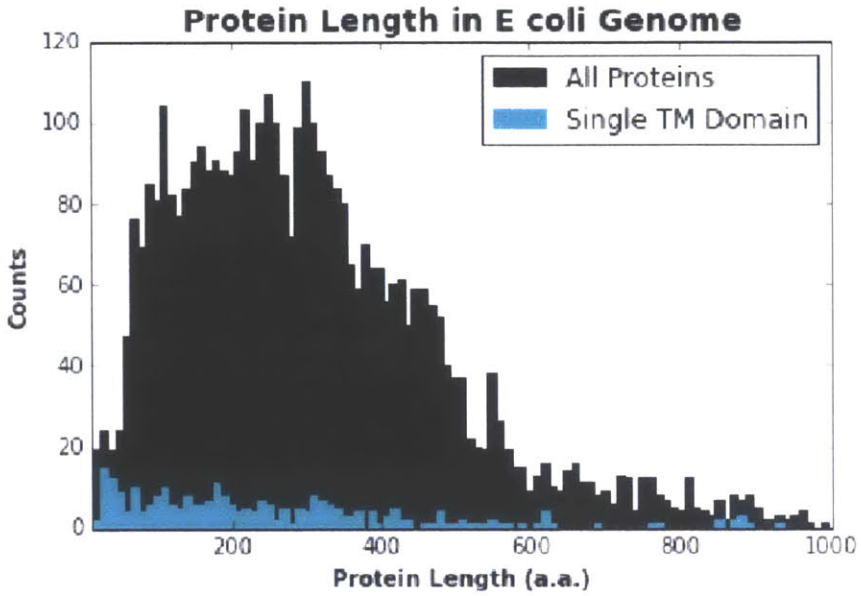

gi	Length	TM Region	Desc
16128018	72	i21-43o	uncharacterized protein b0024
157783151	41	o10-32i	uncharacterized protein b4655
94541122	66	o5-24i	putative membrane protein, UPF0370 family
94541130	67	i7-29o	putative lipoprotein
16130429	63	i20-42o	uncharacterized protein b2504
90111332	34	o10-29i	uncharacterized protein b1788
226524710	34	i7-24o	uncharacterized protein b4672
16129021	46	i21-43o	uncharacterized protein b1058
94541117	35	i7-29o	putative membrane protein
16129780	47	i7-24o	MgrB
635341465	54	i31-53o	uncharacterized protein b4522
226524699	33	i13-32o	uncharacterized protein b4671
16129459	65	i21-40o	SafA
16131155	73	o50-72i	putative outer membrane protein
145698274	35	i13-32o	uncharacterized protein b4535
226524722	32	i7-29o	inner membrane-associated protein
16131151	59	i7-29o	putative membrane protein
226524745	41	i7-29o	uncharacterized protein b4684
145698263	31	i7-26o	inner membrane-associated protein

Figure 3.4: Potential transmembrane regulators of histidine kinases. Top. All *E. coli* proteins sorted by length. Proteins with a single predicted transmembrane region are highlighted in blue. **Bottom.** List of uncharacterized proteins (30-75 amino acids long) with a single transmembrane region.

MgrB-PhoQ characterization in vitro

Although we were able to show that MgrB selectively inhibits the kinase reaction of PhoQ *in vivo*, it may be interesting to further characterize the interaction between the two proteins *in vitro*. By using an *in vitro* transmembrane system and purified full-length PhoQ and MgrB, one could measure how the kinetics of PhoQ autophosphorylation, phosphotransfer, and dephosphorylation of PhoP are influenced by MgrB. Furthermore, by measuring the rates of these reactions while varying the concentration of MgrB, future experiments could show if different concentrations of the MgrB have different effects on the three different reactions, and if there were cooperativity in the function of MgrB, such that multiple MgrB molecules need to function together to influence PhoQ. Understanding the stoichiometry of the MgrB-PhoQ interaction could be especially interesting considering the dimeric nature of PhoQ. Lastly, NMR or other structural studies could be conducted of PhoQ and MgrB variants to better understand the physical aspect of their interaction. It is hypothesized that MgrB interacts with the proposed Mg^{++} binding pocket of PhoQ, but that has yet to be shown experimentally.

PhoQ-PhoP *in vitro* phosphotransfer with ATP regeneration

As discussed in Chapter II, apparent adaptation in PhoP phosphorylation is observed *in vitro* as PhoP~P levels rise and subsequently fall after mixing with phosphorylated PhoQ (Fig. 2.5). Presumably, if ATP levels remain constant instead of decreasing over time, PhoP~P should reach a constant steady state level. However, this approach may be complicated by two factors. First, the *in vitro* rate of PhoQ autophosphorylation is much slower than the rate of PhoP~P dephosphorylation by PhoQ, suggesting that the steady state level of PhoP~P could be zero (Sanowar and Le Moual, 2005).

Furthermore, AMP-PNP has been shown to stimulate PhoP~P intrinsic dephosphorylation *in vitro*, so it is possible that free ATP can further reduce observed PhoP phosphorylation levels (Sanowar and Le Moual, 2005).

Experimental Procedures

Spo0A hierarchical clustering

List of confirmed sporulating *Bacilli* and *Clostridia* was obtained from the literature (Galperin et al., 2012). Reciprocal BLAST of *B. subtilis* Spo0A was performed on the genomes of every sporulating *Bacilli* and *Clostridia* to identify Spo0A orthologues. Heirarchical clustering of Spo0A orthologues was performed using Clustal Omega. Reciprocal BLAST was used to determine the existence of *B. subtilis* Spo0F and Spo0B orthologues in each sporulating bacterial genome.

Protein purification and phosphotransfer experiments

Expression, protein purification, and phosphotransfer experiments were carried out as previously described (Skerker et al., 2005, 2008). Mutagenesis of KinA and Spo0A was performed using round-the-horn PCR.

B. subtilis sporulation

Cells were incubated for 30 hours in Difco Sporulation Medium (DSM) at 37°C with shaking. Half of the culture was then incubated at 80°C for 20 minutes to select for spores, while the other half of the culture was kept at room temperature. Both were plated separately, and the fraction of sporulating cells was defined as the number of

colonies from the boiled culture divided by the number of colonies on the non-boiled culture.

Small transmembrane protein identification

Prediction of transmembrane protein domains was performed using a hidden Markov model for predicting transmembrane helices in protein sequences (Sonnhammer et al., 1998).

References

Burbulys, D., Trach, K.A., and Hoch, J.A. (1991). Initiation of sporulation in B. subtilis is controlled by a multicomponent phosphorelay. Cell *64*, 545–552.

Capra, E.J., and Laub, M.T. (2012). Evolution of two-component signal transduction systems. Annu. Rev. Microbiol. *66*, 325–347.

Galperin, M.Y., Mekhedov, S.L., Puigbo, P., Smirnov, S., Wolf, Y.I., and Rigden, D.J. (2012). Genomic determinants of sporulation in Bacilli and Clostridia: towards the minimal set of sporulation-specific genes. Environ. Microbiol. *14*, 2870–2890.

Groisman, E.A. (2001). The Pleiotropic Two-Component Regulatory System PhoP-PhoQ. J. Bacteriol. *183*, 1835–1842.

Kato, A., and Groisman, E.A. (2008). The PhoQ/PhoP Regulatory Network of Salmonella enterica. In Bacterial Signal Transduction: Networks and Drug Targets, R. Utsumi, ed. (Springer New York), pp. 7–21.

Levine, J.H., Fontes, M.E., Dworkin, J., and Elowitz, M.B. (2012). Pulsed Feedback Defers Cellular Differentiation. PLoS Biol *10*, e1001252.

Lippa, A.M., and Goulian, M. (2009). Feedback inhibition in the PhoQ/PhoP signaling system by a membrane peptide. PLoS Genet. *5*, e1000788.

Salazar, M.E., and Laub, M.T. (2015). Temporal and evolutionary dynamics of two-component signaling pathways. Curr. Opin. Microbiol. *24*, 7–14.

Sanowar, S., and Le Moual, H. (2005). Functional reconstitution of the Salmonella typhimurium PhoQ histidine kinase sensor in proteoliposomes. Biochem. J. *390*, 769–776.

Shin, D., Lee, E.-J., Huang, H., and Groisman, E.A. (2006). A Positive Feedback Loop Promotes Transcription Surge That Jump-Starts Salmonella Virulence Circuit. Science *314*, 1607–1609.

Skerker, J.M., Prasol, M.S., Perchuk, B.S., Biondi, E.G., and Laub, M.T. (2005). Two-Component Signal Transduction Pathways Regulating Growth and Cell Cycle Progression in a Bacterium: A System-Level Analysis. PLoS Biol *3*, e334.

Skerker, J.M., Perchuk, B.S., Siryaporn, A., Lubin, E.A., Ashenberg, O., Goulian, M., and Laub, M.T. (2008). Rewiring the Specificity of Two-Component Signal Transduction Systems. Cell *133*, 1043–1054.

Sonnhammer, E.L., von Heijne, G., and Krogh, A. (1998). A hidden Markov model for predicting transmembrane helices in protein sequences. Proc. Int. Conf. Intell. Syst. Mol. Biol. ISMB Int. Conf. Intell. Syst. Mol. Biol. *6*, 175–182.

Steiner, E., Dago, A.E., Young, D.I., Heap, J.T., Minton, N.P., Hoch, J.A., and Young, M. (2011). Multiple orphan histidine kinases interact directly with Spo0A to control the initiation of endospore formation in Clostridium acetobutylicum. Mol. Microbiol. *80*, 641–654.

Stock, A.M., Robinson, V.L., and Goudreau, P.N. (2000). Two-component signal transduction. Annu. Rev. Biochem. *69*, 183–215.